UTRECHT UNIVERSITY

Department of Earth Sciences

Faculty of Geosciences

THESIS SUBMITTED IN PARTIAL FULFILLMENT OF THE REQUIREMENTS FOR THE DEGREE OF MASTER OF SCIENCE IN EARTH SCIENCES UTRECHT UNIVERSITY

Validating Multidecadal Fluvial Sediment Flux Projections to Major Deltas Under Environmental Change Scenarios

First examiner:
dr. Frances Dunn

Second examiner:
dr. Jaap Nienhuis

Candidate:
J.J.P. Hooijmans

Student number:
7819773

February 2, 2024

Abstract

This thesis presents a critical validation analysis of the pioneering work of (Dunn et al., 2019) in projecting decadal sediment fluxes for major global deltas using the WBMsed model. The study evaluates the model's performance in accurately projecting sediment flux scenarios and its applicability to provide as a 'missing link' in delta sustainability research, especially in projecting relative sea level changes for individual deltas. When substituting empirical data with a model, recognizing its capabilities and limitations is vital for establishing its projection accuracy, reliability and applicability for other global deltas, and to help address the existing knowledge gap in accurately projecting future challenges faced by deltaic systems.

Through a comprehensive operational validity study, insight into how well the WBMsed model captures real-world patterns and behaviours is provided. By evaluating the performance of the model compared to more recent and reliable validation data, significant challenges and areas for improvement in the WBMsed model are revealed. The assessment of mean annual sediment fluxes indicates generally acceptable projection performance, with 37 out of 43 individual rivers falling within one order of magnitude of the validation data. However, the analysis of mean inter-annual variations underscores the model's incapability to accurately capture yearly increase or decrease fluctuations for 21 out of 43 rivers, while simultaneously not representing natural delta system morphology behaviour. The dominance of these extreme inter-annual fluctuations is highlighted by the dominance of these variations on the sediment flux trends. Trendline analysis further analyses the model's sensitivity to chosen periods and event timing, with consistent sediment increase or decrease directions observed for 24 rivers and contradicting direction for 19 rivers between projections and measurements. These findings underscore the need for model refinement to enhance short-term variation projections.

Focussing on the overall sediment flux magnitudes, the WBMsed model demonstrates a pronounced tendency towards overprediction, with fluvial water discharges overestimated up to +1700%, contrasting with underpredictions of -54% in certain rivers. Moreover, the analysis identified that while projections suggest 16 deltas would experience increased pressure on their ability to withstand relative sea level rise as a result of decreasing fluvial sediment flux, observations show that 26 deltas actualy experienced increased pressure.

In this research, the WBMsed model shows promising accuracy in average annual sediment flux predictions for many rivers around the world, however, addressing the identified challenges on overprediction, unnatural inter-annual variability and the exclusion of variables able to influence fluvial sediment fluxes in reality, is crucial for its applicability to a broader range of global deltas and reliable use in delta sustainability projections.

Acknowledgements

I would like to express my sincere gratitude to Prof. Dunn and Prof. Nienhuis for their guidance, support, and encouragement throughout the completion of this thesis. Their expertise and mentorship have been instrumental in shaping my research. Furthermore, I am grateful to my family and friends for their unwavering support.

Contents

List of Figures

List of Tables

1. Introduction

Deltas, home to over 500 million people globally and housing many of the world's megacities, have been identified as one of the most vulnerable coastal environments in the 21st century (Deboulet & Mansour, 2022; R. Nicholls et al., 2016; J. P. Syvitski & Saito, 2007; J. P. Syvitski et al., 2009). Deltas are popular places to live due to abundant resources, including fertile and flat agricultural lands, potential harbour transport, fishing activities and mining resources (Edmonds et al., 2020; Evans, 2012; Hoitink et al., 2020). Additionally, the concentration of freshwater, nutrients and sediment inputs, makes deltas ideal for fostering diverse ecosystems (Adger et al., 2018).

Various climatic, environmental and socioeconomic drivers operate at multiple scales threatening the unique ecosystem services and livelihoods in delta areas. These drivers range from global climate change and sea-level rise to deltaic-scale subsidence, flooding and land cover change (R. Nicholls et al., 2016). While natural occurrences like sediment compaction and incidental flooding are normal, anthropogenic activities exacerbate delta vulnerability (R. J. Nicholls, 2004; Nienhuis et al., 2023; J. Syvitski, 2008; J. Syvitski & Kettner, 2011). As the delta populations and their economies continue to grow, anthropogenic pressures on the delta system are expected to increase (Dunn, 2017).

Deltas form when moving water meets a body of water with a sudden change in flow velocity, causing sediment deposition as the dispersal forces present are not strong enough to prevent sediment accumulation (Evans, 2012). This paper focusses on coastal deltas, with the moving water carrying sediment being the fluvial input, the body of water being an ocean, and wave and tidal processes, along with the river outlet are the dispersion forces referred to. A deltas existence depends on several riverine and oceanic processes, such as a regular sediment supply by fluvial water (Deboulet & Mansour, 2022; Evans, 2012). Aggradation is crucial for a deltas ability to withstand relative sea level rise, requiring regular inundation for sediment deposition and raising the delta surface relative to sea level (Dunn, 2017).

With adequate fluvial sediment supply and minimal human influence, deltas generally maintain their integrity and are able to withstand relative sea level rise due to aggradation mechanism (Ibáñez et al., 2014; Sanchez-Arcilla et al., 1998). However, ex-

panding anthropogenic activity in the last decades, including population and economic development, accompanied by catchment developments, negatively impact aggradation mechanisms (J. Syvitski, 2008; J. Syvitski & Kettner, 2011), reducing the deltas ability to grow and withstand relative sea level rise. Consequently, these regions and their inhabitants face an increasing threat of coastal flooding, depletion of wetlands, shoreline erosion, and infrastructure damage (Ericson et al., 2006; J. P. Syvitski et al., 2009). Interactions between human and natural forcings remain complex and not fully understood, challenging our current predictive capabilities (Sanchez-Arcilla et al., 1998; J. Syvitski et al., 2005).

With climate change driven accelerating sea-level rise, the added uncertainty introduced by non-climatic drivers of relative sea level rise, particularly local sea level rise linked to land level changes resulting from anthropogenic activities, get increasingly researched (Dunn, 2017; Nienhuis et al., 2023; J. Syvitski & Kettner, 2011; J. P. Syvitski et al., 2009).

As we recognise the importance of sediment delivery to deltas and the current reduction due to anthropogenic activity paired with changing sea levels, it is evident that the current situation is unsustainable (Dunn, 2017). Urgent calls for action by the scientific community on the risks faced by deltas with decreasing sediment supplies have increased (Giosan et al., 2014; Kondolf et al., 2022). Conducting more research on the present and potential future conditions of sediment in deltas enhances our scientific understanding of possible trends and can foster more sustainable management approaches (Dunn, 2017).

This study builds on Dunn et al. (2019) pioneering work by validating the decadal sediment flux projections for 43 major global delta rivers. Validated accurate sediment flux projections can be eventually be implemented in delta management strategies planning as it is essential knowledge to project relative sea level rise at individual global deltas, and be able to assess realistic projections of future delta sustainability (Nienhuis & van de Wal, 2021). To detect possible model errors and/or biases, the sediment flux projections will be validated by using historic reliable observations and operational validation.

This research aims to enhance our understanding of future delta sustainability by exploring future sediment flux alterations within global deltas, considering both current and future environmental shifts until the end of the 21st century. Validating the sediment flux projections from Dunn et al. (2019) can help address the existing knowledge gap in

projecting future relative sea level changes in deltaic systems.

To address this problem, the following research question and sub-questions will be answered during this project:

To what extent are the sediment flux projections of Dunn et al. (2019) able to accurately project sediment flux scenarios and thus give a reliable sediment information source to be implemented in projections of global delta land loss?

1. *How do the sediment flux projections perform when compared to recent measurements?*
2. *What factors cause the discrepancies between the projections and the measurements?*
3. *How could the sediment flux projections be improved?*

The research project will build further on existing work on anthropogenic and natural influences on delta sediment fluxes and their impact on delta sustainability on a multidecadal timescale (Dunn et al., 2019). Due to relative stable natural influences on sediment fluxes, there will be a focus on anthropogenic influences on sediment fluxes in this study, as these are harder to predict on a longer timescale and are therefore more likely to cause projection errors (Dunn, 2017).

In Chapter 2, the intricacies governing delta sustainability and overall delta functioning are explained. This includes an exploration of processes influencing delta surface elevation relative to sea level and an examination of the drivers of change impacting these deltaic processes, a detailed description of the WBMsed model employed for projections along with the data utilized in shaping these projections. Also, the importance of validating the projections established by Dunn (2017) is explained, shedding light on potential errors inherent in the model or the data employed. In Chapter 3, the validation method and dataset are introduced, followed by preparation of the projection data. Chapters 4 and 5 contain the results and discussion of the validation analysis, beginning by fulfilling objective 1 through the presentation of direct comparison results between the projections and validation data. Objective 2 is subsequently achieved as the comparisons are examined, delving into potential factors contributing to observed discrepancies. This thorough analysis results in the identification of points of improvement, offering valuable insights into refining the projection model and fulfilling objective 3.

2. The difficulty of projecting delta sustainability

Coastal delta systems are highly dynamic landscapes, facing sustainability challenges due to the disturbance of delta processes (Wagner et al., 2017; Zonneveld & Nadin, 2020). The equilibrium of mechanisms creating and deteriorating deltas is globally disturbed, causing deltas to currently be among the most stressed and vulnerable systems (Day et al., 2016; IPCC, 2007). They are vulnerable to the impacts of climate change and anthropogenic factors influencing inland precipitation patterns and the fluvial runoff and sediment delivery patterns. However, these same drivers also influence the ability of the delta to keep up with sea level rise, and especially as low-lying plains, deltas are highly sensitive to changes in relative sea level (Wong et al., 2014). This prompted a recent increase in research efforts, with a surge in studies focusing on monitoring and projecting future sediment fluxes (Cohen et al., 2022; Dunn et al., 2018; Moragoda & Cohen, 2020). Notably, Dunn (2017) performed pioneering work in this domain, offering insights on expected effects of environmental changes on sediment fluxes to the worlds' major deltas. However, the interaction of different mechanisms makes it difficult to make correct projections for future delta risks and their magnitudes (Ericson et al., 2006). Therefore, ensuring the reliability of these projections is essential, as undisclosed discrepancies could lead to misleading results (Valle et al., 2009).

2.1 The influence of delta elevation change processes

Delta sensitivity to relative sea level rise is only enlarged due to the natural subsidence of deltaic sedimentary environments, which itself is accelerated by anthropogenic activities in densely populated areas (Dunn, 2017; R. J. Nicholls & Cazenave, 2010). The sensitivity lies in coastal threats such as floods and coastal erosion due to relative sea level rise (R. Nicholls et al., 2007). Dunn (2017) prioritised relative sea level rise as a key risk factor for deltas as a result of environmental change, focussing on eustatic sea level changes, sediment compaction and aggradation. All these elements can be influenced by anthropogenic factors, thereby impacting relative sea level rise.

2.1.1 Eustatic sea level changes

While it has been recognised for decades that anthropogenic-driven climate change contributes to ice mass-retreat and ocean warming, changing eustatic sea levels (Fairbridge, 1961; Rovere et al., 2016), are likely to accelerate as warming of (sub)polar glaciers continues (Meier et al., 2007; Sames et al., 2020). Important to note is that the global sea level rise will never be uniformly distributed globally due to self-gravitation in the surface mass load. Meaning, as ice melts, mass is lost locally and water will be redistributed from the local area to further locations (Mitrovica et al., 2001). The differing global distribution of global eustatic sea level changes influence deltas globally in different manners. Some deltas will experience eustatic sea level rise, whereas others may experience a drop (Yin et al., 2010). The unpredictability of (sub)polar ice masses add complexity to accurate future projections, as changes in glacier behaviour can occur on short time scales (Rignot & Thomas, 2002).

2.1.2 Sediment Compaction

Subsidence is a well-known phenomenon in deltaic areas consisting of natural and anthropogenic drivers (Nguyen et al., 2023). Natural compaction and consolidation is common in delta areas due to the relatively young sediment composition (Truong & Nguyen, 2020; Zoccarato et al., 2018). However, these natural compaction rates can be intensified by anthropogenic influence. Water extraction results in aquifer compaction (Jordan et al., 2019; Parker, 2020), and as cities grow, the weight on the delta subsurface increases, driving further compaction of the sediments (Parsons et al., 2023; Waltham, 2002). Delta sediment compaction strongly increases the deltas' vulnerability to flooding, coastal erosion and ultimately permanent inundation (Minderhoud et al., 2020). The anthropogenic activities currently dominate the main drivers for delta subsidence (Saito et al., 2007), making the projection of future subsidence rates more complicated. The few studies that exist on projecting anthropogenic intensified delta compaction rates rely on extrapolated extraction and mining activity rates. This creates uncertainties as increased weight of growing cities and other land use changes are not accounted for (Dunn, 2017; Minderhoud et al., 2020).

2.1.3 Aggradation

According to J. P. Syvitski et al. (2009), *"A delta's aggradation rate is determined from the volume of sediment delivered to and retained on the subaerial delta surface as new sedimentary layers"*. As relative sea levels rise is either a result of rising sea levels or delta land sub-

sidence, accommodation space is created. If sufficient fluvial sediment is provided, this accommodation space is filled and the delta is maintained (J. Syvitski, 2008). Alternatively, if the accommodation space exceeds delivered sediment supply rate or volume, the delta area will retreat (Nienhuis & van de Wal, 2021). Sustainable deltas are thus characterized by an adequate sediment supply to withstand marine forcing and relative sea level rise (Besset et al., 2019). Therefore, with current accelerated sea level rise, there is also an increase in sediment supply needed to maintain modern deltas. However, where at the start of classic civilizations anthropogenic activities induced fluvial sediment delivery due to large-scale implementation of deforestation, agricultural practices and other land use changes (Ibáñez et al., 2014; Maselli & Trincardi, 2013), anthropogenic activities negatively impact delta aggradation capabilities in the modern day. Upstream damming, instream sediment mining and canal- and levee construction has been reducing sediment delivery to deltas for decades (Ericson et al., 2006; J. Syvitski, 2008). Besides sediment delivery, the ability to retain this sediment is equally important for delta aggradation (J. P. Syvitski et al., 2009). However, even this retention capability is affected by anthropogenic activities, with flood defence efforts being of highest influence (Dunn, 2017). Being ironic, as the natural process of aggradation is essential for deltas to keep up with relative sea level rise. (Dunn, 2017) comprised the magnitudes of eustatic change, crustal deformation, and compaction for 47 global deltas. These values were compared to the accompanying aggradation values, showing that even with current aggradation processes, 14 out of 16 deltas which had data available on all processes, cannot keep up with current relative sea level rise.

2.2 Sediment delivery challenges

The importance of delta aggradation, and thus sediment delivery to deltas, to be able to keep up with RSLR is recognised. However, modern deltas face escalating challenges in fluvial runoff and sediment delivery patterns, stemming from climate change and increasing anthropogenic activities.

2.2.1 Climate drivers

Anthropogenic-driven climate change is a global phenomenon, but manifests in diverse effects on individual deltas. Precipitation and temperature alterations significantly influence fluvial sediment fluxes (Dunn, 2017). Climate change-induced precipitation changes, whether intensifying or decreasing, impact erosive processes and sediment transport.

Increasing and intensifying precipitation has an erosive effect, increasing precipitation runoff needed to transport this eroded sediment, ultimately increasing the fluvial sediment transport (Çakmak et al., 2021; Dunn, 2017; Hancock, 2009). Temperature also conducts its own influence on these processes. For example, an increase in global temperatures is expected to increase sediment fluxes in cold environments due to the melting of frozen sediment and glaciers or due to increased fluid precipitation (J. P. Syvitski, 2003; T. Zhang et al., 2022). The effects of both precipitation and temperature changes on sediment fluxes is complex and varies per individual delta, which makes it hard to project the influence of climate change on deltas' aggradation abilities (Dunn, 2017).

2.2.2 Anthropogenic drivers

Anthropogenic activities drastically transformed deltaic environments since the 20th century (Day et al., 2016), primarily due to land use changes, reservoir construction and channel activities like mining. According to (J. P. Syvitski et al., 2009), the construction of reservoirs has the biggest negative impact on sediment delivery to deltas, as dams retain substantial amounts of fluvial sediment (Vörösmarty et al., 2003). According to J. Syvitski et al. (2022)

> "If it were not for sequestration of sediment behind dams, global rivers would have increased their particulate loads by 212% between 1950 and 2010".

Channel mining and engineering, as well as flow diversion, further influence sediment fluxes, often resulting in declines (Kondolf, 1997; McManus, 2002). Channel engineering activities are related to economically prosperous communities with higher GNP, linking to the correlation of declining sediment fluxes as thriving deltaic economies continue to grow (Dunn, 2017). Flow diversion, implemented for consumption purposes, further reduces fluvial sediment fluxes due to increased evaporation and consumption losses leading to less discharge (Ericson et al., 2006; Vörösmarty et al., 2003). The dominant impact of anthropogenic drivers on sediment flux is emphasized by Moragoda and Cohen (2020), projecting future sediment flux scenario's under climate change effects as temperature and discharge, along with current anthropogenic influences and without the anthropogenic influences. They identified that already existing anthropogenic activities, which already diminish sediment fluxes, hinder the climate's positive influence on increasing sediment flux. As such, for some deltas the projected sediment fluxes was decreasing with current anthropogenic activities taken into account, but shifted to an increase in sediment flux when climate change effects were isolated.

2.3 Projecting future delta sustainability using WBMsed v2.0

Dunn employed the WBMsed v2.0 model for the sediment flux projections, which is an extension of WBMplus, which itself is an updated version of the original WBM (Water Balance Model) (Cohen et al., 2013). The original WBM was able to project soil moisture, evapotranspiration and runoff for individual cells. Due to the grid being two-dimensional, the discharge transfer between cells depended on the topology of the channel network, storage times of cells, and floodplain inundation (Dunn, 2017; Vörösmarty et al., 1989). The WBMplus extension of Wisser et al. (2008) introduces anthropogenic irrigation, evapotranspiration and additional reservoir components to better represent the grid based water balance (Wisser et al., 2010). In the WBMsed v2.0 extension, the cell discharge output computed by WBMplus is modified by adjusting daily water discharge for each grid-cell based on its bankfull discharge(maximum capacity). If projected water discharge surpasses the bankfull discharge, the surplus will be stored in an infinite modelled floodplain, and the water discharge will be limited to the bankfull discharge level. When predicted water discharge drops below bankfull levels again, water stored in the floodplain will be reintroduced to the river grid-cell. The amount of water returning to the river is proportional to the deficit of the river grid-cell from bankfull level. In other words, very low river discharge after a period of very high river discharge, will lead to a higher reintroduction of floodplain water. Additionally, floodplain storage allows the reduction of sediment flux projections as settling of sediment occurs (Cohen et al., 2014; Dunn, 2017).

WBMsed v2.0 integrates the BQART sediment delivery model of J. P. Syvitski and Saito (2007), which computes long-term suspended sediment loads at river mouths, taking into account the influence of geomorphic and tectonic influences (basin area and relief), geography (temperature, runoff), geology (lithology, ice cover), and human activities (reservoir trapping, soil erosion) on sediment fluxes to coastal zones (J. P. M. Syvitski & Kettner, 2011):

$$Q_S = \omega B Q^{0.31} A_B^{0.5} RT \text{ when } T \geq 2^{\circ}\text{C} \tag{2.1}$$

$$Q_S = 2\omega B Q^{0.31} A_B^{0.5} R \text{ when } T < 2^{\circ}\text{C} \tag{2.2}$$

Where Q_S is suspended sediment (kg/s), B are the catchment factors of glacial ero-

sion, lithology and anthropogenic soil erosion, A_B is basin area (km^2), R is maximum relief difference (m), T is the spatially averaged basin temperature (°C), Q is discharge (m^3/s) and ω is a proportionality coefficient (0.02 for kg/s or 0.0006 for Mt per year) (Dunn, 2017). To account for intra- and interannual variability, the Psi sediment delivery model by Morehead et al. (2003) is introduced along the BQART model. By merging the BQART and Psi models, WBMsed achieves the capability to simulate global daily water transport, enabling the spatial and temporal simulation of global sediment fluxes (Cohen et al., 2013). WBMsed is not a mass conservative model, as it does not explicitly compute sediment transport, but calculated sediment flux from the upstream basin at each individual pixel. Overall key fluvial basin input factors to the WBMsed with the potential to systematically affect performance according to Dunn (2017) are: Temperature, precipitation, flow channel network, contributing area, maximum- and minimum relief, minimum slope, ice cover, population density, GNP, large- and small reservoir capacity, irrigation area, -intensity and -efficiency, crop fraction, lithology factors, soil parameters, bankfull discharge, river bed slope and floodplain to river flow.

2.3.1 Composing Dunn et al. (2019) projections

In applying WBMsed for global delta sediment fluxes till 2100, corresponding input datasets are required. Dunn et al. (2019) used Jones et al. (2011) climate data, Murakami and Yamagata (2017) socioeconomic data, and Grill et al. (2015) together with Zarfl et al. (2015) for projected global reservoir capacity. To investigate fluvial sediment flux sensitivity to future climate- or socioeconomic changes, 12 scenarios of different climate and socioeconomic combinations are projected for the time period 1980-2099. This time period is chosen to provide sufficient historic years for validation of the research and beyond the end of the 21st century, confidence in projected datasets diminish as anthropogenic and natural projection uncertainties increase with time (Dunn, 2017). The 12 scenarios used in Dunn et al. (2019) are combinations of the four Representative Concentration Pathways (RCPs) and the first three Shared Socioeconomic Pathways (SSPs), SSP1 to SSP3 (shown in Figure 2.1).

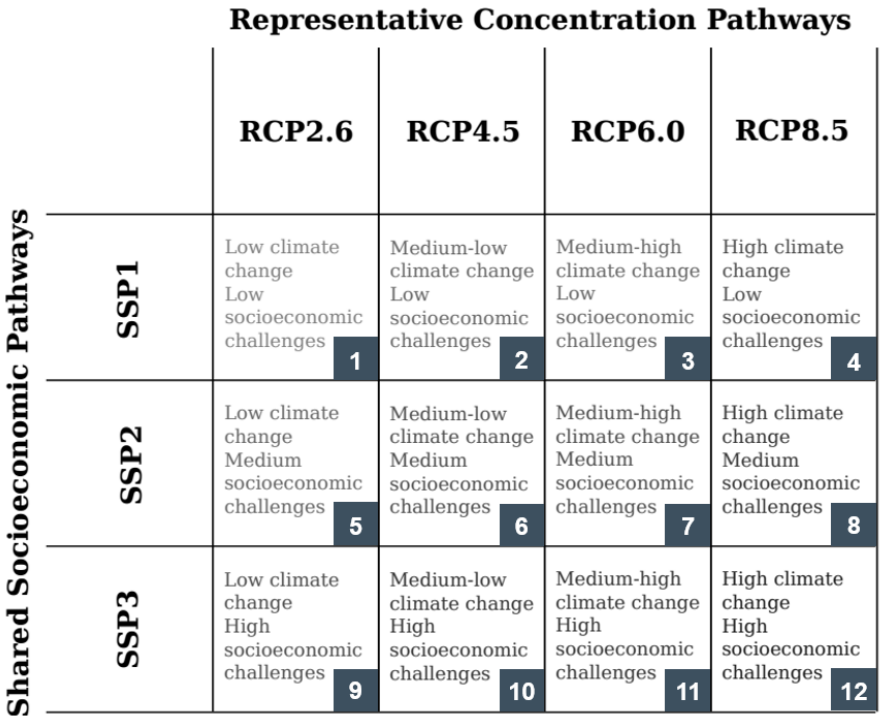

Figure 2.1: Matrix of the 12 future climate scenarios, constructed using all four RCP's and SSP1 to SSP3 from Dunn (2017)

2.3.1.1 Climate

The four RCPs project four different magnitudes and extents of climate change under different levels of radiative forcing (van Vuuren et al., 2014). Each RCP number represents the stabilised radiative forcing before the end of the 21st century (4.5 and 6.5) or the radiative forcing reached at 2100(2.6 and 8.5) (Dunn, 2017). The RCPs translate emissions, concentrations and accompanying land use and land cover to radiative forcing, and then this forcing is expressed in climate change (van Vuuren et al., 2011). The data used for climate change of Jones et al. (2011) utilizes atmospheric pollutant concentrations and land use from the RCPs, and additional solar irradiance and stratospheric volcanic aerosols to produce climate projections from 1950 to 2100 at 0.5 degree resolution. However, as the RCPs diverge from 2005 onward, climate data between 1950-2004 is the same for all pathways per basin. The climate variables used for implementation in WBMsed are the annual mean air temperature and precipitation (Dunn, 2017).

2.3.1.2 Socioeconomics

As RCPs are established for global socioeconomic assumptions, there is no detailed RCP data available for individual basins (Dunn, 2017). To be able to understand and work

with possible societal futures, five Shared Socioeconomic Pathways(SSPs) were constructed to characterize five future social trends. These SSPs consist of quantitative and qualitative elements describing how the future might develop in terms of population growth, governance efficiency, inequality across and within countries, socio-economic developments, institutional factors, technology change, and environmental conditions (O'Neill et al., 2014; van Vuuren et al., 2014). Murakami and Yamagata (2017) have used pre-existing data and interpolation to produce yearly, databases on population and demographics, urbanisation and GDP for SSP1-3 at a 0.5 degree resolution for the years 1980-2100.

2.3.1.3 Dams

Due to their earlier established significant impact on sediment delivery to deltas, Dunn (2017) implemented dam construction as a separate consistent variable in projecting the future sediment fluxes. The used reservoir data of Zarfl et al. (2015) consists of hydropower dams with at least 1MW capacity which are under construction, planned, financed and assigned, in a feasibility assessment stage or even in a pre-feasibility stage. These dams are corresponded with information on the dam location, hydroelectric capacity and construction timeline. To be used in the WBMsed model, the hydroelectric capacity of the dams are translated to reservoir volumes using Grill et al. (2015). To implement these constructed reservoir volumes at the correct location on the timeline used in the WBMsed model, the previously mentioned dam construction stages are used. Dunn (2017) assumed that dams under construction in 2015 come online in 2020; dams financed and signed as off 2015 come online in 2030; dams in the 'feasibility assessment' stage per 2015 come online in 2040; and all other dams (planned or in the 'pre-feasibility' stage) come online in 2050. An important note in the use of this particular reservoir dataset, is the exclusion of smaller, or other types of dams, giving rise to under-estimates of future dam reservoir volume present in the delta basins. Also, in reality, at the time of dam 'employment' sediment carrying capacity is not fully reduced at once (Lai et al., 2017).

2.4 The need for validation

When substituting empirical data with a model, recognizing its capabilities and possible limitations is vital, along with the accuracy of the utilized variables and external datasets, used in Dunn (2017).

2.4.1 Modelled water discharge

According to Dunn (2017), the model tends to overpredict mean annual water discharge, especially for rivers with lower annual water discharges (<8km^3/year). Additionally, the study reveals that rivers in temperate climates, especially those below 11°C, have more accurate discharge projections, likely due to temperatures impact on vegetation growth. The models representation of cropping locations in lower temperatures is more accurate than in hotter regions, explaining discrepancies. Similarly, rivers with high precipitation are more likely to have less projection discrepancies, which could be caused by the models crop location representation. However, where high temperature is combined with high precipitation, the discrepancy ratio of the projections is even lower than just high temperatures alone, suggesting a complex model bias for crop growth assumptions (Dunn, 2017). Important to note, WBMsed struggles to accurately represent the river discharge in the presence of dams, as extreme alterations in flow occur and predicting global dam operation magnitudes and schedules is challenging in itself (Cohen et al., 2014).

In contrast to the mean annual flow, the model underpredicts the annual peak discharge at lower discharges and overpredicts for higher discharges (Cohen et al., 2013). However, looking closer at the peak discharges, rivers with high annual water discharges (>160 km^3 per year) are more likely to have well predicted peak discharges. For rivers with low annual water discharges or when large reservoir volumes are present in the basin(>100,000km^3), peak discharges tend to be overpredicted. Indicating WBMsed not being able to appropriately capture water discharge dynamics when basins contain a large total reservoir volume, and thus is not able to accurately simulate the effect of large reservoirs on flood peaks (Dunn, 2017).

2.4.2 Anthropogenic soil erosion

One of the catchment factors introduced in the WBMsed model is the anthropogenic soil erosion factor. Inspired from Saito et al. (2007), and based on population density and Gross National Product (GNP) per capita. Dunn (2017) enabled the possibility to fluctuate this value in the projections, making the values used for the anthropogenic soil erosion factor as illustrated in Table 2.1. A problem that can arise by implementing the possibility for GNP value variability, is the abrupt changes in sediment flux projections due to slight shifts in GNP per capita. This mechanism is unrealistic, as the transition of a community to anthropogenic drivers influencing soil erosion occurs gradually (Dunn, 2017).

Table 2.1: Values of the anthropogenic factor in the WBMsed model (Dunn, 2017)

		Population Density		
		<30 per km^2	**30-140/km^2**	**>140 per km^2**
GNP per Capita	**<$2,500**	1	1	2
	$2,500-$20,000	1	1	1
	>$20,000	1	0.3	0.3

2.4.3 Sediment fluxes

Dunn (2017) made an effort to validate the projected sediment fluxes, however, there was limited reliable sediment data available. The used sediment data carried uncertainties as the quality varied and duration of observations of sediment measurements were relatively short. Most sources did not specify their methods or location even, and the coverage was often measured in years rather than decades, if the time period was even indicated at all (Dunn, 2017). On top of that, the most recent sediment data of some sources dated from Milliman and Meade (1983) or Milliman and Syvitski (1992). Due to the high uncertainty in this data, primarily the magnitude of the measurements was taken into account. The comparison showed larger overprediction than underprediction, and even errors larger than an order of magnitude away. The overprediction is no surprise considering earlier mentioned discharge overprojections. To reassess this validation and theory, a new validation with more accurate measurement data is needed to make substantiated assumptions. Ideally, the validation data consist of real-life sediment flux measurements of the specific projected deltas. As highlighted by Dethier et al. (2022) and Dunn (2017), there is a vast challenge associated with collecting such data, as many rivers lack suspended sediment observation data. Therefore, datasets derived from alternative observation methods which underwent thorough substantiation and validation using reliable methods, would be a good data source for validation. One such promising validation dataset is sourced from Dethier et al. (2022). Dethier et al. (2022) investigated historical and recent changes in suspended sediment flux in 414 major rivers worldwide, emphasizing the crucial role of sediment flux in delta sustainability and underscoring the influences of different stressors such as dams and anthropogenic influences. Concentrating on rivers >90 m at their outlet, draining areas >20,000 km^2, and utilizing satellite image analysis combined with algorithms trained on 130,000 ground truth measurements from 340 sites in North- and South America and Taiwan, the algorithm estimated accurate suspended sediment concentration for 414 global rivers from 1984 to 2020.

2.5 Data limitations

Besides the WBMsed model discrepancies, the projected sediment fluxes for global deltas are based on multiple external datasets, introducing fundamental issues in the sediment flux projections. Examples of this are the previously mentioned capability to project reliable anthropogenic factors for long-term periods or data limitations in the used climate, socioeconomic and dam datasets. The different temporal variations of the data sources used for the input and validation datasets for the model, represented in figure 2.2, and more general limitations of global climate and hydrological models, should be taken into account (Dunn, 2017; Fekete et al., 2016). These uncertainty factors highlight the need for validation of the projections made in Dunn et al. (2019), before it can be confidently used in delta morphology projections.

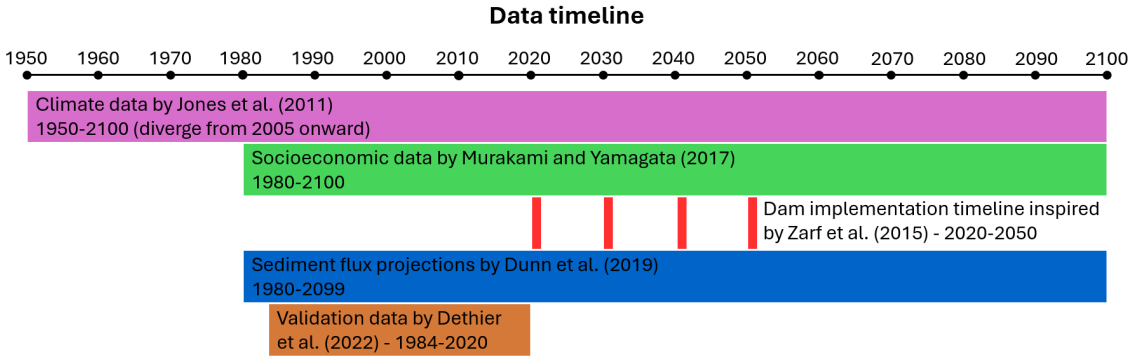

Figure 2.2: Temporal variability of different relevant datasets used in the study of Dunn et al. (2019) and this research

3. Validation method and datasets

This chapter outlines the research methodology employed to validate the global delta sediment flux projections from Dunn et al. (2019) using more recent and validated sediment flux data. The purpose of this research is to assess the accuracy, reliability, and applicability of the existing findings of Dunn et al. (2019) by systematically comparing them with data derived from an external source. A comparative research design is adopted for this study, allowing for systematic comparison of both datasets. By employing a comparative approach, this research aims to identify consistencies, discrepancies and trends between the base dataset of Dunn et al. (2019) and the validation dataset, providing a comprehensive understanding of the validity of the findings from Dunn et al. (2019).

3.1 Operational validity

Operational validity, as defined by Sargent (2010), involves determining whether the simulation model's output behaviours have the required accuracy for its intended purpose over the model's domain. In the context of the sediment flux projections, operational validity provides insight into how well the WBMsed model captures real-world patterns and behaviours (Thacker et al., 2004). With a focus on projecting sediment flux behaviour and patterns rather than precise magnitudes due to inherent uncertainties in natural systems (Refsgaard et al., 2013), the operational validity analysis is conducted mostly qualitatively with supporting quantitative details, emphasizing the model's ability to portray expected behavioural aspects.

3.1.1 Exploring model behaviour

Understanding the WBMsed models' behaviour is crucial, as it involves uncertainties and complexities inherent in natural systems. Behaviour analysis can be done qualitatively and quantitatively. Qualitative analysis focusses on output directions and if the model outputs lie within 'reasonable' intervals, aiming at the models ability to simulate expected patterns and processes. Quantitative analysis delves into numerical accuracy, providing insights into the ability of the model to precisely project exact sediment flux magnitudes (Sargent, 2010). In this study, the primary focus lies within assessing

the model's ability to depict the expected behavioural aspects of the sediment flux projections, therefore, the operational validity is conducted dominantly qualitatively with supporting quantitative analysis. To compare the models behaviour and patterns on the global delta sediment fluxes with real measurements, the datasets are graphed in various ways, including time series plots, barplots, and scatter plots. Statistical significance testing ensures the reliability of findings. Identified discrepancies trigger further validation and expert consultations, enhancing the overall study reliability. Assessing the quality of model projections involves comparing sediment flux projections with validation data. If projections lie within one order of magnitude of validation data, the model's quality is deemed 'reasonable' (Dunn, 2017). While parameter variability-sensitivity analysis and various statistical methods could enhance operational validity analyses (Sargent, 2010), the unavailability of original input data limits these aspects in this study.

3.1.2 Limitations

Acknowledging limitations is crucial for interpreting the research results in the correct context, interpreting the validity of the research and the conclusions provided. The understanding of the limitations goes beyond just listing magnitudes and directions of validation problems, but requires interpretation of the influence of potential errors on the eventual findings (Ioannidis, 2007).

One limitation is the availability and quality of the validation dataset, which might affect the depth of the comparative analysis. Additionally, differences in data collection methods between the base and validation datasets could introduce biases in validation results, compromising the consistency and accuracy or the validation analysis. Finally, validating model outputs directly with test data takes on the entire model system, which can be problematic as the model comprises multiple components with complex connections and the original input data is not accessible. If there proves to be poor agreement between the projections and the validation measurements, it is difficult if not impossible to isolate which subsystem of the model is responsible for the discrepancy (Thacker et al., 2004).

3.2 Datasets

In this section, we delve into the foundational datasets that form the backbone of our comparative study. The datasets are categorized into two main components: Base data and Validation data.

The Base Data encompasses the original dataset containing global delta sediment flux projections from Dunn et al. (2019), forming the basis of this comparative study and is the work of F.E. Dunn, the researcher and creator of the dataset. It incorporates information concerning 47 deltas with each its own directory with .csv files. The file names are the coordinates where the data is from, which is simultaneously the starting point of the delta area. In cases where deltas are fed by more than one river, there are multiple .csv files, resulting in a total of 62 different river model outputs. An overview of the 47 deltas and their river coordinates are in Appendix A. The files contain the annual sediment flux projection results over a period of 1980 to 2099 on 0.5 degree resolution, portraying 12 scenarios that combine 4 RCPs and 3 SSPs (as explained in Section 2.3.1). The direct access to the dataset and insights from F.E. Dunn ensures the authenticity and accuracy of the data used for this research.

Validation data is essential in assessing the reliability of the sediment flux projections. The validation data will consists of the suspended sediment fluxes from the study of Dethier et al. (2022), explained in 2.4.3. By validating Dunn et al. (2019) sediment flux projections with the validated historic suspended sediment fluxes by Dethier et al. (2022), the uncertainty and reliability of the projections will be evaluated. This thorough evaluation using more recent and precise sediment data will enhance our understanding of sediment delivery processes and contribute to the development of effective and sustainable management strategies.

3.3 Data Preparation

To ensure compatibility and consistency, both datasets are in need of preprocessing using Python. This involves converting the datasets into a uniform format and eliminating irrelevant data for analysis. By intersecting both datasets, common deltas or individual rivers shared by both, are identified, setting the stage for meaningful comparative analysis. Also, the individual Dunn et al. (2019) data will be statistically analysed, to determine which of the 12 scenarios will serve as the basis for validation. This process evaluates the occurrence of specific RCP and SSP combinations within the relevant time period for validation practices, aligning the projection data with the available validation data.

3.3.1 Data intersection

The Dethier et al. (2022) study incorporates a wide range of sediment flux measurements from 414 rivers, but may not include all 47 deltas and corresponding rivers from the Dunn et al. (2019) study due to potential limitations in remotely sensed imagery and field monitoring data availability. If there is a lack of overlap for certain deltas or individual rivers, they are excluded from the study. Identifying trustworthy or complete supplementary validation datasets for the missing rivers proves challenging, as freely available river discharge and suspended sediment flux records for long historical periods are extremely rare (Cohen et al., 2014).

The exclusion of specific rivers or entire deltas from the analysis due to limited availability of validation data introduces limitations to the study's findings. The lack of reliable or complete additional validation data for these missing rivers underscores the need for standardized sediment flux data collection methods across various sources to ensure consistency in global fluvial sediment data.

In tables 3.1 and 3.2, Dunn et al. (2019)'s rivers are shown alongside their corresponding validation dataset. In some cases, partial joins were conducted for Dunn et al. (2019) rivers upstream of the corresponding Dethier et al. (2022) location. These couples are the Pasak & Menam river in the Chao Phraya delta, the MacKenzie & Peel river in the Mackenzie delta, the Limpopo & Changane river in the Limpopo delta, the Magdalena & Brazo De Mompos in the Magdalena delta and the Brahmani & Baiterani river in the Mahanadi Brahmani Baiterani delta, resulting in 53 distinct Dunn et al. (2019) rivers for further analysis. For the comparative analysis, the datasets of these combined rivers are also joined. While this may introduce variability, it allows for a comprehensive comparative analysis of the datasets.

Table 3.1: Data intersection of Dunn et al. (2019) rivers with Dethier et al. (2022) data locations. Continents: AF = Africa, AS = Asia, EU = Europe, OC = Oceania, NA = North-America and SA = South-America

River Nr.	River Name(s) (Dunn et al., 2019)	Designation in Dethier et al. (2022)	Continent
1	Amazon	'Amazon'	SA
2	Amur	'Amur'	AS
3	Burdekin	'Burdekin'	AS
4	MaeKlong (Chao Phraya delta)	'MaeKlong'	AS
5	Pasak-Menam (Chao Phraya delta)	'Chao Phraya'	AS
6	BangPakong (Chao Phraya delta)	X	AS
7	Colorado	X	NA
8	Congo	'Congo'	AF
9	Ebro	'Ebro'	EU
10	Fly	'Fly'	OC
11	Meghna (Ganges Brahmaputra Meghna delta)	'Meghna'	AS
12	Ganges (Ganges Brahmaputra Meghna delta)	'Ganges'	AS
13	Brahmaputra (Ganges Brahmaputra Meghna delta)	'Brahmaputra'	AS
14	Godavari	'Godavari'	AS
15	Grijalva	X	NA
16	Han (Han delta)	'Han'	AS
17	Imijn (Han delta)	X	AS
18	Ryesong (Han delta)	X	AS
19	Indus	'Indus'	AS
20	Irrawaddy	'Irrawaddy'	AS
21	Krishna	'Krishna'	AS
22	Lena	X	AS
23	Limpopo-Changane (Limpopo delta)	'Limpopo'	AF
24	MacKenzie-Peel (Mackenzie delta)	'MacKenzie'	NA
25	Magdalena-Brazo De Mompos (Magdalena delta)	'Magdalena'	SA
26	Mahakam	'Mahakam'	AS

Table 3.2: Data intersection of Dunn et al. (2019) rivers with Dethier et al. (2022) data locations. Continents: AF = Africa, AS = Asia, EU = Europe, OC = Oceania, NA = North-America and SA = South-America

River Nr.	River Name(s) (Dunn et al., 2019)	Designation in Dethier et al. (2022)	Continent
27	Mahanadi (Mahanadi Brahmani Baiterani delta)	'Mahanadi'	AS
28	Brahmani-Baiterani (Mahanadi Brahmani Baiterani delta)	'Brahmani'	AS
29	Mekong	'Mekong'	AS
30	Mississippi	'Mississippi'	NA
31	Moulouya	'Moulouya'	AF
32	Murray	'Murray Darling'	OC
33	Niger	'Niger'	AF
34	Nile	'Nile'	AF
35	Orinoco - Caroni	X	SA
36	Orinoco - Orinoco	X	SA
37	Paraná	'Parana'	SA
38	Pearl - Xi Jiang	'Zhujiang'	AS
39	Pearl - Bei Jiang	X	AS
40	Pearl - Dong Jiang	X	AS
41	Po	'Po'	EU
42	Red	'Song Hong'	AS
43	Rhine	X	EU
44	Rhône	'Rhone'	EU
45	Rio Grande	'RioGrande'	SA
46	São Francisco	X	SA
47	Sebou	'Sebou'	AF
48	Senegal	'Senegal'	AF
49	Tana	'Tana'	AF
50	Tigris Euphrates	'Shatt el Arab'	AS
51	Tone	X	AS
52	Vistula	'Vistula'	EU
53	Volta	X	AF
54	Yangtze	'Changjiang'	AS
55	Yellow	'Huanghe'	AS
56	Yukon	'Yukon'	NA
57	Zambezi	'Zambezi'	AF

3.3.2 Dunn et al. (2019) data preparation

For the 62 distinct model outputs of Dunn et al. (2019), it is key to identify significant differences among the 12 scenario outputs and to determine which best represents the reality for the timeframe 1980-2020. Finding significant output differences between the 12 scenarios is crucial for understanding the level of variability in the model outputs and identifying potential sources of uncertainty. Additionally, comparing the scenarios can provide insights into the driving factors that have the greatest influence on delta dynamics, which can inform management strategies and adaptation plans. However, a challenge arises when the original WBMsed inputs are not available, preventing direct comparison between historical climate- and socioeconomic data, hindering the discovery of which scenario aligns best with reality. Therefore, a statistical analysis is undertaken to determine the most suitable Dunn et al. (2019) data scenario for the comparative analysis. Ensuring that the chosen scenario portrays the most accurate representation of reality.

3.3.2.1 Inter-scenario comparison

A distinctive feature of the literature on climate change and socio-economic change scenarios is the use of a 'baseline' scenario to analyse various target levels (Birkmann et al., 2015; Riahi et al., 2007). In this research, the first and final cells of the 12 scenario matrix represent opposite ends of a spectrum in terms of climate change and socio-economic challenges. By using scenario one as baseline, the other eleven scenarios can be assessed in relation to it. This approach streamlines the comparison process, providing a clear understanding of the most extreme differences possible between scenarios. Absolute differences are transformed into relative differences, facilitating a comprehensive comparison and analysis of inter-scenario differences for individual rivers. Statistical outliers are crucial in identifying abnormal inter-scenario differences. Outliers are data points that significantly deviate from the norm and therefore provide valuable insights into the potential impacts of socio-economic and climate challenges on individual river systems (Aguinis et al., 2013). To identify these outliers, three widely employed techniques are used: histograms, the standard deviation, and a quantile-quantile plot (Q-Q plot) for visual and quantitative inspection (Ghasemi & Zahediasl, 2012). These techniques help visualize the distribution of inter-scenario differences and determine which values are more likely to appear if the sediment flux projection dataset is expanded. During this analysis the period 1980-2020 is used from the Dunn et al. (2019) data to represent the validation period.

Visual inspection

The initial step in visual inspection involves constructing a histogram (Figure 3.1), containing intervals representing the inter-scenario differences for all data points of scenarios 2-12, with the base scenario 1. Within these intervals, the height of the vertical bar represents the number of datapoints which hold inter-scenario differences within the particular intervals. Notably, the interval between -10% and +10% holds the highest number of datapoints, 27526 from the total of 27962, with each 62 rivers spanning 41 years (1980-2020) and containing 11 inter-scenario values.

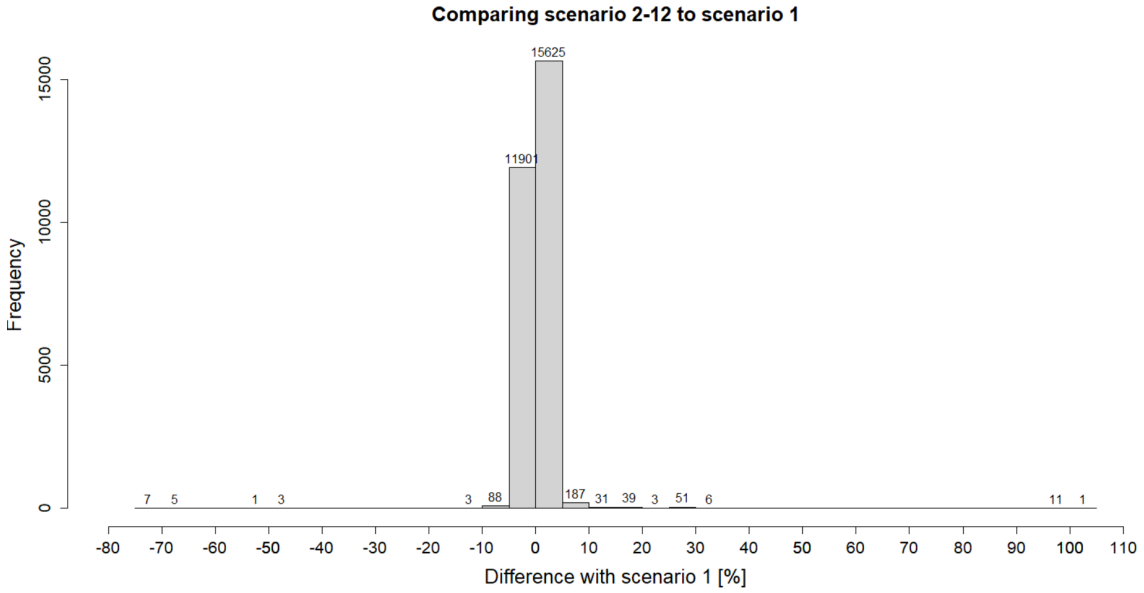

Figure 3.1: Relative inter-scenario differences of scenario 2-12 with base scenario 1 for annual data for all 62 rivers.

While the histogram in Figure 3.1 provided insights into data distribution, its shape is influenced by the chosen number of bins. To refine the data distribution shape, we create a probability density function (PDF) displayed in Figure 3.2 (Scott, 2015). The PDF describes likelihood observing a certain outcome from a data-generating process (Grinstead & Snell, 2006). Each black line along the x-axis represents a measured inter-scenario difference value in the Dunn et al. (2019) dataset for the period 1980-2020.

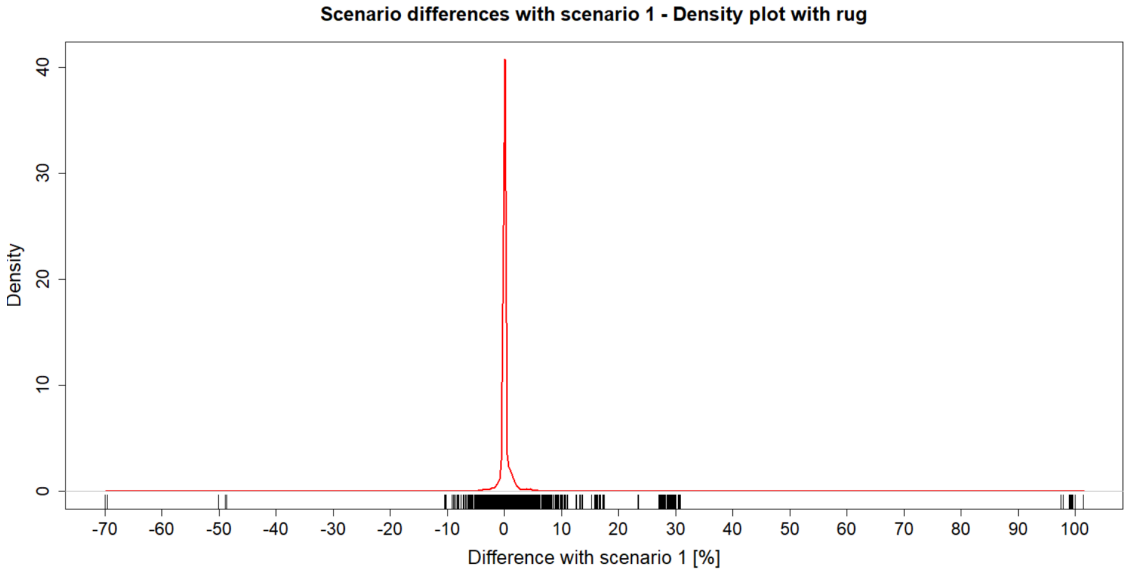

Figure 3.2: Probability density function of the relative inter-scenario differences of scenario 2-12 with base scenario 1 for annual data for all 62 rivers.

In the context of this research, the density plot provides a visual representation of the distribution of differences between inter-scenario sediment flux projections in the projection dataset of the interval 1980-2020. By examining the density plot, we can gain insights into the likelihood of observing certain outcomes and identify which values are more probable compared to others. Suggesting that when expanding the dataset globally, for 1980-2020, the relative inter-scenario differences in projected sediment flux are likely to fall between -10% and 10% with a concentration around the 0

Looking at the histogram and PDF, it seems that the sediment flux projections for the 62 rivers in the period 1980-2020 portrays a steep normal distribution. To test this assumption, a Quantile-Quantile (Q-Q) plot is constructed and displayed in Figure 3.3. It illustrates the correlation between the datasets and a normal distribution (Ford, 2015), plotted along the ideal match reference line.

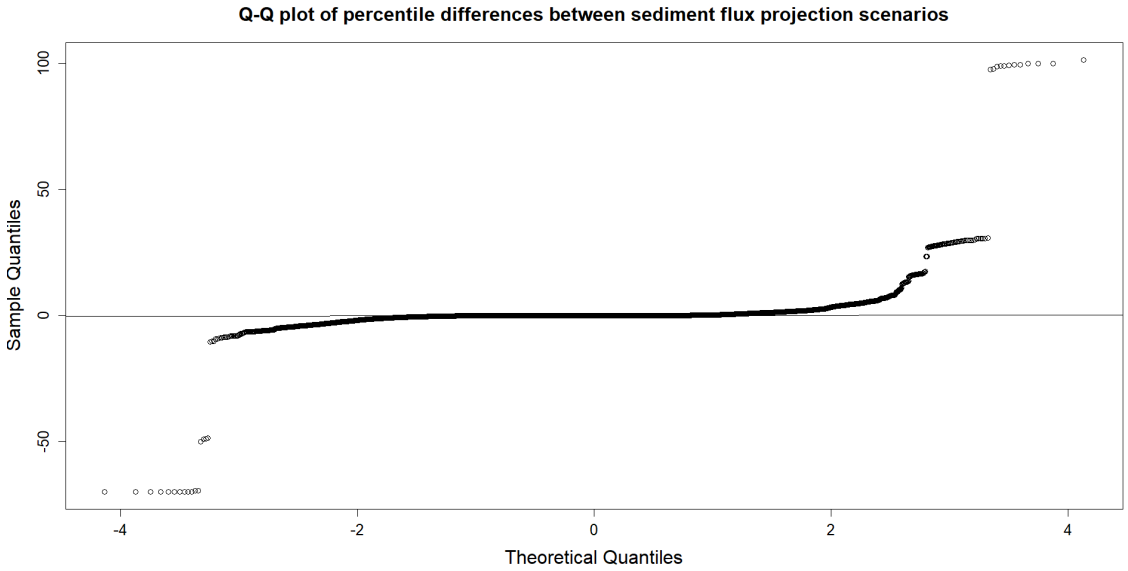

Figure 3.3: Quantile-quantile plot of relative inter-scenario differences for annual sediment flux projections for the period 1908-2020 for 62 rivers

Notice the points fall along the reference line in the middle of the graph, but curve off in the extremities. Normal Q-Q plots that exhibit this behaviour usually suggest the data possesses more extreme values than would be expected if they truly came from a normal distribution (Ford, 2015). These extreme values are exactly what we want to look further into because extreme values in the delta datasets mean that within a certain year, for a certain river, there is an abnormally large inter-annual difference between delta flux scenarios.

From the Q-Q plot and the histogram, we assume that the mutual difference within the sediment delta flux projections from Dunn et al. (2019), follow a steep normal distribution with extreme values at the tails. To identify the extreme scenario difference values, the standard deviation from the normal distribution is used. According to Streiner (1996) and Altman and Bland (2005), the Standard Deviation (SD) is an index of the variability of the original data points, it is an index of how closely the individual data points cluster around the mean.

Standard deviation formula (Wan et al., 2014):

$$S = \left[\sum_{i=1}^{n} \frac{(X_i - \bar{X})^2}{(n-1)} \right]^{1/2} \tag{3.1}$$

Where $\bar{X}$ is the Arithmetic mean of the observations, X the certain value in the data distribution, and n the number of observations.

Table 3.3: Outcomes calculation Standard Deviation and outliers

Mean	0.202
Standard deviation	3.163
Large outliers (extreme values > 3*SD)	145
Small outliers (extreme values < 3*SD)	19
Total number of outliers	164

Due to the large dataset and small standard deviation (Table 3.3), meaning that there is a high concentration of the data points around the mean, the rule of using three standard deviations to find extreme values is applied. A value that falls outside $+-$ three standard deviations, which consist of 99,7% of all data points, is part of the distribution but it is an unlikely or rare event. These values are applied to the dataset and visualised in Figure 3.4.

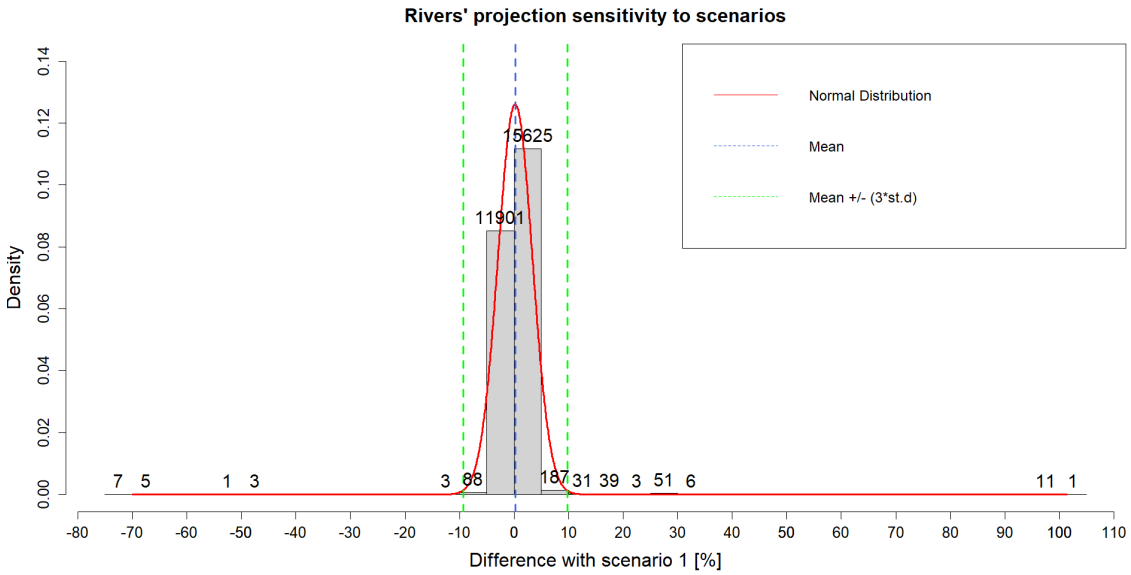

Figure 3.4: Overview of the relative inter-scenario differences for 62 rivers for the period 1980-2020

The results show 145 data points >3SD and 19 data points <3SD, indicating 164 extreme values in the sediment flux projections of the 47 deltas, accounting for 0.59% of all inter-annual scenario values. The presence of these extreme values shows that for some deltas, certain scenarios have an extreme impact on the sediment flux projections when compared to scenario 1. The delta rivers which pose extreme values are: Dong Jiang, Changane, Han, Imijn, Limpopo, Mahanandi, Meghna, Rio Grande, Sebou and Tigris.

Among these 10 delta rivers, the extreme values manifest in two distinct ways. Firstly, some outliers occur in just one or two years of the dataset and are associated with Specific Scenario Pathways (SSP), shown by the fact that the 4 scenarios belonging to a specific SSP scenario, show large extreme outliers. When looking at these sudden isolated shifts, it suggests that the responsible socio-economic values surpassed a threshold into a new category on the GDP table, influencing sediment projections. The robustness of this theory is challenged by instances where SSP2 induces outliers, while SSP1 and SSP3 do not exhibit similar patterns. This discrepancy is illogical given that SSP2 depicts the intermediate challenges, suggesting that SSP1 or SSP3 would surpass a certain threshold prior to SSP2. This inconsistency suggests issues in the SSP input data for sediment flux projections in Dunn et al. (2019). This theory is substantiated by the fact that in all other years the sediment flux projections don't show outstanding values. The inconsistency of the SSP input data is also substantiated by the fact that for the concerning datasets, a single SSP is one or two years ahead of the other SSP's in their values, therefore, in those specific instances, the extreme values are removed from the dataset. After removal of the outliers linked to the single varying SSP years, the reliability of the dataset is restored and data distortions caused by inconsistent SSP input data is minimized.

Other observed outliers are RCP bound, represented by the fact that the extreme values in the dataset are for multiple years and are repeated in the same RCP bound scenarios. These RCP-related outliers arise due to variations in global climate data influenced by factors like geographical location, topography, and regional climate patterns. These factors contribute to the different rates and intensities of climate change experienced globally. Consequently, for different deltas, climate change has a more outspoken influence on the sediment flux projections for the different scenarios, resulting in larger mutual differences between the sediment flux projections. This phenomenon is especially prominent in the later 2010s as the difference between the RCPs become more prominent. The varied representations of the outliers in different rivers are detailed in Table 3.4, while their global positions are visualised in Figure 3.5, with the Category 2 and Category 3 rivers annotated.

Table 3.4: Categorization (Cat.) of inter-scenario comparison of individual rivers with characteristics (Char.)

Cat.	Char.	Datasets
1	No outliers in individual delta dataset	Amazon, Amur, Baiterani, Bang Pakong, Beijiang, Brahmani, Brahmaputra, Brazo De Mompos, Burdekin, Caroni, Colorado, Congo, Ebro, Fly, Ganges, Godavari, Grijalva, Indus, Irrawaddy, Krishna, Lena, Mackenzie, MaeKlong, Magdalena, Mahakam, Mekong, Menam, Mississippi, Moulouya, Murray, Niger, Nile, Orinoco, Paraná, Pasak, Peel, Po, Red, Rhine, Rhône, Ryesong, São Francisco, Senegal, Tana, Tone, Vistula, Volta, Xijiang, Yangtze, Yellow, Yukon, Zambezi
2	1 or 2 years in the individual delta dataset holds outliers on SSP base	Dong Jiang, Han, Imijn, Mahanadi, Meghna, Sebou
3	Multiple outliers with a shown dependence on climate change	Changane, Limpopo, Rio Grande, Tigris

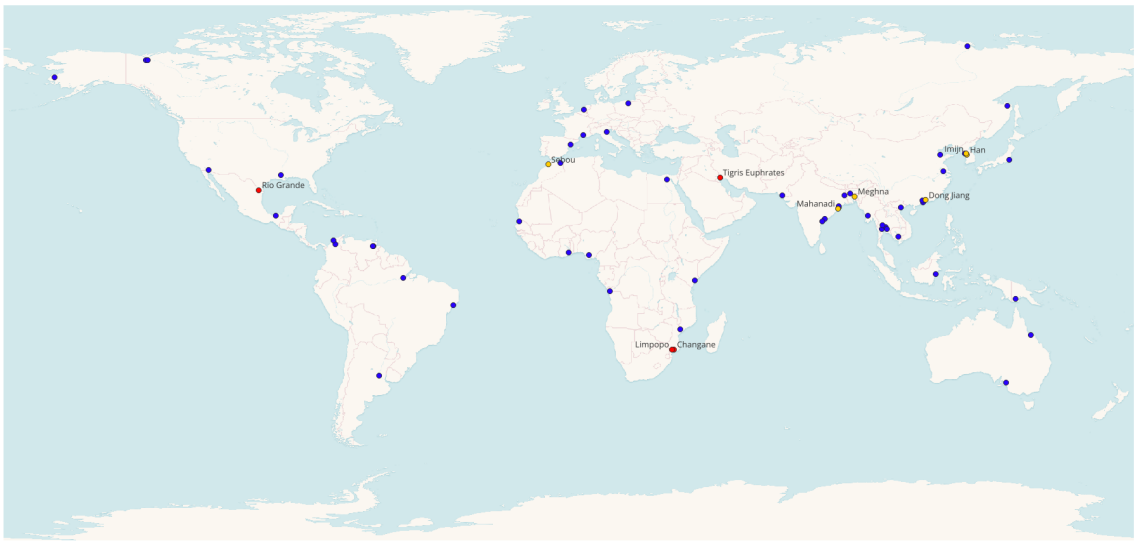

Figure 3.5: Visualisation of relative inter-scenario difference categorisation of individual rivers. Green: Category 1 river, Orange: Category 2 river and Red: Category 3 river.

Managing the varied represented outliers depends on their characteristics. Category 1 rivers do not possess any remarkable inter-scenario differences for their projected sediment fluxes, therefore the 12 scenarios are averaged to represent one sediment flux value per year per river. In Category 2, the outliers on the SSP base are removed because they are linked to inconsistencies in the SSP input data, and the 12 scenarios are averaged to represent one sediment flux value per year per river. By removing these outliers, the dataset becomes more reliable for analysis and minimizes distortions or biases caused by the inconsistent SSP input data. In Category 3, the 12 scenarios are reduced to averaged 4 RCP scenarios because these rivers show a higher sensitivity to different RCP scenarios. Due to the limitations in consulting local historic climate changes, comparing the RCP scenarios to validation data allows for the selection of the best fitting scenario sediment flux projection data. For the deltas of Category 3, the RCP scenario with the lowest mean absolute difference will be used in the comparative analysis, ensuring that the comparative analysis is based on the most accurate and reliable data, of which the results are displayed in Table 3.5. Showing the use of RCP2.6 for Limpopo-Changane and Rio Grande, and RCP8.5 for TigrisEuphrates. By using the scenario that closely matches the validation dataset, the results of the analysis will be more relevant. This approach reduces the potential for discrepancies between the projections and the observed sediment dynamics.

Table 3.5: Mean absolute and percentile differences of the four RCP scenarios of Category 3 deltas, with the validation data.

	Mean difference with validation dataset [Mt/a]			
Delta	**RCP2.6**	**RCP4.5**	**RCP6.0**	**RCP8.5**
Limpopo-Changane	3.023 (+114.71%)	3.025 (+114.80%)	3.225 (+122.36%)	3.414 (+129.55%)
Rio Grande	0.430 (+122.37%)	0.443 (+126.09%)	0.441 (+125.52%)	0.494 (+140.63%)
TigrisEuphrates	35.932 (+1667.11%)	35.516 (+1647.8%)	35.960 (+1668.33%)	35.427 (+1643.67%)

By completing the necessary preparations, the Dunn et al. (2019) data is now ready for comparative analysis. The data has been reduced to single sediment flux values for each of the 43 rivers, covering the period from 1984 to 2020. These single values provide a concise representation of the sediment flux projections for each river, allowing for easier comparisons and analysis of the data.

4. Validating the accuracy of the projections

In this section, the results are presented of the validation process conducted to assess the reliability of the global delta sediment flux projections from Dunn et al. (2019). The validation aims to assess the agreement of the projections with the validation dataset of Dethier et al. (2022), and the overall consistency between the datasets. The focus extends beyond numerical comparisons, emphasizing a qualitative analysis that delves into the trends and behaviours of the datasets. Statistical tests are used to substantiate the validation process, but not as a validation analysis technique.

4.1 Absolute magnitudes

The first step in the validation process is to create an overview of the absolute measurement plots illustrating the raw data of the projections and the real-life measurements for the individual rivers. The rivers are displayed in Figures 4.1, 4.2, 4.3, 4.4, 4.5 and 4.6, divided in their respective continents.

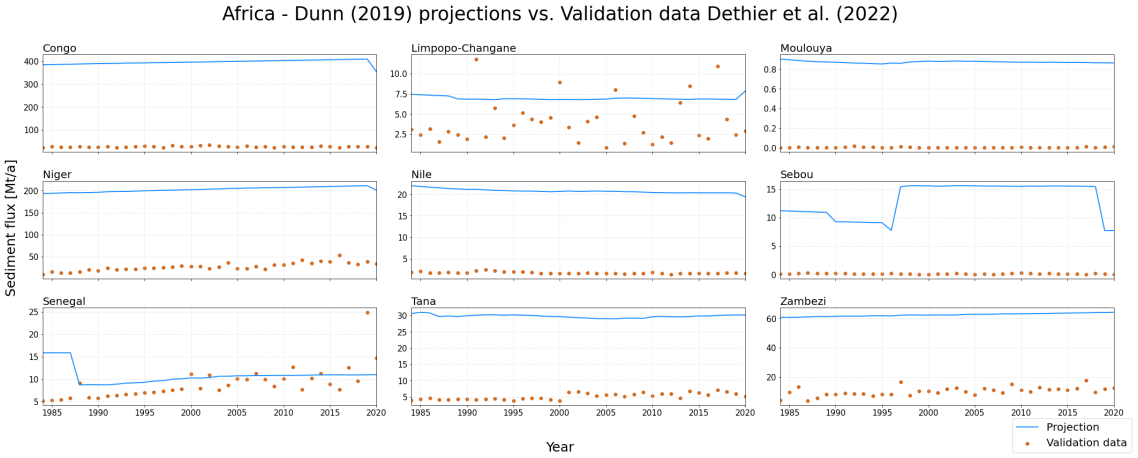

Figure 4.1: Absolute magnitudes of Dunn et al. (2019) projections and of the validation data of Dethier et al. (2022) for rivers in Africa

Figure 4.2: Absolute magnitudes of Dunn et al. (2019) projections and of the validation data of Dethier et al. (2022) for rivers in Asia

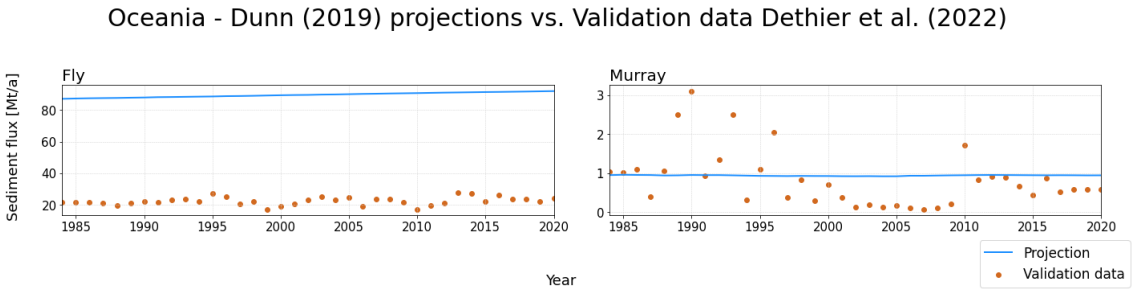

Figure 4.3: Absolute magnitudes of Dunn et al. (2019) projections and of the validation data of Dethier et al. (2022) for rivers in Oceania

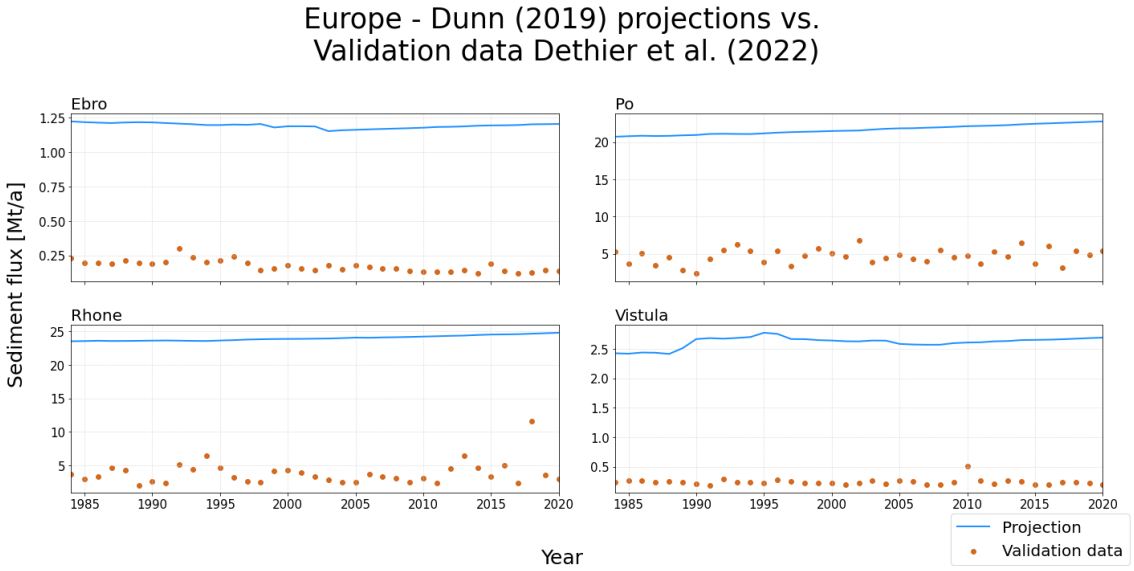

Figure 4.4: Absolute magnitudes of Dunn et al. (2019) projections and of the validation data of Dethier et al. (2022) for rivers in Europe

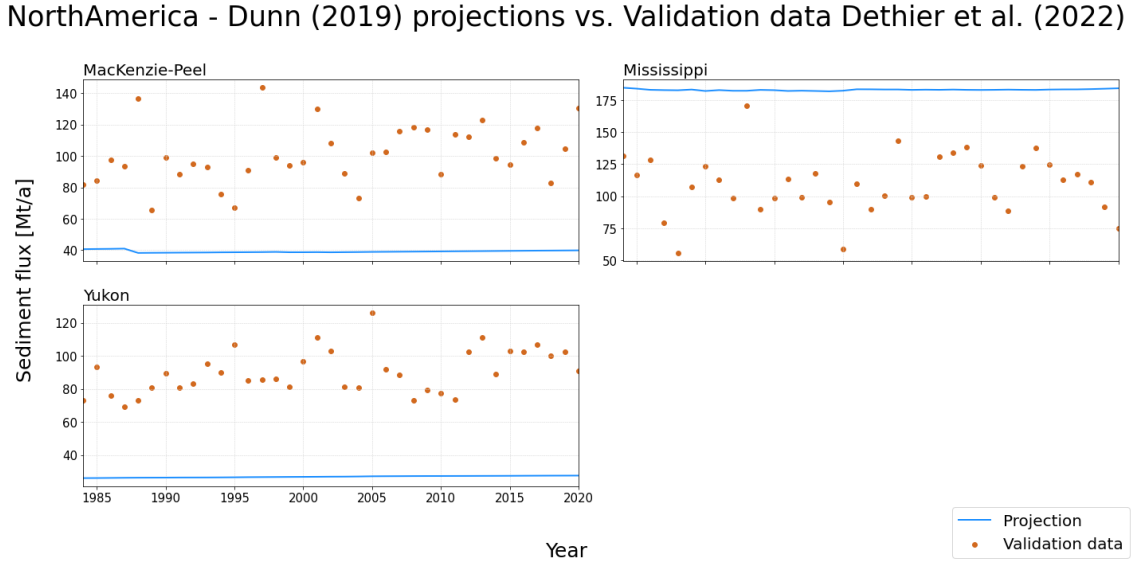

Figure 4.5: Absolute magnitudes of Dunn et al. (2019) projections and of the validation data of Dethier et al. (2022) for rivers in North-America

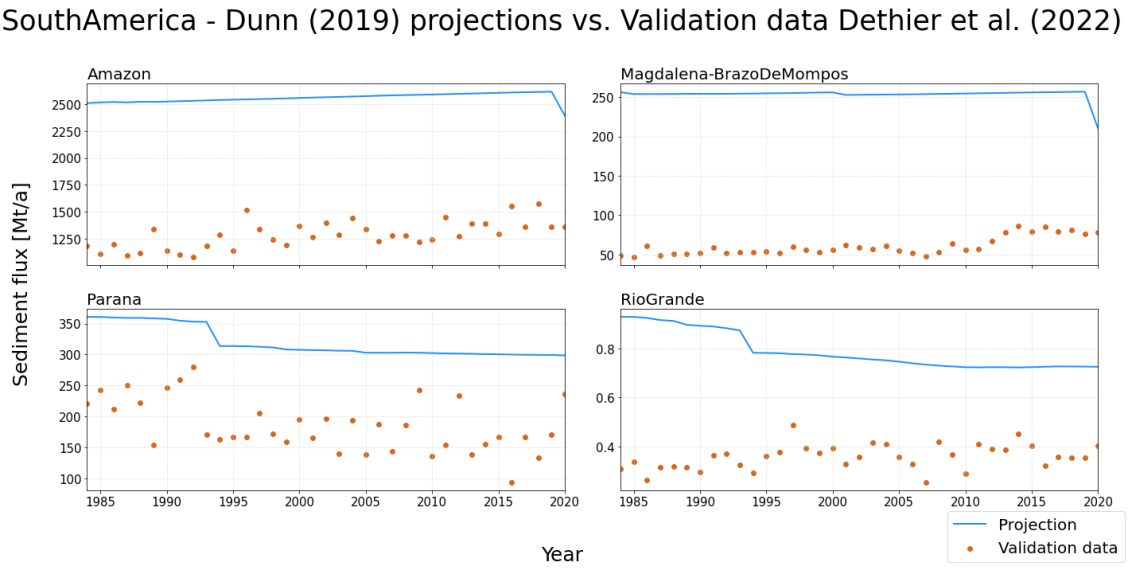

Figure 4.6: Absolute magnitudes of Dunn et al. (2019) projections and of the validation data of Dethier et al. (2022) for rivers in South-America

In analysing the raw data plots of the projections and the validation data, three observations stand out:

Inter-annual Variability

The projections exhibit a remarkable inter-annual variability, displaying abrupt changes in sediment flux from one year to another. This characteristic is at odds with the expected behaviour of natural fluvial systems, where sediment fluxes tend to change gradually over time. The unnaturally sharp fluctuations in Dunn's projections raise concerns about the model's ability to capture the gradual and more continuous nature of sediment transport in reality. These sharp annual fluctuations are probably related to a number of possibilities. First being the Anthropogenic factor that can shift inter-annually to another threshold, influencing the sediment flux projections suddenly. Another influence can be that certain dams are being introduced in a certain year. This will suddenly dramatically decrease the sediment flux in the river. Also from 2010 onwards, the RCPs begin to deviate, increasing climate influence on the sediment projections suddenly.

Overall Sediment Flux Discrepancies

The projections often significantly overpredict, and sometimes underpredict the overall sediment flux. While there may be structural similarities between the projections and real-life measurements, the projections are almost in every instance located far above or below the validated observations in the plot. This over- and underprediction lacks a structured pattern, making it challenging to quantify precisely how much the projections deviate from actual measurements. This suggests a need for refinement in the model to

bring it in closer agreement with real-world sediment flux dynamics.

Timing Discrepancies

An additional noteworthy observation pertains to timing discrepancies in the projections. There are instances where the model inaccurately projects sudden drops or increases in sediment flux, which do not align with the gradual changes observed in reality. Conversely, there are cases where the initial projection deviates significantly from actual measurements, but subsequent adjustments lead to a sudden alignment with the observed data. These timing irregularities underscore the complexity of accurately capturing the temporal dynamics of sediment transport in the model.

To conclude, the Absolute Measurements Plot highlights substantial challenges in the accuracy of Dunn's sediment flux projections, particularly in terms of inter-annual variability, overall sediment flux discrepancies, and timing inaccuracies. These findings emphasize the necessity for further validation analysis to get a more nuanced understanding of the level of similarity between the projections and real-life events.

4.2 Euclidean distance

The Euclidean distance is a widely used technique to measure dissimilarity between time series of the same time lengths. It is a straightforward measure, calculating the distance between two time series as the straight-line distance between matching time points based on a distance metric. As we are calculating the distance and not direct similarity, a smaller distance suggests more similarity between the timeseries (Barrett, 2005; Ding et al., 2008; Faloutsos et al., 1994; Jiang et al., 2019; Puri et al., 2022). The Euclidean distance is parameter-free and requires minimal computation, making it suitable for large datasets. Also, as presented by Ding et al. (2008), the Euclidean distance is competitive to other more complex approaches, especially with large datasets.

$$\text{Euclidean distance} = \sqrt{\sum_{i=1}^{n} (x_i - y_i)^2} \tag{4.1}$$

There are two facts making this method problematic. Firstly, the Euclidean distance is sensitive to outliers and is strongly influenced by scale differences between the two time series datasets, therefore many statisticians recommend normalizing the data (Stoddard, 1979). Otherwise the variables measured in large valued units will dominate the computed dissimilarity. The second problem is that there is no set value for the maximum distance, making the similarity between the datasets hard to target as 'good' or 'bad'.

To achieve reliable interpretation about the degree of similarity between the projections and the validation data, the initial used data and resultant Euclidean distance need to be transformed into a 0-1 metric using a strictly linear method. This rescaling is achieved by using the maximum possible distance observable between the two datasets at a certain year for each individual river, referred to as *md* (Barrett, 2005). The rivers are individually normalised due to large magnitude scale differences between rivers and the fact that we want to analyse possible structured proportional dissimilarity embedded in the projections.

The particular maximum observable discrepancy at a certain year is then used to initially normalise the individual squared discrepancy of the Euclidean distance calculation for each individual river. Then the square root of the sum of these normalised squared values represent the raw Euclidean distance of these normalised values:

$$\text{Raw Euclidean distance } = \sqrt{\sum_{i=1}^{n} \frac{(x_i - y_i)^2}{md_i{}^2}} \tag{4.2}$$

The final step to scale back the Euclidean distance itself to a metric between 0 and 1.0, the scaled squared discrepancies are divided by the square root of the number of data points in the individual datasets (v), which is constantly 37 in this case for the time period 1984-2020:

$$\text{Scaled Euclidean distance } = \frac{\sqrt{\sum_{i=1}^{n} \frac{(x_i - y_i)^2}{md_i{}^2}}}{\sqrt{v}} \tag{4.3}$$

Formulas from Barrett (2005)

The resulting metrics represent scaled Euclidean distances, capturing the dissimilarity between both the projected and validation time series for the individual rivers. Where 1 would mean the maximum dissimilarity between datasets, meaning a consistent maximum observed distance across the scaled datasets, while values closer to 0 show that the majority of the time series data are closer to the validation data compared to the maximum observed distance. Scaling all Euclidean distances of individual rivers ensures direct comparability.

Table 4.1: Scaled Euclidean distances between the projections and validation dataset

River nr.	River name	Scaled Euclidean Distance (0-1)
1	Amazon	0.831176419
2	Amur	0.369617725
3	Brahmani-Baiterani	0.59349487
4	Brahmaputra	0.764167409
5	Burdekin	0.325435311
6	Congo	0.954702773
7	Ebro	0.92281828
8	Fly	0.896613286
9	Ganges	0.518386791
10	Godavari	0.593472567
11	Han	0.549976293
12	Indus	0.486701125
13	Irrawaddy	0.687324145
14	Krishna	0.676439912
15	Limpopo-Changane	0.576728769
16	MacKenzie-Peel	0.611246999
17	MaeKlong	0.487527591
18	Magdalena-BrazoDeMompos	0.921477023
19	Mahakam	0.909825817
20	Mahanadi	0.270524058
21	Meghna	0.904082471
22	Mekong	0.732752311
23	Mississippi	0.598057771
24	Moulouya	0.963430173
25	Murray	0.33035611

Continued on next page

Table 4.1: Scaled Euclidean distances between the projections and validation dataset (Continued)

26	Niger	0.871648809
27	Nile	0.922377283
28	Parana	0.515869783
29	Pasak-Menam	0.400284905
30	Po	0.832087126
31	Red	0.340166487
32	Rhone	0.891340487
33	RioGrande	0.656494708
34	Sebou	0.858462956
35	Senegal	0.282391465
36	Tana	0.906800953
37	TigrisEuphrates	0.753173716
38	Vistula	0.920183467
39	Xijiang	0.37231285
40	Yangtze	0.280639309
41	Yellow	0.427983539
42	Yukon	0.646852909
43	Zambezi	0.865091183

This type of dissimilarity analysis does not disclose the magnitude of the differences, however, our focus is on identifying consistent dissimilarity ranges or structures between projections and observations. As can be observed in table 4.2, there is a large range of values, meaning there is no consistent dissimilarity between the projections from Dunn et al. (2019) and the validation data of Dethier et al. (2022), suggesting there is no structured dissimilarity between datasets. However, Dunn (2017) already suspected that discharge is at the core of possible anomalies in the projections, stating "The results from rivers with naturally low discharge, high temperature or low precipitation need to be treated with caution". To explore this theory, we can use the individually calculated Euclidean distances to explore connections between structural dissimilarity in the datasets and the dif-

ferent input variables used by Dunn et al. (2019) to model the sediment flux projections. Unfortunately, as stated before, the original input data is unavailable, but there are a few averages of the WBMsed input data recorded per delta: Delta Area (km^2), Delta Area Average Temperature (°C), Delta Area Average Precipitation (mm/year), Delta Population (millions), Delta GNP (bnUS$2005/year) and the estimated water discharge value (km^3/a). To test if the statement of Dunn is true, the estimated water discharge value (km^3/a) is plotted against the Euclidean distances in Figure 4.7.

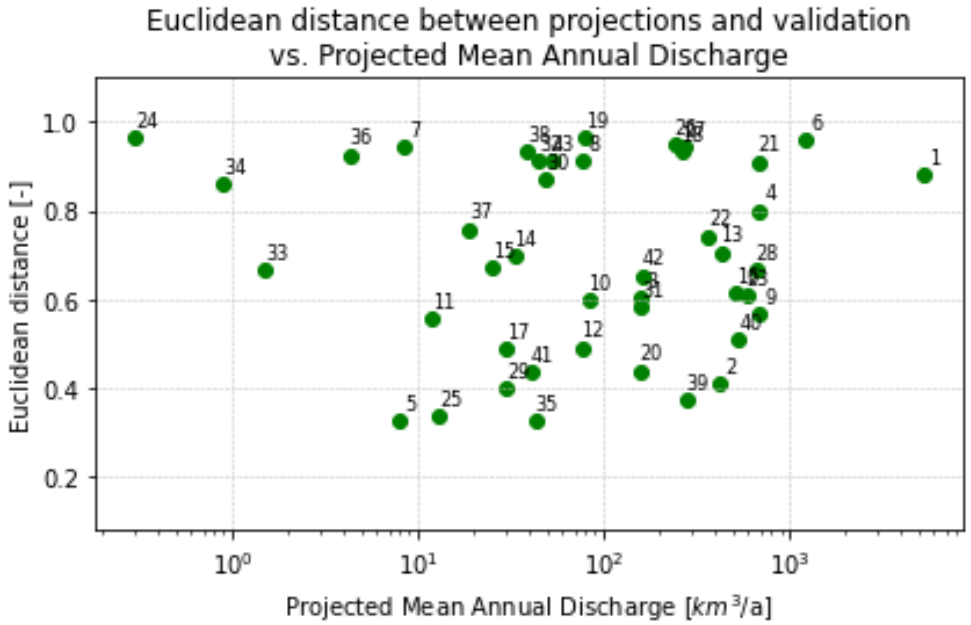

Figure 4.7: Scaled Euclidean distances plotted against the average annual discharge of the individual rivers: 1)Amazon, 2)Amur, 3)Brahmani-Baiterani, 4)Brahmaputra, 5)Burdekin, 6)Congo, 7)Ebro, 8)Fly, 9)Ganges, 10)Godavari, 11)Han, 12)Indus, 13)Irrawaddy, 14)Krishna, 15)Limpopo-Changane, 6)MacKenzie-Peel, 17)MaeKlong, 18)Magdalena-BrazoDeMompos, 19)Mahakam, 20)Mahanadi, 21)Meghna, 22)Mekong, 23)Mississippi, 24)Moulouya, 25)Murray, 26)Niger, 27)Nile, 28)Parana, 29)Pasak-Menam, 30)Po, Z1)Red, 32)Rhone, 33)RioGrande, 34)Sebou, 35)Senegal, 36)Tana, 37)TigrisEuphrates, 38)Vistula, 39)Xijiang, 40)Yangtze, 41)Yellow, 42)Yukon, 43)Zambezi

We observe at the lower discharge values higher Euclidean distance values. However at higher discharges there are both relatively high and low Euclidean distances observed, indicating there is no structural dissimilarity to be observed related to the projected mean annual discharge. Also, when plotting the Euclidean distance against the other available variables that influence the eventual sediment flux projections of Dunn, there was no structural connection between the dissimilarity of the datasets with any of the variables used in WBMsed by Dunn (2017), of which the plots are in Appendix B. Therefore, further qualitative validation analysis is needed on the similarity of the projections versus the validation measurements.

4.3 Mean absolute differences

To provide insight into the overall magnitude similarity performance of the Dunn's sediment flux projections, a mean absolute difference bar chart is displayed in Figure 4.8. Showcasing the mean differences between the projections and the validation data for each individual river, illustrating how much Megatons[Mt] the projections are in their entirety over- or underestimated.

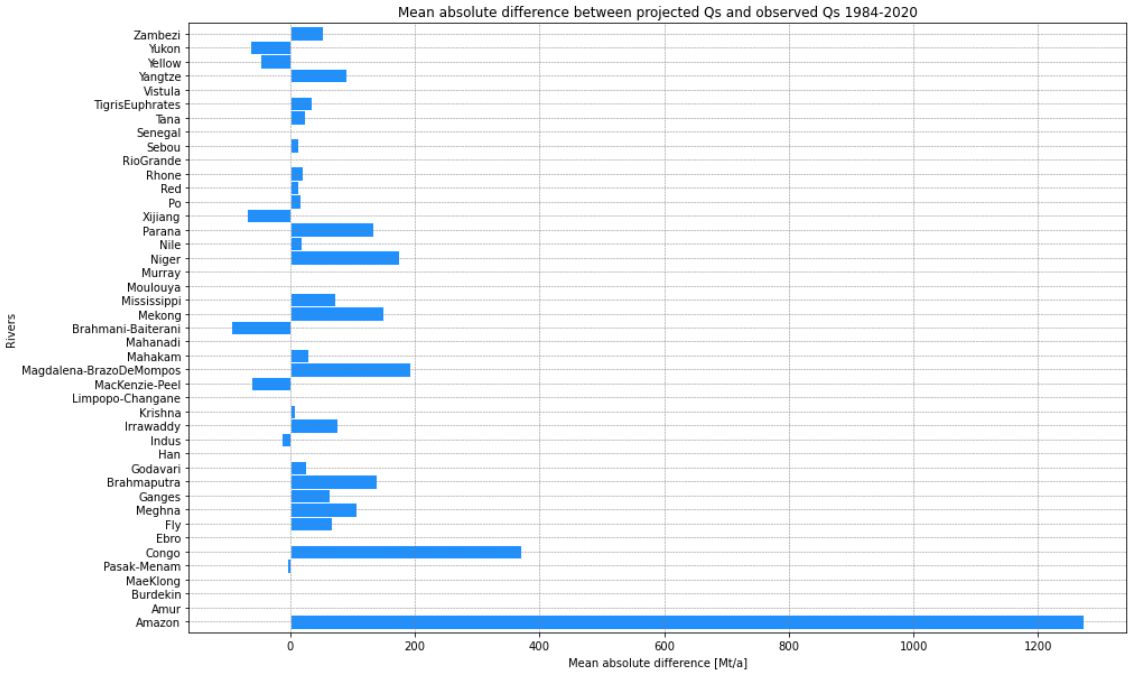

Figure 4.8: Barchart on the mean absolute difference between the projections and validation data in Megaton.

The barchart illustrates that the mean absolute differences between the projections and measurements vary in direction. While only 8 rivers show negative differences, indicating underprediction by the model, the majority of 35 rivers exhibit positive differences, confirming an overall tendency of overpredicting sediment fluxes by the WBMsed model. This confirmation has implications for model reliability, indicating a potential need to adjust model parameters to cancel out the overprediction. The dispersion in magnitudes of the mean absolute differences highlights the complexity of the overprediction of the WBMsed model, emphasizing the difficulty in isolating the causes for overprediction and the universal difficulty in capturing the diverse dynamics of sediment transport in different river systems. Further effort in understanding the patterns and magnitudes of projection inaccuracies is necessary to improve the capabilities of the WBMsed model in usage of projecting accurate sediment fluxes for global deltas.

4.4 Average annual sediment fluxes

As the overprediction characteristic of the WBMsed model is established, it is important to understand if these overpredicted magnitudes are relatively significant. The scatterplot in Figure 4.9 compares the projected average annual sediment fluxes versus the observed average annual sediment fluxes, providing insight into their relative difference.

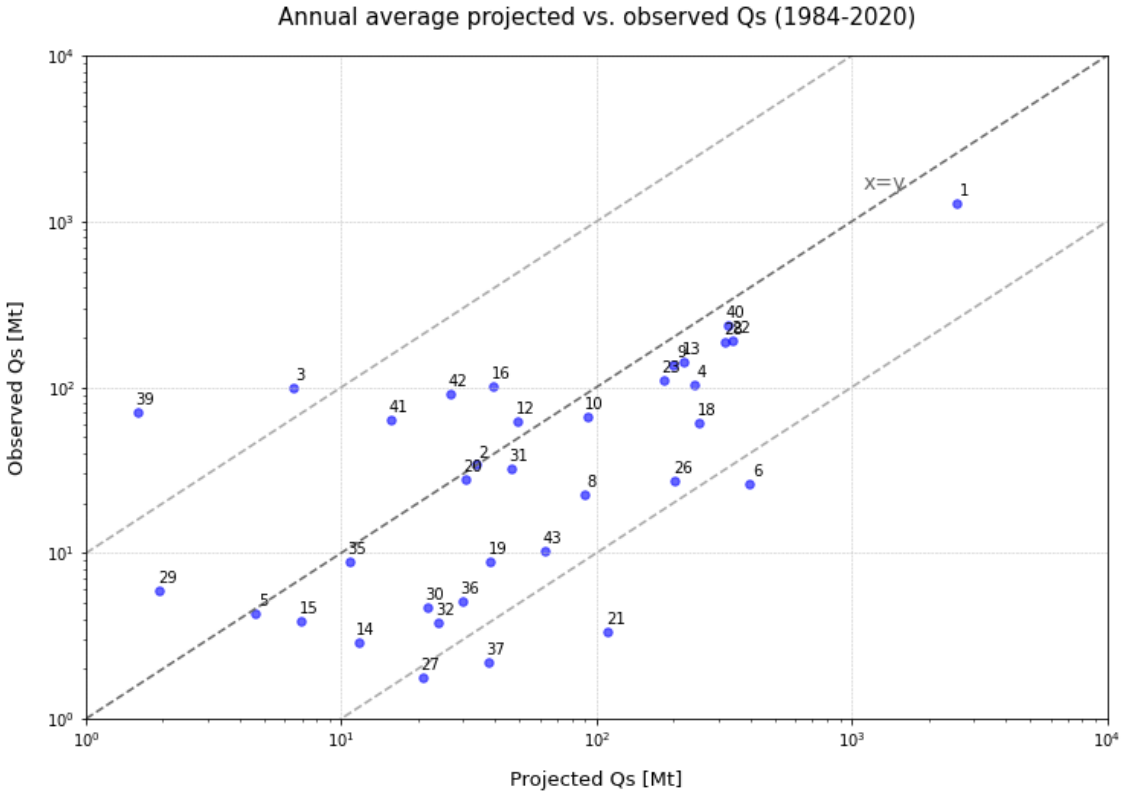

Figure 4.9: Average annual sediment flux projections versus the average annual sediment flux observations for the individual rivers: 1)Amazon, 2)Amur, 3)Brahmani-Baiterani, 4)Brahmaputra, 5)Burdekin, 6)Congo, 7)Ebro, 8)Fly, 9)Ganges, 10)Godavari, 11)Han, 12)Indus, 13)Irrawaddy, 14)Krishna, 15)Limpopo-Changane, 6)MacKenzie-Peel, 17)MaeKlong, 18)Magdalena-BrazoDeMompos, 19)Mahakam, 20)Mahanadi, 21)Meghna, 22)Mekong, 23)Mississippi, 24)Moulouya, 25)Murray, 26)Niger, 27)Nile, 28)Parana, 29)Pasak-Menam, 30)Po, Z1)Red, 32)Rhone, 33)RioGrande, 34)Sebou, 35)Senegal, 36)Tana, 37)TigrisEuphrates, 38)Vistula, 39)Xijiang, 40)Yangtze, 41)Yellow, 42)Yukon, 43)Zambezi, with reference lines: black) y=x and grey) y=0.1x and y=10x

In this study we established the qualitative threshold of one order of magnitude. If the average annual sediment fluxes of the projections lie within one order of magnitude or the average annual sediment fluxes of the validation data, the overprediction characteristic of the model is not labelled as a 'bad' projection. Solely looking at the average annual sediment fluxes, the projection performance for 37 out of 43 rivers is within one degree of magnitude margin and is thus an encouraging indication of the models

multi year average projection capabilities. While the scatterplot highlights the acceptable overall projection performance, the significant variation in relative differences among the rivers without a consistent bias, encourages further investigation. Also, while the over-predicting characteristic of the WBMsed model might look acceptable in the scatterplot above, its lack of trend and consisting of averages, makes it essential to investigate possible causes for these variations in the projections before the model is applicable for deltas globally.

4.5 Inter-annual variations

To gain a more detailed understanding, the analysis delves into annual fluctuations, focusing on mean inter-annual changes for each river. Aiming to uncover patterns in the model's ability to capture fluctuations in sediment flux on a yearly basis. The mean inter-annual variations of the projections are plotted against the mean inter-annual variations of the validation data in Figure 4.10.

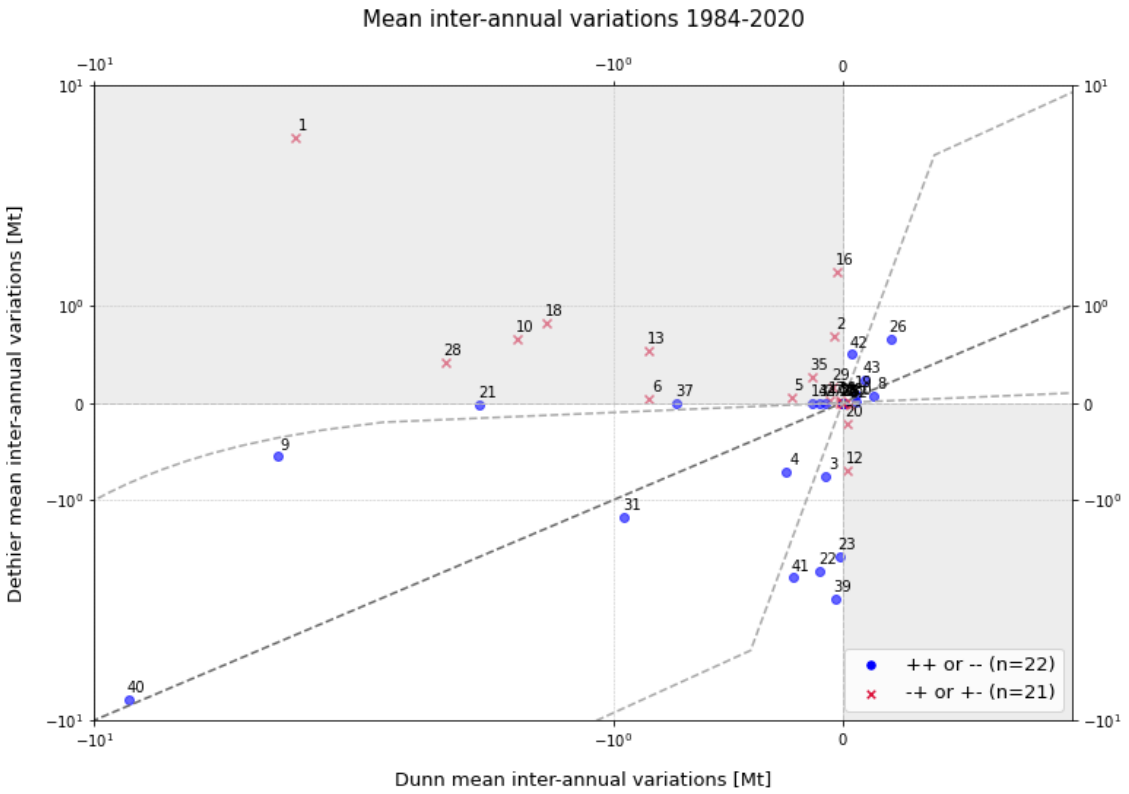

Figure 4.10: Mean inter-annual changes for all individual rivers: 1)Amazon, 2)Amur, 3)Brahmani-Baiterani, 4)Brahmaputra, 5)Burdekin, 6)Congo, 7)Ebro, 8)Fly, 9)Ganges, 10)Godavari, 11)Han, 12)Indus, 13)Irrawaddy, 14)Krishna, 15)Limpopo-Changane, 6)MacKenzie-Peel, 17)MaeKlong, 18)Magdalena-BrazoDeMompos, 19)Mahakam, 20)Mahanadi, 21)Meghna, 22)Mekong, 23)Mississippi, 24)Moulouya, 25)Murray, 26)Niger, 27)Nile, 28)Parana, 29)Pasak-Menam, 30)Po, Z1)Red, 32)Rhone, 33)RioGrande, 34)Sebou, 35)Senegal, 36)Tana, 37)TigrisEuphrates, 38)Vistula, 39)Xijiang, 40)Yangtze, 41)Yellow, 42)Yukon, 43)Zambezi, with reference lines: black) y=x and grey) y=0.1x and y=10x

For the similarity between the projections and the validation data being assessed as 'reasonable', again the threshold of one order of magnitude above or below the y=x line is applied. However, as inter-annual variations are harder to project for natural systems, rivers should fall into quadrants with a common direction ($++$, $--$) to be assessed as 'reasonable'. The plot indicates that 22 out of 43 rivers fall within this threshold, displaying similar directional behaviour in both projections and measurements. On the other hand, 21 rivers exhibit contradicting directions in their mean inter-annual variations. To clarify, a river in the Dethier et al. (2022) dataset might show a positive mean inter-annual variation but Dunn et al. (2019) projected a negative mean annual variation. This indicates a discrepancy in the ability of the WBMsed model in capturing the correct growth or decrease in annual sediment flux amounts, which is at the core of a reliable projection, and is a critical anomaly. Seeing that for 21 out of 43 rivers the mean inter-annual variation is in contradicting directions, draws questions to the reliability of the statements

made in Dunn et al. (2019) about global deltas retreating or growing in the future. Increasing the accuracy of capturing short-term variations by the projections makes the model less dependent on a chosen period, signaling a need for refinement in the model.

4.6 Trends

As part of the validation process, a linear regression analysis can show similarity in behaviour and direction between the projections and the observations. Allowing for an in depth analysis of the dominant trajectories of the datasets and unexpected deviations which may prompt a closer examination of possible causes for the anomalies.

4.6.1 Trends for period 1984-2020

Trend analysis involves using a linear regression model with time as the independent variable to explore the long-term behaviour of the series (Nugus, 2009). The objective when estimating a linear regression model is to minimize the sum of the squared error, also called 'least-squares', between the concerning y-value of the data and the trendline (Jenkins-Smith et al., 2017). The resulting linear regression is the best fit for the data in the sense of minimizing the sum of the deviations of each y-value from the line (Lee et al., 2014). Therefore, the trendline strongly depends on the y-value behaviour and distribution of the data. The absolute data for each individual river of the Dunn et al. (2019) and Dethier et al. (2022) datasets along their respective first order trendlines are displayed in Figures 4.11, 4.12, 4.13, 4.14, 4.15 and 4.16.

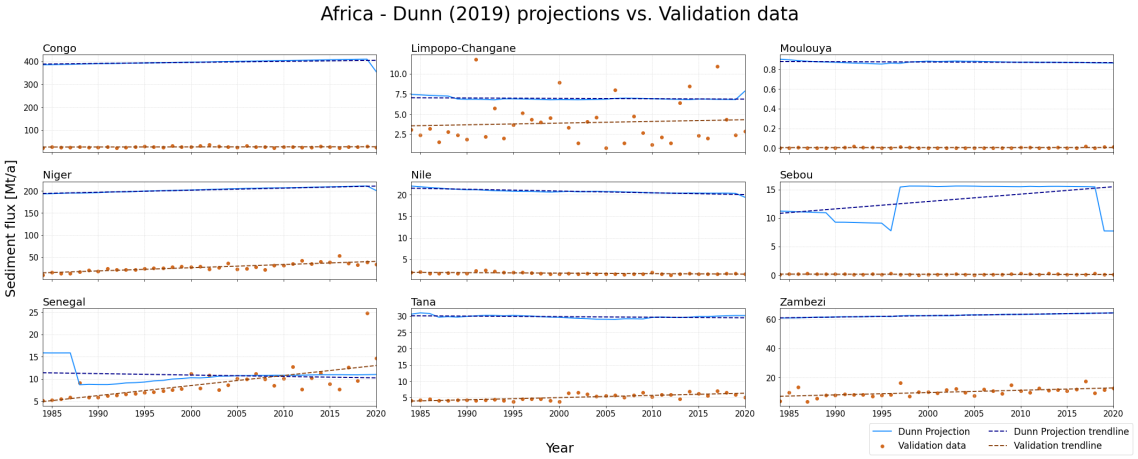

Figure 4.11: Absolute magnitudes of Dunn et al. (2019) projections and of the validation data of Dethier et al. (2022) for rivers in Africa with their corresponding trendlines

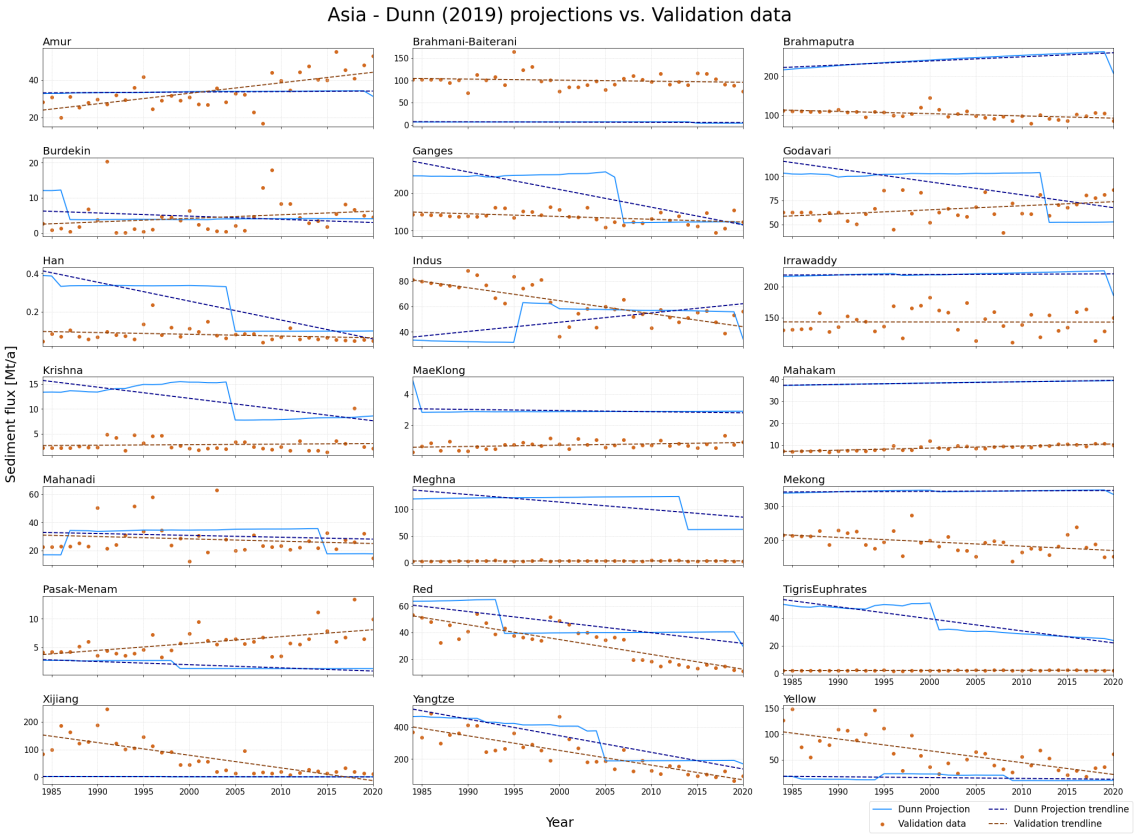

Figure 4.12: Absolute magnitudes of Dunn et al. (2019) projections and of the validation data of Dethier et al. (2022) for rivers in Asia with their corresponding trendlines

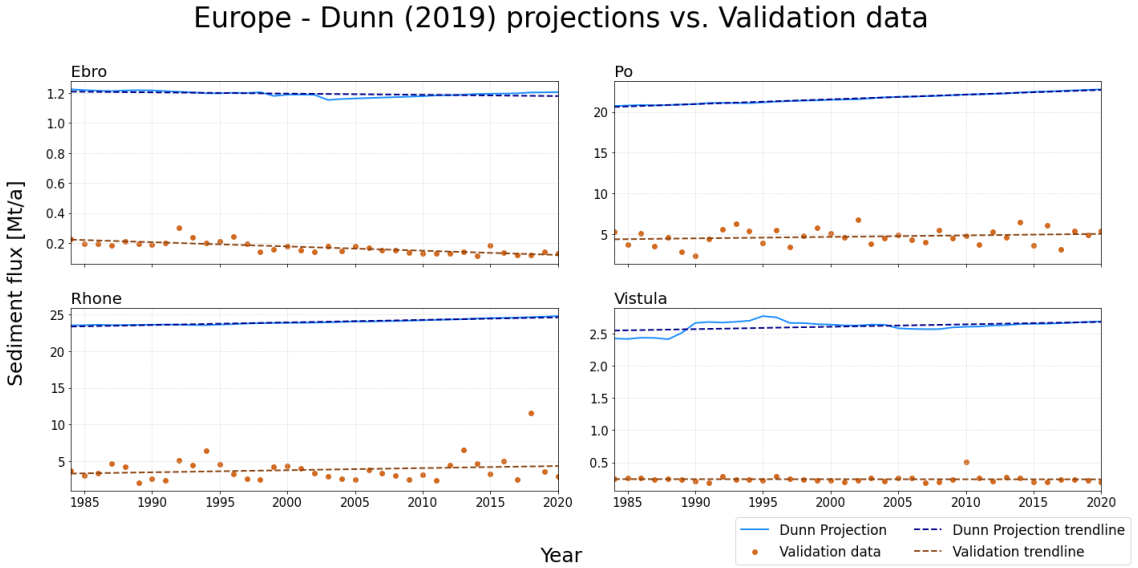

Figure 4.13: Absolute magnitudes of Dunn et al. (2019) projections and of the validation data of Dethier et al. (2022) for rivers in Europe with their corresponding trendlines

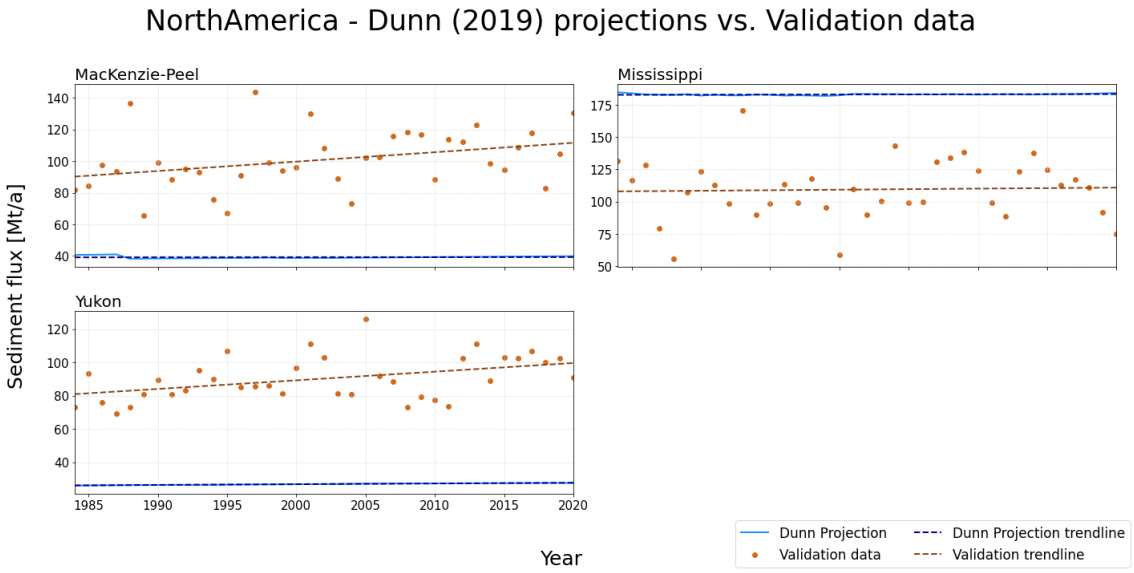

Figure 4.14: Absolute magnitudes of Dunn et al. (2019) projections and of the validation data of Dethier et al. (2022) for rivers in North-America with their corresponding trendlines

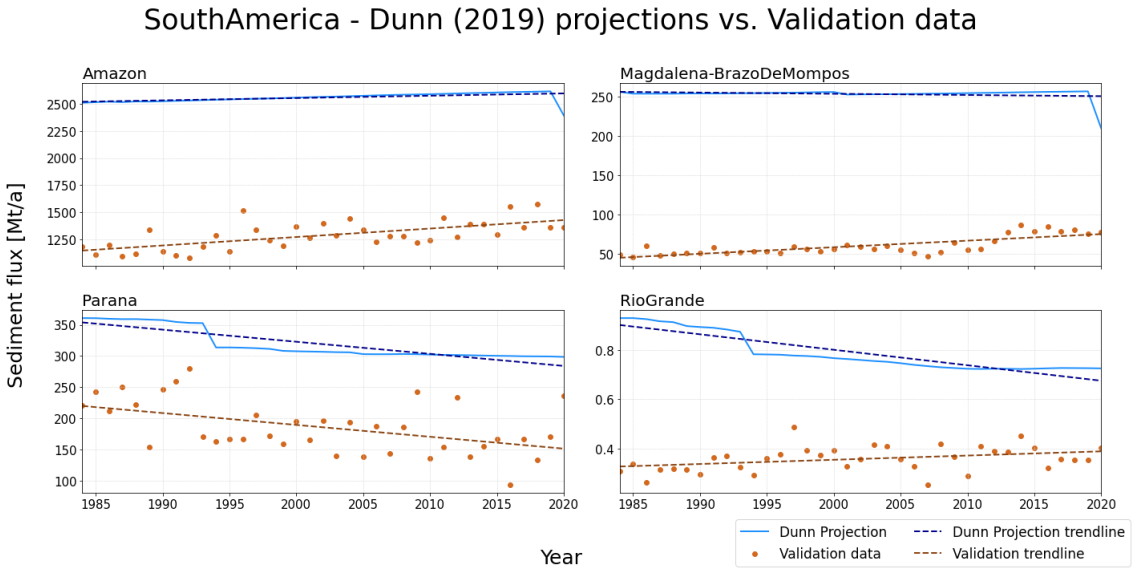

Figure 4.15: Absolute magnitudes of Dunn et al. (2019) projections and of the validation data of Dethier et al. (2022) for rivers in South-America with their corresponding trendlines

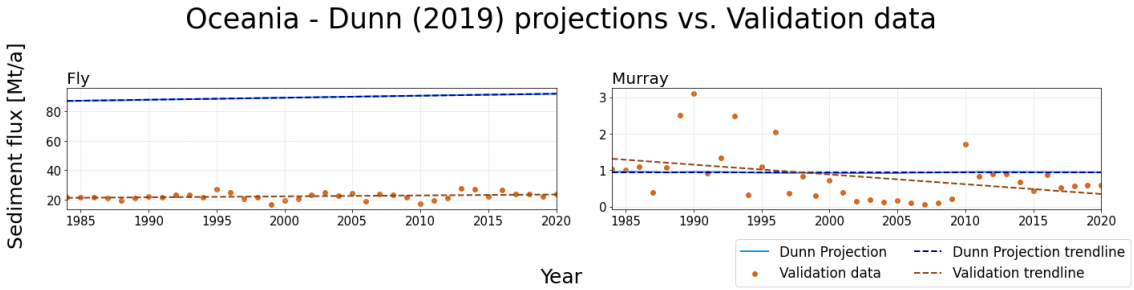

Figure 4.16: Absolute magnitudes of Dunn et al. (2019) projections and of the validation data of Dethier et al. (2022) for rivers in Oceania with their corresponding trendlines

As observed in Figures 4.11, 4.12, 4.13, 4.14, 4.15 and 4.16, performing linear regression often results in non-zero trends. To test the significance of the linear regression of the trendlines, the classical t-test is applied with the following null hypothesis and its alternative:

H_0: There is no significant trend

H_1: There is a significant trend

The t-value, representing the deviation ratio of the values from the regression line (Allen, 1997), is calculated for each trendline with its respective dataset. With the t-value we can calculate the p-value, indicating the probability of observing the data if the null-hypothesis is true (Dahiru, 2008). Compare the p-value to the conventional significance level 0.05. A p-value < 0.05 rejects H0, signifying statistical significance (Allen, 1997). The t-test outcomes for Dunn et al. (2019) and Dethier et al. (2022) are in Appendix C.

Results suggest some trendlines lack evidence to reject H0, indicating 'time [year]' insignificantly predicts 'sediment flux [Mt]'. This is not surprising as the observation data is influenced by uncertainties related to natural systems and anthropogenic influence that is not always possible to detect. To assess the overall directional variations in sediment flux projections compared to measurements, a scatterplot was created in Figure 4.17, plotting the slopes of the trendlines for both projections and measurements, aiming for $++$ or $--$ scatters for data behaviour similarity.

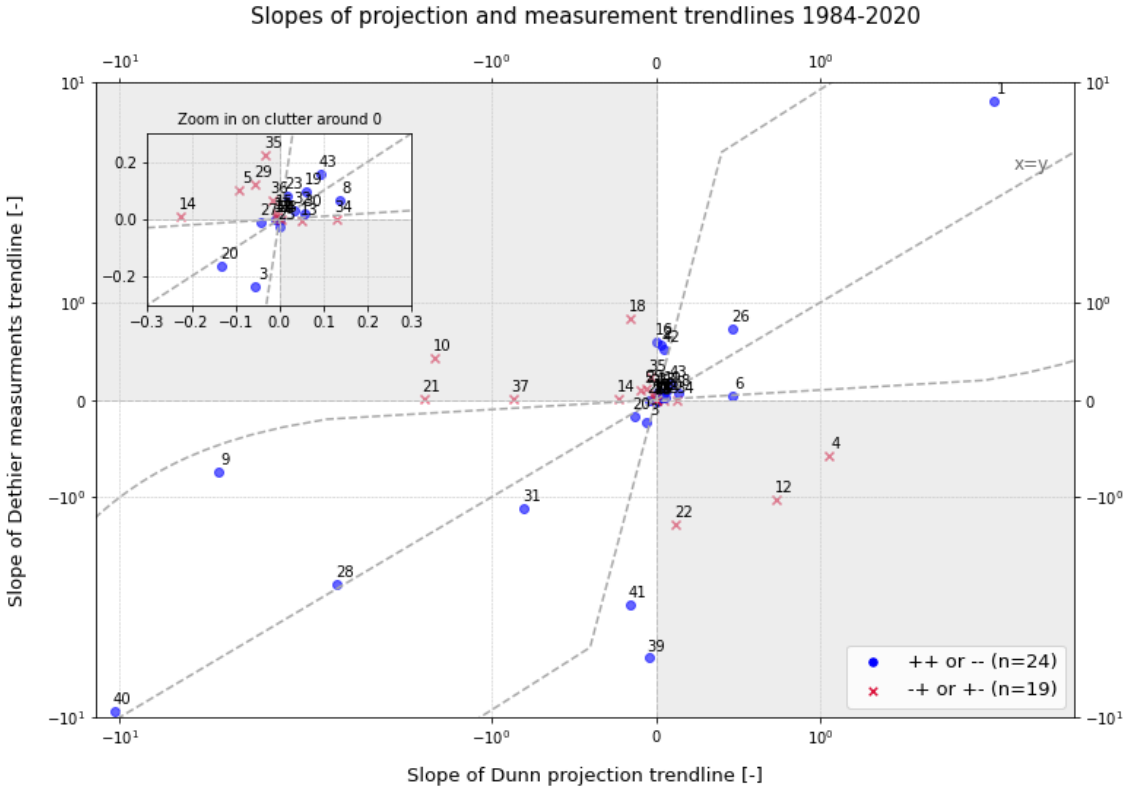

Figure 4.17: Slopes of projections versus the slopes of the validation data fort the period 1984-2020 for individual rivers: 1)Amazon, 2)Amur, 3)Brahmani-Baiterani, 4)Brahmaputra, 5)Burdekin, 6)Congo, 7)Ebro, 8)Fly, 9)Ganges, 10)Godavari, 11)Han, 12)Indus, 13)Irrawaddy, 14)Krishna, 15)Limpopo-Changane, 6)MacKenzie-Peel, 17)MaeKlong, 18)Magdalena-BrazoDeMompos, 19)Mahakam, 20)Mahanadi, 21)Meghna, 22)Mekong, 23)Mississippi, 24)Moulouya, 25)Murray, 26)Niger, 27)Nile, 28)Parana, 29)Pasak-Menam, 30)Po, Z1)Red, 32)Rhone, 33)RioGrande, 34)Sebou, 35)Senegal, 36)Tana, 37)TigrisEuphrates, 38)Vistula, 39)Xijiang, 40)Yangtze, 41)Yellow, 42)Yukon, 43)Zambezi, with reference lines: black) y=x and grey) y=0.1x and y=10x

For the similarity between the projections and the validation data being assessed as 'reasonable', again the threshold of one order of magnitude above or below the y=x line is applied. However, in terms of the ability of the model being able to project the correct sediment flux behaviour, rivers should fall into quadrants with a common direction ($++$, $--$) to be assessed as 'reasonable'. The plot indicates that out of the 43 rivers analysed, 24 rivers exhibit consistent slopes, portraying the desired similarity, a key element in a models ability to make valid projections. 19 rivers show contradicting slopes between projections and measurements, again suggesting a discrepancy in the model's ability to replicate the directional behaviour observed in real-life measurements.

4.6.2 Robustness of the trends

To assess the robustness of the projections, the average inter-annual variations (Section 4.5) of individual rivers and their respective trendline slopes should portray similar directions, irrespective of the sample period, to ensure the alignment between inter-annual variations and trendline behaviour. There is a discrepancy observed on this matter regarding the Dunn et al. (2019) data, 11 rivers show contradiction between their inter-annual variation direction and their respective trendline slope (Table 4.2).

Table 4.2: Rivers with contradicting mean inter-annual variations and trendline slope for (Dunn et al., 2019) data

River nr.	**River name(s)**	**Average inter-annual var. [Mt/a]**	**Trendline Slope**
1	Amazon	-3.266150031	2.144361903
2	Amur	-0.03961666	0.026546929
4	Brahmaputra	-0.243399929	1.049954897
6	Congo	-0.843580871	0.460860899
13	Irrawaddy	-0.842424776	0.051568833
15	LimpopoChangane	0.011212474	-0.004672634
16	MacKenziePeel	-0.021557927	0.005210705
20	Mahanadi	0.019103384	-0.131646453
22	Mekong	-0.098669908	0.122714937
23	Mississippi	-0.013241373	0.015753771
34	Sebou	-0.097148566	0.129728765

This phenomenon is due to the nature of the theory behind calculating the mean inter-annual variation and the first order trendline. The mean inter-annual variations are calculated by summing all inter-annual differences and dividing that sum the number of inter-annual variations. Therefore, the inter-annual behaviour is dominated by large inter-annual magnitude drops in the graphs, regardless of their timing. On the contrary, first order trend lines follow the dominant trajectory of the projections, as they strive for minimization of the total error between the data points and the trendline. Consequently when at the end of the concerning period a large inter-annual difference is projected in the

opposite direction of the previous dominant trajectory, the trendline is not redirected and keeps its slope in the direction of the dominant trajectory. This results in conflicting directions of the mean inter-annual variations and their respective trendlines, which when interpolated would result in conflicting future projections. This is an undesirable key issue of the WBMsed model, as now the projected trends highly depend on the chosen period and when events are timed within this period. While this issue is likely present in most time series, it highlights the models sensitivity to chosen periods and event timing, necessitating smoothing of significant inter-annual differences.

This theory is supported by the use of the available projection data for the years 1980-2099. Figure 4.18 illustrates the impact of interpolating incorrect trendlines, showcasing Dethier et al. (2022) validation data for its time period 1984-2020, the projections from Dunn et al. (2019) for the available period 1980-2099 and the previous trendlines with interpolation to the year 2099.

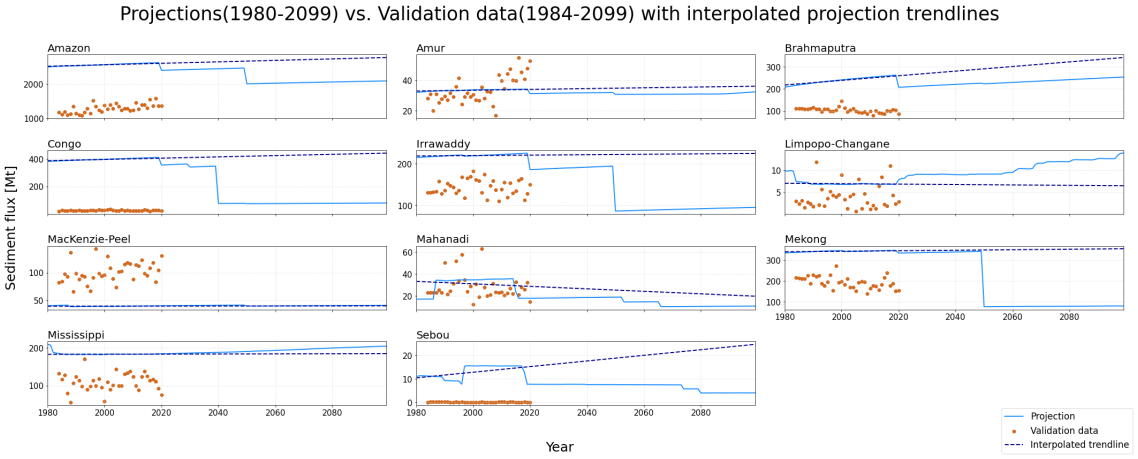

Figure 4.18: Absolute magnitudes of Dunn et al. (2019) projections for the period 1980-2099, the validation data of Dethier et al. (2022) for the period 1984-2020 and the interpolated trendlines for the Dunn et al. (2019) data.

Figure 4.18 confirms that most of the computed trendlines are in need of redirection. Due to the trendline directions conflicting with the behavioural direction of the data, the dissimilarity between the sediment flux projections and interpolated trendline increases with increasing time.

For the Amur, Mississippi and the MacKenziePeel the trend lines seem quite a good fit, however this can be related to the small difference in slopes between the mean-inter annual differences, being less than a 0.07 Mt/a difference, which visually would not notably influence the course of the trendline.

4.7 Diminishing inter-annual extremes

As we now know, the inter-annual sediment flux extremes greatly influence the interpretation of the WBMsed model results. From literature we know that these sudden inter-annual changes can be related to a shift in GNP per capita, leading to a different anthropogenic soil erosion factor, instantly influencing sediment flux projections. The rapid impact of dam employment on sediment flux projections adds to this complexity, which could be observed only in 2020 for this concerning period. Neither implementation of these mechanisms in the model is realistic, as the transition of a community to anthropogenic drivers of soil erosion are implemented gradually and the geomorphic change of a delta as an effect of sediment trapping by dams also occurs moderately. To show the dominance of the current implementation of anthropogenic mechanisms in the WBMsed model, inter-annual variations >20% of its previous magnitude have been removed from the dataset, focussing on 32 rivers where the projected mean inter-annual variation differs more than one order of magnitude from the mean inter-annual variations of the observed sediment fluxes (Figure 4.11, Section 4.5). These 32 rivers with original projection and validation data are shown in Figure 4.19.

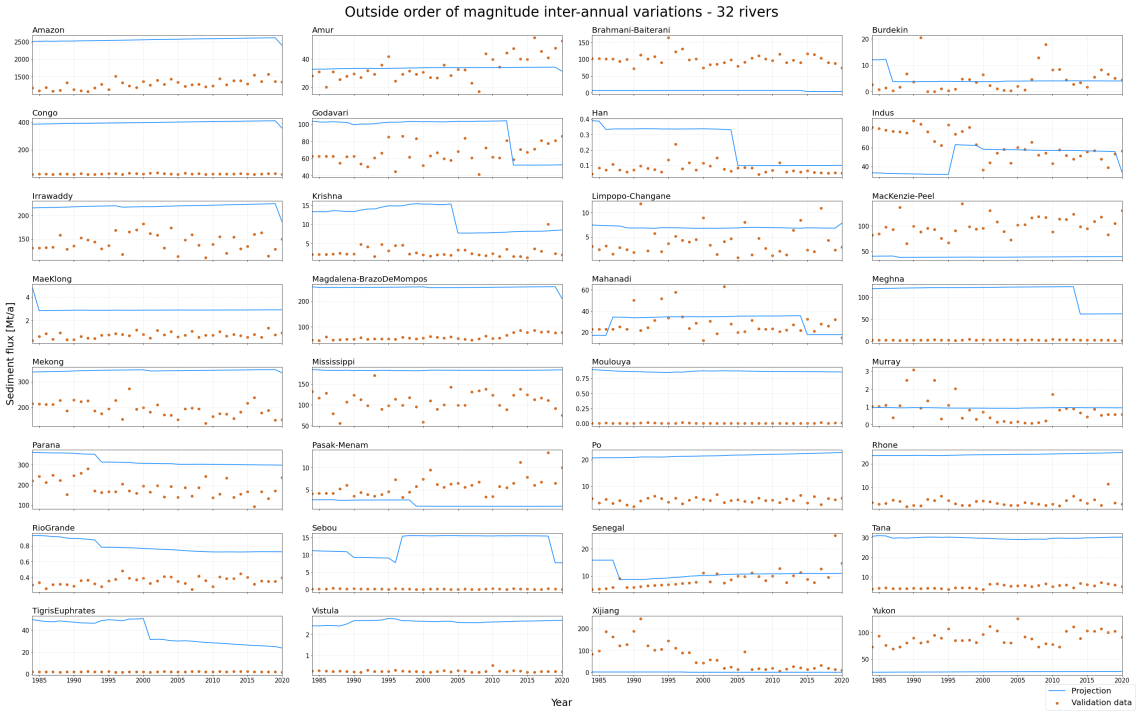

Figure 4.19: Projection and validation data of 32 rivers of which the mean inter-annual variation differs more than one order of magnitude from the mean inter-annual variations of the observed sediment fluxes.

Out of these 32 rivers, 14 rivers had inter-annual differences >20%, the BrahmaniBaiterani, Burdekin, Godavari, Han, Indus, Krishna, MaeKlong, Mahanadi, Meghna, Pasak-Menam, Sebou, Senegal, TigrisEuphrates and the Xijiang. Emphasising the large occurrence of the presence of inter-annual differences >20%, confirms the fact that this is a key issue to resolve before the model is implemented for more global deltas. In Figure 4.20 the projection and validation data is visualised without the inter-annual variations >20%, showing the behaviour of the projections without the abrupt variations.

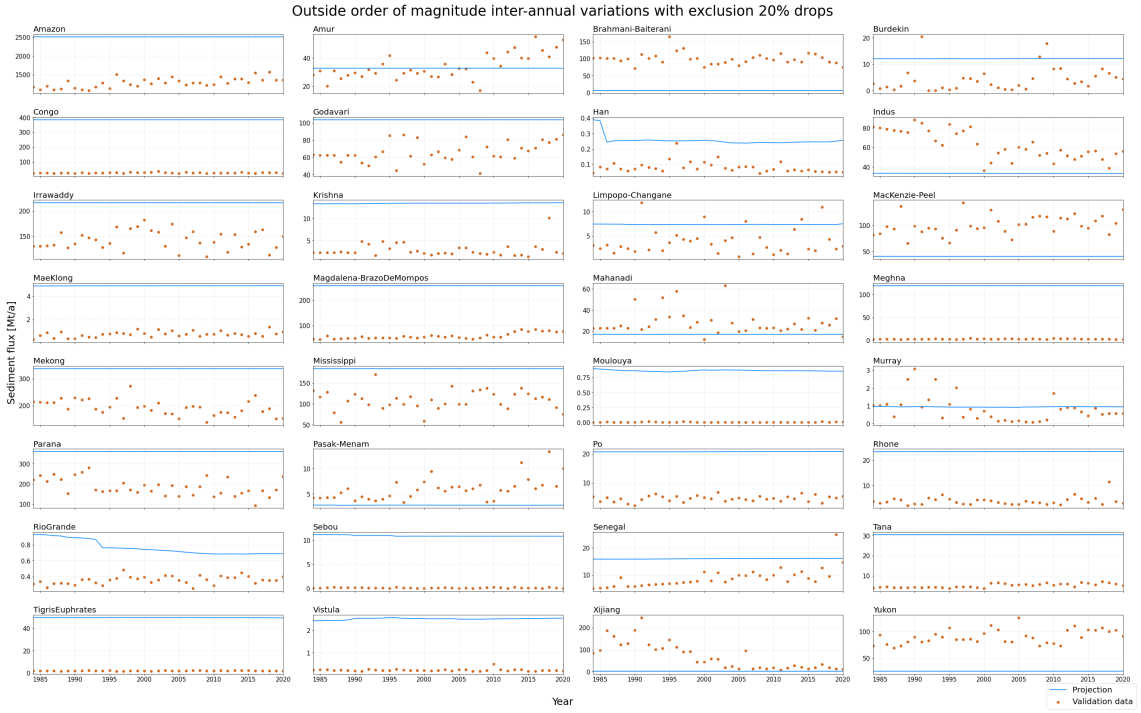

Figure 4.20: Projection and validation data of 32 rivers of which the mean inter-annual variation differs more than one order of magnitude from the mean inter-annual variations of the observed sediment fluxes with their projection data plotted with inter-annual variations >20% removed.

Figure 4.20 illustrates that excluding these extremes enhances the overall behaviour of the projections, aligning more closely with observations. The need for the anthropogenic effects on sediment flux projections in terms of correctly projecting the absolute sediment flux magnitudes is emphasized. Without the anthropogenic effects, the sediment flux projections do not advance towards the observed sediment flux amounts and in some cases even deflects from it.

At 18 out of the 32 rivers: the Amazon, Amur, Congo, Irrawaddy, Limpopo-Changane, MacKenzie-Peel, Magdalena-BrazoDeMompos, Mekong, Mississippi, Moulouya, Murray, Parana, Po, Rhone, RioGrande, Tana, Vistula, and Yukon, there was not an inter-

annual difference >20% in the data. However, as the mean-inter annual variations from the projections for these rivers showed a dissimilarity larger than one order of magnitude with the observations, the underlying cause for this similarity needs attention. One thing that stands out for the data concerning these 18 rivers is the fact that their behaviour and direction visually are quite good, but the difference in the absolute magnitudes of their observations and projections show large differences. From literature we understand that the WBMsed model tends to overpredict the water discharge which could result in an overprediction of the sediment fluxes.

4.8 Overpredictions

To test if the difference in projected and observed water discharge[km^3/a] is the cause for the anomalies observed in the overall magnitude differences, we construct a scatterplot containing the average annual discharge(Qa) for the projections and the observations for all 43 rivers, shown in Figure 4.21.

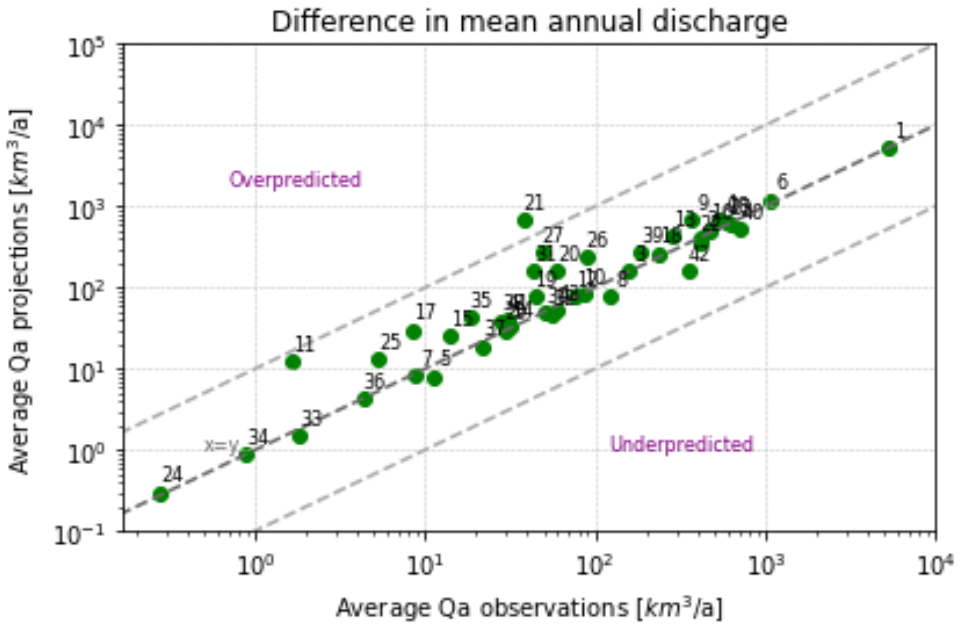

Figure 4.21: Does the model indeed under- and overpredict according to literature for the individual rivers: 1)Amazon, 2)Amur, 3)Brahmani-Baiterani, 4)Brahmaputra, 5)Burdekin, 6)Congo, 7)Ebro, 8)Fly, 9)Ganges, 10)Godavari, 11)Han, 12)Indus, 13)Irrawaddy, 14)Krishna, 15)Limpopo-Changane, 6)MacKenzie-Peel, 17)MaeKlong, 18)Magdalena-BrazoDeMompos, 19)Mahakam, 20)Mahanadi, 21)Meghna, 22)Mekong, 23)Mississippi, 24)Moulouya, 25)Murray, 26)Niger, 27)Nile, 28)Parana, 29)Pasak-Menam, 30)Po, Z1)Red, 32)Rhone, 33)RioGrande, 34)Sebou, 35)Senegal, 36)Tana, 37)TigrisEuphrates, 38)Vistula, 39)Xijiang, 40)Yangtze, 41)Yellow, 42)Yukon, 43)Zambezi, with reference lines: black) y=x and grey) y=0.1x and y=10x y=x.

Figure 4.21 shows that the WBMsed model under- and overpredicts the fluvial discharge, with a larger tendency to overpredict, across all observed water discharges from the validation data. The actual magnitude of these under- and overpredictions is displayed by the plot in Figure 4.22. Representing the relationship between the relative difference in annual Qa between the projections and observations and the average Qa observed for the individual rivers. The relative difference in Qa shows the percentile proportion of the projected annual Qa in relation to the observed Qa. For example, when the projected average Qa is of twice the magnitude of the observed Qa, the relative difference is +100%.

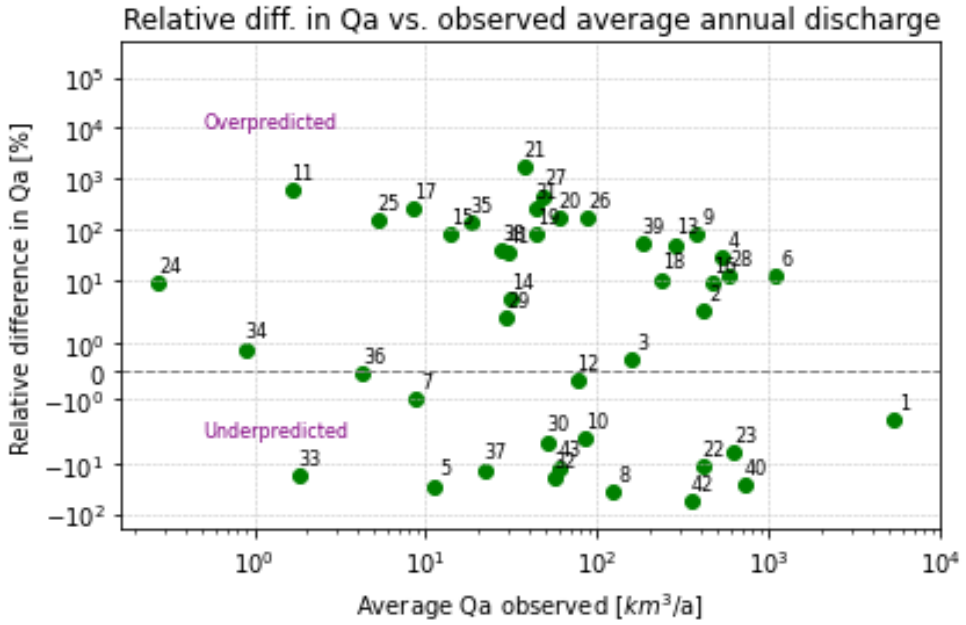

Figure 4.22: How do the under- and overpredictions translate to the relative difference between the projected and observed annual discharges for the individual rivers: 1)Amazon, 2)Amur, 3)Brahmani-Baiterani, 4)Brahmaputra, 5)Burdekin, 6)Congo, 7)Ebro, 8)Fly, 9)Ganges, 10)Godavari, 11)Han, 12)Indus, 13)Irrawaddy, 14)Krishna, 15)Limpopo-Changane, 6)MacKenzie-Peel, 17)MaeKlong, 18)Magdalena-BrazoDeMompos, 19)Mahakam, 20)Mahanadi, 21)Meghna, 22)Mekong, 23)Mississippi, 24)Moulouya, 25)Murray, 26)Niger, 27)Nile, 28)Parana, 29)Pasak-Menam, 30)Po, Z1)Red, 32)Rhone, 33)RioGrande, 34)Sebou, 35)Senegal, 36)Tana, 37)TigrisEuphrates, 38)Vistula, 39)Xijiang, 40)Yangtze, 41)Yellow, 42)Yukon, 43)Zambezi, with reference line y=0.

Figure 4.22 shows the significant dominance of the overprediction characteristic of the WBMsed model as overpredicted water discharges are up to 1700% overpredicted, while other rivers are only underpredicted by -54%. There is no correlation observed on when the model over- or underpredicts based on the observed discharges, which are related to the basins climate characteristics and inputs used in the model. To test if the under- and overproduction of the fluvial discharge is the dominant factor for the under-

and overpredicting the sediment flux [Mt], Figure 4.23 represents the relative difference in average sediment flux(Qs) magnitudes in relation to the observed Qa. Similar to the explanation for Figure 4.22, the relative difference in Qs shows the percentile proportion of the projected annual Qs in relation to the observed Qs.

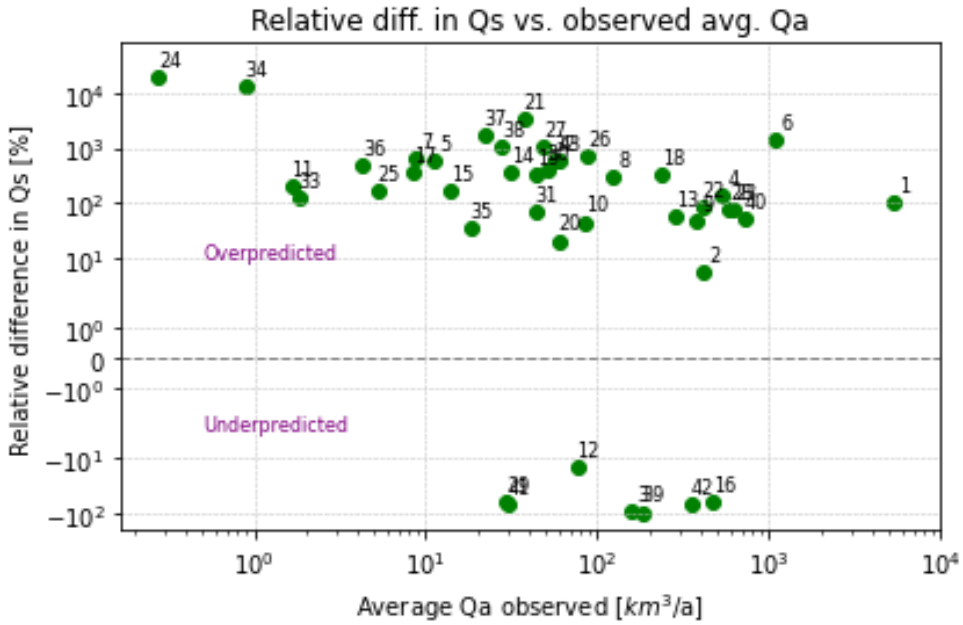

Figure 4.23: How do the under- and overpredictions translate to the mean relative difference between the projected and observed sediment fluxes for the individual rivers: 1)Amazon, 2)Amur, 3)Brahmani-Baiterani, 4)Brahmaputra, 5)Burdekin, 6)Congo, 7)Ebro, 8)Fly, 9)Ganges, 10)Godavari, 11)Han, 12)Indus, 13)Irrawaddy, 14)Krishna, 15)Limpopo-Changane, 6)MacKenzie-Peel, 17)MaeKlong, 18)Magdalena-BrazoDeMompos, 19)Mahakam, 20)Mahanadi, 21)Meghna, 22)Mekong, 23)Mississippi, 24)Moulouya, 25)Murray, 26)Niger, 27)Nile, 28)Parana, 29)Pasak-Menam, 30)Po, Z1)Red, 32)Rhone, 33)RioGrande, 34)Sebou, 35)Senegal, 36)Tana, 37)TigrisEuphrates, 38)Vistula, 39)Xijiang, 40)Yangtze, 41)Yellow, 42)Yukon, 43)Zambezi, with reference line y=0.

The dissimilarity between plots shows a certain anomaly in the steps between the discharge and the eventual projected sediment fluxes. If the under- and overprediction of the discharge is the main reason for differences in the projected and observed sediment flux projections, the distribution of the relative sediment flux difference would be similar. However, that is not the case, 9 of the 16 rivers with underpredicted fluvial discharge shows overpredicted sediment fluxes. Also, several rivers with already overpredicted fluvial discharge, show an even greater overprediction in the sediment flux projections.

4.9 Sediment starvation risk

Dunn (2017) focussed on sediment starvation as a key risk factor driving changes in relative sea level rise and thus the sustainability of global deltas. The mentioned drivers of change in relative sea level rise in Section 2.1 are eustatic sea level changes, sediment compaction and aggradation. Aggradation is the primary mechanism which makes it possible for deltas to oppose relative sea level rise. In this Section the projected aggradation abilities of individual deltas are compared to the aggradation abilities calculated with the validation data, to see if this key element for delta sustainability is correctly projected and thus reliable to use for delta sustainability management. To assess if the projected sediment fluxes suffice the amount of sediment needed for individual rivers to aggradate, the Sediment Starvation Risk Index (SSRI) is utilised in Dunn (2017):

$$SSRI = \frac{QsS - QsE}{A} \tag{4.4}$$

QsS: Sediment flux at the start of the concerning period [m^3/a]
QsE: Sediment flux at the end of the concerning period [m^3/a]
A: Delta area [m^2]

The sediment load is calculated with bulk density of 2 t/m^3 and the trapping efficiency is assumed as 100%, resulting in the SSRI representing change in sediment flux per unit of delta area(m/a) (Dunn, 2017). In the study of Dunn (2017), the SSRI is calculated for the full projection period of 1980-2099 however, as we focus on the validation of the projections with available observation data, the SSRI is calculated for the 43 individual rivers for the relevant period 1984-2020. Due to the shorter period, the 'start' of the period will be assessed as 1984-1988 and the 'end' as 2016-2020. The SSRI does not take into account the current state of each delta, it only shows if certain deltas are likely to face increased sustainability difficulties in the concerned period. The results of these calculations are in Appendix D. These calculated SSRI values show for the projections 16 out of 43 rivers would have been expected to experience more aggradation difficulties due to decreasing sediment fluxes between 1984 and 2020. Whereas the observations show that actually 26 out of 43 rivers were likely to have experienced more aggradation difficulties as a result of decreasing sediment fluxes. This error in the projected SSRI values enforces the model limitations in representing all real life factors influencing fluvial sediment fluxes. It is necessary to correctly project the capacity of the delta to keep pace with relative sea level rise as this is a key factor in delta sustainability.

5. Discussion

Literature addresses the difficulty in making correct projections for future delta risks regarding sediment fluxes due to the intricate interaction of different climate- or anthropogenic threats with delta mechanisms. Therefore, the goal of this study was to uncover to what extent the sediment flux projections made by Dunn et al. (2019) were representative for the actual situation, ensuring the reliability of the used methods and results for global delta management implementation.

5.1 Interpreting raw data comparison results

The projection data of Dunn et al. (2019) was visually compared to validation data of Dethier et al. (2022), representing historic sediment flux data, for the period 1984-2020. The analysis highlights a notable extreme inter-annual variability in the sediment flux projections, inconsistent with the gradual nature expected in natural fluvial systems. Possible contributing factors to these fluctuations include anthropogenic influences and dam activation, of which their effect on sediment fluxes is modelled instantly, and the timing for all dam implementation is set in 2020, an unrealistic assumption.

While structural similarities in the data behaviour exist, the sediment flux projections by the WBMsed model are heavily overpredicted and sometimes underpredicted in comparison to real-life observations. The lack of a clear pattern in this under- and overprediction complicates quantification of discrepancies, emphasizing the need for model refinement to achieve better representation of reality by the projections. To quantify the measure of dissimilarity between the projections and the validation data, the scaled Euclidean distance was calculated, and the results were analysed for a possible structural dissimilarity in the use of the WBMsed model to project global delta sediment fluxes. The lack of this expected consistent dissimilarity across the datasets suggest complexities that extend beyond a single metric. Emphasized by the attempt to correlate dissimilarity with input variables of the model like discharge[km^3/a], no clear structural connection is observed.

5.2 Interpreting overall tendencies comparison results

In order to test the models tendencies compared to the validation data, similarity between the projections and validation data was measured in their mean absolute differences[Mt] and average annual sediment fluxes[Mt/a]. For the model's projections to be classified as 'reasonable' in reflecting the validation data, it has to lie within one order of magnitude.

Results showed varying directions of the mean absolute differences between the projections and observations, with a dominance in overprediction, confirming the underprediction of the model but mainly confirming the overpredictive tendencies of the WBMsed model. The dispersion in differing magnitudes highlights the complexity in isolating the reasons for dominant overprediction by the model, demanding a detailed understanding of projection inaccuracies. While the overprediction characteristic of the WBMsed model is established, the mean annual sediment flux of 37 out of 43 individual rivers being within one order of magnitude different from the validation data suggests acceptable overall projection performance. However, the significant variation in relative differences among rivers, without a consistent bias, calls for a deeper investigation into the causes for these variations.

5.3 Interpreting time-dependency analysis results

To explore the sensitivity of the WBMsed model on specific time periods, the model's ability to accurately project sediment fluxes on a yearly basis is explored and using a linear regression analysis provided the assessment of the sensitivity of the WBMsed model interpretations regarding the timing of large inter-annual variations.

The analysis of mean inter-annual variations explores the model's ability to capture fluctuations on a yearly basis. The divergence in directional behaviour for 21 out of 43 rivers signals a need for refinement in the model to improve short-term variation projections, as these short term projections are the basis for specific projection periods. Seeing that for 21 out of 43 rivers the mean inter-annual variation is in contradicting directions, this draws questions regarding the reliability of the statements made in Dunn et al. (2019) about global deltas retreating or growing in the future. However, the conclusions drawn by Dunn et al. (2019) were based on the comparison of the beginning and end of a century-long timeframe, which contrasts with the decadal scope of this study. This longer period may render their findings more resilient to the introduced variability stemming from extreme inter-annual variations, although not entirely immune, as extending

the period with just one extra year could already drastically alter the results.

The scatterplot of the linear regression trend analysis in Section 4.6, suggests both consistent slopes for 24 rivers and contradicting slopes for 19 rivers between projections and measurements, suggesting a discrepancy in the model's ability to replicate the directional behaviour of reality. Testing the robustness of these trendlines highlights discrepancies between mean inter-annual variations and trendline slopes, indicating the model's sensitivity to chosen periods and event timing. This sensitivity can be related to the extreme inter-annual variations and especially the timing of these variations within the specific period, as they are able to redirect trend lines significantly, necessitating smoothing of the significant inter-annual differences.

5.4 Interpreting error factor influence analysis results

As the research revealed several possible factors influencing the reliability of the sediment flux projections using the WBMsed model, the actual influence of these factors was established by exclusion and correlation analysis.

Focusing on 32 rivers where the projected mean inter-annual variation differs more than one order of magnitude from the mean inter-annual variations of the observed sediment fluxes, inter-annual extremes greater than 20% were present in 14 rivers and excluded. This exclusion results in visual enhancement of the overall behaviour of the projects, aligning more closely with the observations. Because these extreme inter-annual variations are related to anthropogenic influences or dam construction, the implementation of these factors should be reassessed as their effect on the sediment flux projections is needed to represent a more accurate magnitude range.

According to Dunn et al. (2019), the threshold for expecting overprediction of the discharge is for rivers with Qa<8km^3/year. This statement is not supported by the data, which can be a reuslt of the use of different historic validation data in the Dunn et al. (2019) study and this research. There is no clear threshold to be observed for over-, under- or correctly projecting the discharge. A similarity observed with the mean annual discharge validation conducted by Dunn et al. (2019), is the overall dominance of the overprediction characteristic of the WBMsed model, as overpredicted water discharges are up to 1700% overpredicted, while other rivers are only underpredicted by -54%. The lack of trend in the under- or overpredictions suggest there is a certain influence that causes particular rivers to be overpredicted and others to be underpredicted while their observed discharges are roughly equal.

This discharge projection discrepancy could be related to underlying error within the used data to project water discharge. The water discharge calculation is impacted by climate drivers and anthropogenic changes such as precipitation, temperature, soil moisture balance, irrigation water demand and reservoir construction. According to Wisser et al. (2010), there is a large uncertainty in correctly documenting precipitation data on a global-scale water balance context, which can translate to errors in water discharge projections. Another reason for water discharge projection discrepancies is the lack of inclusion of smaller dams in the used dam dataset, as they collectively have a significant impact on river flow by irrigation expansion and seasonality change of the discharge (Vörösmarty et al., 2003). Also, presented by Cohen et al. (2013), introducing a flood plain reservoir component would improve the models discharge projections. However, in the study of Dunn et al. (2019), a floodplain component was added, but still resulted in both underprediction and significant overprediction of the fluvial discharge. This could potentially be related to the fact that this mechanism instigates a higher reintroduction of floodplain water at very low discharges.

Remarkably, the under- and overpredictive behaviour at designated discharge levels is not translated to the sediment flux projections, leading to a conclusion that observed sediment fluxes might vary from the projections due to unincluded natural delta processes in the WBMsed model, and thus the under- and overprediction of the sediment flux would still occur to some degree, even if realistic water discharge amounts are used for the projections. The WBMsed model was build on the BQART sediment delivery model of J. P. Syvitski and Saito (2007), making the computed sediment fluxes based on basin area and relief, temperature, runoff, lithology, glacial erosion, reservoir trapping and anthropogenic soil erosion. According to Dunn et al. (2019) it is unlikely that the basin area and relief, temperature and glacial erosion would produce errors in the projections. As explained before, the discharge is not the only prominent factor for the under- and overprediction of the sediment fluxes, and according to Dunn et al. (2019) the conversion of lithology data to usable factor values for the model may be a key source of potential error in that variable, but that statement can not be validated as the original data and model is unavailable. This leaves reservoir trapping and anthropogenic soil erosion as possible dominant factors responsible for the yet unexplained projection discrepancies, primarily stemming from the absence of specific factors in the provided anthropogenic datasets, like the smaller reservoirs or other variables unaccounted for in their totality. Once again highlighting the complex interplay between anthropogenic and natural drivers of fluvial sediment fluxes and the difficulty in accurately projecting

this interplay. Indicating that improving the accuracy of sediment flux projections by the WBMsed model takes more than only adjusting parameters within the model.

Possible variables unaccounted for in the model are:

Anthropogenic changes

Anthropogenic activities significantly impact fluvial sediment fluxes, and WBMsed primarily considers population density and GNP per capita for anthropogenic soil erosion. However, rapid socio-economic shifts, beyond GNP per capita, can impact land use and human activities. Undocumented local human activities, such as deforestation, mining, and urbanization, can significantly impact sediment fluxes but are not explicitly incorporated into the model. These activities alter land cover and contribute to erosion, affecting sediment transport in rivers (Maaß et al., 2021; MacKenzie et al., 2022). For example, a study by Dethier et al. (2023) showed that in 80% of their researched rivers in the tropics, the suspended sediment concentrations were more than double their pre-mining sediment concentrations.

Future dam construction is solely implemented in the model for hydropower dams with at least 1MW capacity. However, regardless of their size, dams have the capacity to trap sediment and thus decrease the fluvial sediment flux (Moragoda et al., 2023). Therefore, not all global sediment trapping by dams is portrayed in the model. This is undermining the great dominance of fluvial sediment flux reduction caused by dams, as there are currently ∼58,000 dams with heights >15m in the world and an additional ∼3,700 dams that are under construction or planned (Best & Darby, 2020; Moragoda et al., 2023). Alongside dam construction, sand and gravel mining is also one of the most common forms of anthropogenic intervention in fluvial systems. Removal of sediment directly from the river bed affects the channel geometry head-on, affecting flow and sediment mechanisms, ultimately causing sediment deficits (Preciso et al., 2012; Rascher et al., 2018). Integrating more accurate anthropogenic effects in the WBMsed model is essential, as according to Moragoda and Cohen (2020) and Y. Zhang et al. (2023), the influence of anthropogenic activities on fluvial sediment flux dominate climate change impacts, even extreme events.

Extreme events

Climate change is incorporated in the model as the mean annual air temperature and precipitation. However, there is also an increase in extreme events as a result to climate change which can have a drastic and complex impact on global sediment fluxes (Moragoda & Cohen, 2020). Even a few extreme precipitation events can increase the sediment flux greatly due to their high impact on soil erosion, affecting fluvial sediment load (Y. Zhang et al., 2023). The magnitude of these extreme events dominate their influence

on sediment delivery. Therefore, the ability to project the occurrence and magnitude of future extreme events caused by future climate change, is crucial in accurately projecting future delta sediment fluxes (Fryirs, 2013). An extra complexity in this matter is, the threshold for an event to be extreme can shift, as the catchment-equilibrium could change due to climate change, making accurately projecting these extreme events difficult (Reid et al., 2007). However, as the number of studies on regional climate effects on extreme events increase, it has potential to be implemented in the WBMsed model (Li et al., 2022; Y. Zhang et al., 2023).

Ecological factors

One of many ecosystem functions is their ability to stabilize and trap sediment (Hillman et al., 2020). However due to climate change or dam construction, these ecosystems are impacted, accompanied by their sediment trapping ability. Besides the implemented negative effect of dam construction on sediment fluxes, it also decreases the frequency of overbank flooding, increasing vegetation within or along the river channel, increasing sediment trapping and further decreases sediment fluxes (van Oorschot et al., 2018). Also, an increase in drought frequency, intensity or duration as a result of climate change can increase the fluvial sediment flux as a consequence of vegetation reduction in the basin due to drier conditions (Juracek & Fitzpatrick, 2022). Ecological factors and sediment flux are finely interlinked making it a complicated factor to include in the WBMsed model, but potentially enhances projection reliability.

Finally, the Sediment Starvation Risk Index showed a discrepancy of the models reliability to correctly project delta aggradation abilities. The analysis revealed that there were 26 deltas which their ability to withstand relative sea level rise are likely to become more pressured by sediment starvation, in contrast to the projected amount of 16 deltas. This inaccuracy could be caused by the presence of an extreme inter-annual variation at the end of the concerning period, as this would impact the sediment flux change increase or decrease direction in the calculation, but it could also result from inability of the model to accurately reflect real life factors impacting delta sediment fluxes.

5.5 Implications

The analysis of the WBMsed model's performance in projecting sediment fluxes reveals both strengths and areas needing attention. The model generally performs acceptably regarding average annual sediment fluxes with the majority of rivers falling within an

acceptable margin, in line with Cohen et al. (2013), suggesting that WBMsed can project multi-year average sediment loads well. However, investigation is necessary when examining inter-annual variations, as a substantial number of rivers exhibit contradictory directions between projections and measurements during the temporal scale of this research.

Linear regression analysis provides insights into long-term behaviour, but discrepancies between mean inter-annual variations and trendline slopes raise questions about the model's robustness. This discrepancy, linked to the nature of calculating mean inter-annual variations and the model's trendline, highlights the need for a more natural representation of environmental changes due to changing anthropogenic drivers in the delta. Aligning the WBMsed model parameters with more extensive and detailed real-world sediment dynamics is crucial, particularly the gradual transition of communities to anthropogenic drivers of soil erosion and the impact of dam employment, to reduce the model result dependency on specific periods.

While the Euclidean distance analysis attempts to correlate dissimilarity with input variables, the lack of a clear structural connection raises questions about the relevance and accuracy of the variables used by Dunn et al. (2019) in WBMsed or the validation data. However, as the actual used datasets for the projections cannot be consulted, and there is insufficient validation data available, this analysis would be in need of further research. Additionally, the large magnitude differences between the projections and the observations highlight the discharge overprediction within the WBMsed model and highlights that real-life factors influencing sediment fluxes, such as sediment mining, smaller reservoir construction, urbanization and changed ecosystems, are not fully accounted for.

All of these results imply that this specific version of the WBMsed model is not fully reliable for long term delta management strategies, as it is highly dependent on the chosen timeframe, significantly over- and underpredicts and does not display sediment alterations due to several anthropogenic or environmental effects naturally, making the projections not robust. However, the model's reliability improves when used to project long-term changes in sediment fluxes far into the future, as extending the projection period diminishes the influence of extreme inter-annual variations on the trend direction over this period.

5.6 Limitations

For interpreting the research findings, it is crucial to acknowledge several potential limitations. Firstly, reliance on existing datasets introduces concerns about their accuracy and representativeness, potentially impacting the robustness of the outcomes. As stated, there is a global shortage of sufficient sediment flux data, therefore the validation data could not be evaluated or expanded with other sources. Additionally, the subsequent exclusion of specific rivers or entire deltas from the analysis due to limited availability of validation data introduces limitations to the study's findings. Moreover, unavailability of the original input data used in WBMsed restricts a comprehensive analysis of the relationship between dissimilarity and specific input variables. As RCP's started to differ from 2005 onward, the models ability to accurately represent the different RCP pathways could not be assessed in this study, which might hold certain discrepancies. During this study fundamental methods are used, such as the Euclidean distance and first order trendlines to examine the basic characteristics and behaviour of the projections. Also, with the used SSRI calculation, it is assumed that 100% of the fluvial sediment output is retained in the delta, while this is not naturally accurate. Finally, generalizing findings of this research to other global deltas requires caution, considering the study's specific focus on certain datasets and regions. The qualitative analysis of trends and behaviours involves subjectivity, and different interpretations of these trends may impact the overall assessment of model performance. Recognizing these limitations is essential, providing insights into areas for future refinement and guiding subsequent research efforts.

5.7 Future research

The lack of reliable or complete additional validation data for these missing rivers emphasizes the need for standardized sediment flux data collection methods across various sources to ensure consistency in global fluvial sediment data. Also expanding the input datasets with more accurate, consistent and comprehensive global data along with more validation and calibration sources can further ensure model reliability. As mentioned in Section 5.3, due to negligible small differences between the 12 projected scenarios, the average of these scenarios were taken for most of the individual rivers. However as the RCP scenarios are increasingly differing in the future, a closer examination on which scenario used for the projections is needed as inter-scenario changes will increase. There would be research needed on global data to determine the RCP trajectories of global deltas. Dynamic time warping is proposed as a future method to depict dissimilarity

between the model and validation data, as this will introduce the ability to account for timing discrepancies within the model, delving into more intricate aspects beyond the basic forms analysed in this study. Further research in the method of discharge projections is needed on the certain influence causing particular rivers to be under- or overpredicted while their observed discharges are equal. Additionally, a more realistic representation of delta aggradation could be achieved if time-dependent trapping efficiencies for individual deltas were calculated.

Moragoda and Cohen (2020) underscore the intricate challenge of accurately simulating global fluvial sediment fluxes due to their multiscale nature, highlighting the need for advanced methodologies for incorporating additional factors like sediment mining, dam construction, urbanization, and changed ecosystems into the model, to significantly improve projections. If possible regional characteristics can be implemented such as the mining boom across the tropics increasing local sediment fluxes as researched by Dethier et al. (2023). In Dunn (2017), there were crop growth assumptions made, based on precipitation and temperature, to validate certain projection biases. This same theory could perhaps be applied to incorporate certain ecological systems and their effects on sediment fluxes in the model, after further research about their ideal conditions, behaviour and effects. Another example can be the study of Y. Zhang et al. (2023), in which the temporal trends and spatial patterns of sediment load as a response to climate change, especially climate extremes, was investigated. They found a dominant influence of rainstorms on soil loss and the key factor for local sediment flux changes. Studies like this could be combined with studies projecting global exposure to rainstorms as an effect of climate change(Liao et al., 2019), and could be applied to the WBMsed model for increased accuracy. Ongoing research should explore ways to integrate these complexities, which could mean the inclusion of algorithms or analysing trends bound to regional variables, ensuring the model's accuracy for diverse global delta mechanisms.

The impact of inter-annual extremes on projections is evident. While transforming these abrupt inter-annual variations to a more natural effect on the sediment fluxes enhances projection behaviour, accurately representing anthropogenic effects remains a challenge. Future research should focus on refining anthropogenic effect modelling for more realistic projections.

6. Conclusion

As Dunn et al. (2019) provided pioneering work in projecting decadal sediment fluxes for 47 global deltas, this study set out to discover to what extent the projections are able to accurately project sediment flux scenarios and provide a reliable sediment information source for delta sustainability research such as projections of global delta land loss.

The comprehensive analysis of sediment flux projections by the WBMsed model reveals several challenges and areas for improvement. The model exhibits significant inter-annual variability, overall sediment flux discrepancies and timing inaccuracies, indicating limitations in capturing the complex dynamics of sediment transport. While the Euclidean distance analysis and mean absolute differences offer quantitative insights, the lack of consistent dissimilarity and a clear structural connection with model input variables necessitates further qualitative validation.

The trend analysis emphasizes the need for refinement in the model, considering both the significance of trendlines and the robustness of trends across different sample periods. The sensitivity of the model to chosen periods and event timing endorses the importance of addressing such issues for reliable projections, which would create a more reliable basis for global delta management strategies. Ensuring the extreme inter-annual variations are more naturally incorporated in the model will enhance the alignment of projections with observations, but knowing how to account for the impact of unforeseeable anthropogenic effects remains a key challenge.

The overprediction analysis and dissimilar delta aggradation capabilities between projections and observations highlight potential factors influencing sediment fluxes not accounted for in the model. The influence of real-life factors, as sediment mining, small reservoir construction, extreme events, and ecosystems, show the need for further model improvements and its difficulty.

To conclude, Dunn et al. (2019)'s projections show promising accuracy in average annual sediment flux projections for major global deltas. However, addressing the identified challenges on overprediction, unnatural inter-annual variability and the exclusion of variables able to influence fluvial sediment fluxes in reality, is crucial for its applicability to a broader range of global deltas and reliable use in delta sustainability projections.

A. List of Dunn (2017) deltas and their river coordinates

Table A.1: List of 47 deltas and their rivers coordinates (Dunn, 2017)

Delta	**Apex Latitude, Longitude**
Amazon	-1.54368, -52.72264
Amur	53.09969, 139.85332
Burdekin	-19.71295, 147.29023
Chao Phraya	15.25714, 100.0575; 14.64947, 100.9637; 13.95067, 101.37038; 13.89303, 99.89099
Colorado	32.75106, -114.64291
Congo	-5.75414, 13.24175
Ebro	40.7729, 0.64739
Fly	-8.25786, 142.55464
Ganges Brahmaputra Meghna	24.84539, 87.95208; 25.23968, 89.75353; 24.25343, 91.15707
Godavari	17.21379, 81.6839
Grijalva	18.18004, -93.33626
Han	37.99815, 126.39846; 37.89964, 126.79678; 37.56986, 127.001
Indus	24.73682, 68.14388
Irrawaddy	18.2891, 95.41181
Krishna	16.35835, 80.84568
Lena	72.0949, 127.10557
Limpopo	-24.406, 33.01334; -24.36311, 33.55294
Mackenzie	67.65721, -133.96667; 67.64299, -134.75189

Continued on next page

Table A.1: List of 47 deltas and their rivers coordinates (Dunn, 2017) (Continued)

Magdalena	10.41469, -74.77455; 9.15114, -74.24994
Mahakam	-0.34527, 116.9483
Mahanadi Brahmani Baiterani	20.4557, 85.81554; 20.85188, 86.14747; 21.22313, 86.16526
Mekong	11.55579, 105.04546
Mississippi	31.05813, -91.62047
Moulouya	35.12365, -2.51588
Murray	-34.97861, 139.35589
Niger	5.57685, 6.55163
Nile	29.75918, 31.25468
Orinoco	8.56811, -62.32174; 8.48602, -62.21823
Paraná	-32.67496, -60.341
Pearl	23.15196, 112.71086; 23.29473, 112.80009; 23.44827, 112.94642
Po	44.96045, 12.160156
Red	20.91594, 105.95295
Rhine	51.85382, 4.90113
Rhône	43.9163, 4.73445
Rio Grande	26.35338, -98.74988
São Francisco	-10.16007, -36.63488
Sebou	34.54216, -6.35319
Senegal	16.45329, -15.64329
Tana	-2.43558, 40.25205
Tigris Euphrates	30.35235, 48.25008
Tone	36.04321, 140.52154
Vistula	54.02423, 18.94498
Volta	6.54507, 0.05753
Yangtze	32.33372, 119.52415

Continued on next page

Table A.1: List of 47 deltas and their rivers coordinates (Dunn, 2017) (Continued)

Yellow	37.62862, 118.42554
Yukon	62.19093, -163.84877
Zambezi	-18.04213, 35.66087

B. Scaled Euclidean distances vs. different variables

For all plots the numbers represent the individual rivers: 1)Amazon, 2)Amur, 3)Brahmani-Baiterani, 4)Brahmaputra, 5)Burdekin, 6)Congo, 7)Ebro, 8)Fly, 9)Ganges, 10)Godavari, 11)Han, 12)Indus, 13)Irrawaddy, 14)Krishna, 15)Limpopo-Changane, 6)MacKenzie-Peel, 17)MaeKlong, 18)Magdalena-BrazoDeMompos, 19)Mahakam, 20)Mahanadi, 21)Meghna, 22)Mekong, 23)Mississippi, 24)Moulouya, 25)Murray, 26)Niger, 27)Nile, 28)Parana, 29)Pasak-Menam, 30)Po, Z1)Red, 32)Rhone, 33)RioGrande, 34)Sebou, 35)Senegal, 36)Tana, 37)TigrisEuphrates, 38)Vistula, 39)Xijiang, 40)Yangtze, 41)Yellow, 42)Yukon, 43)Zambezi.

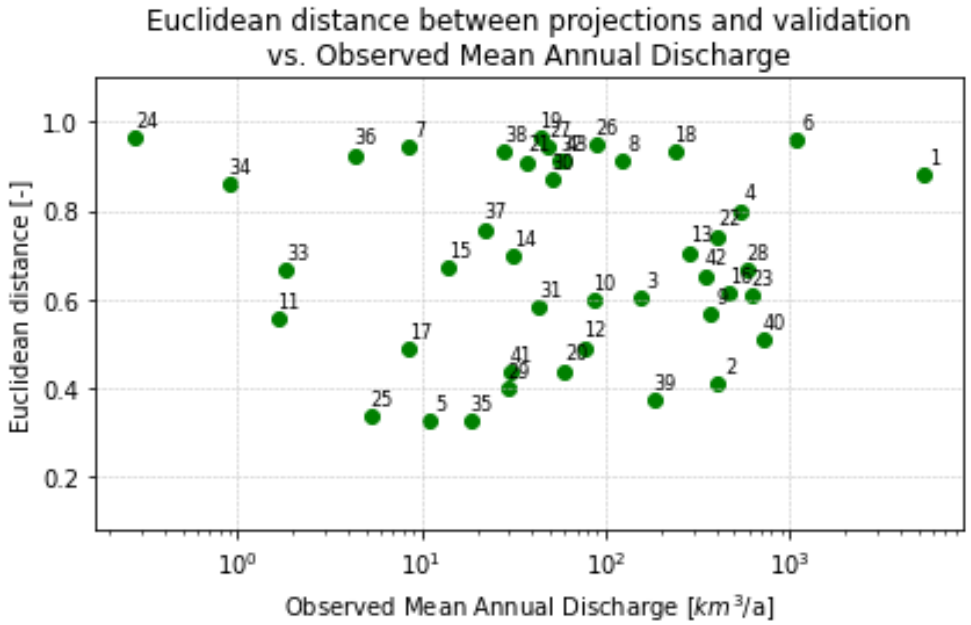

Figure B.1: Scaled Euclidean distance vs. Validation data's average annual discharge[km^3/a]

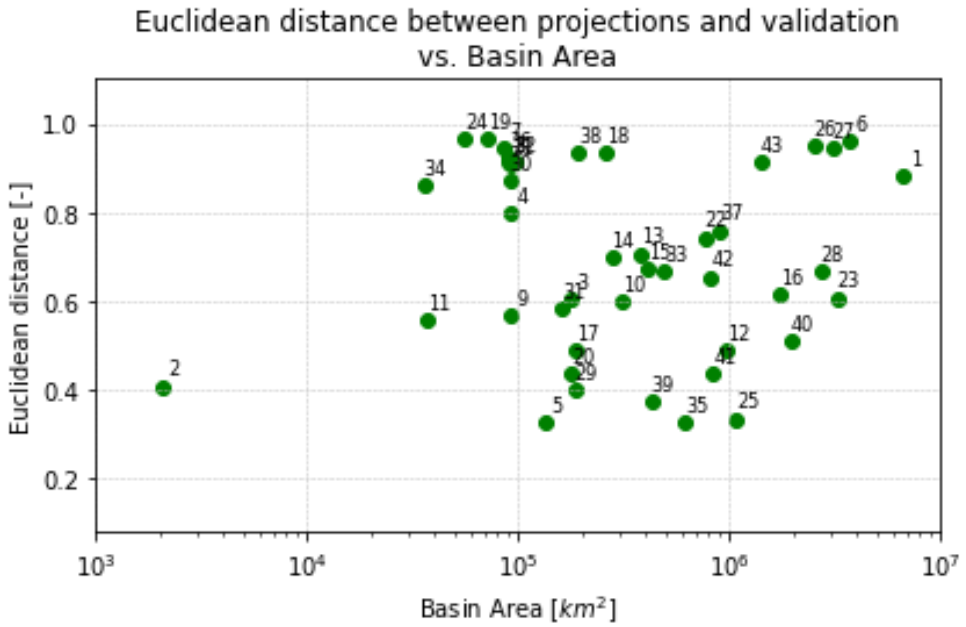

Figure B.2: Scaled Euclidean distance vs. Dunn's (2017) input variable 'Basin Area [km^2]'

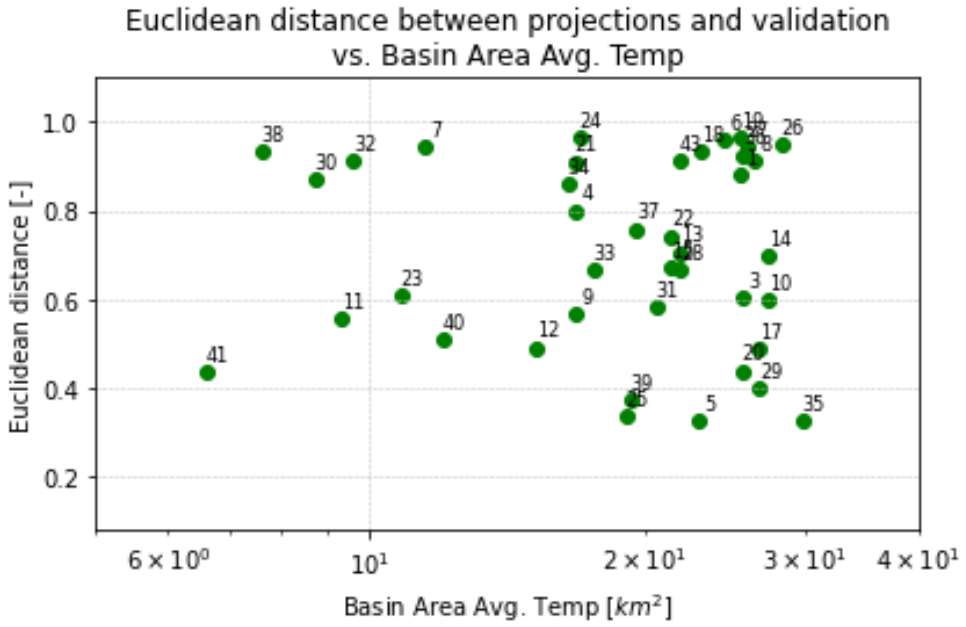

Figure B.3: SScaled Euclidean distance vs. Dunn's (2017) input variable 'Basin Area average temperature [°C]'

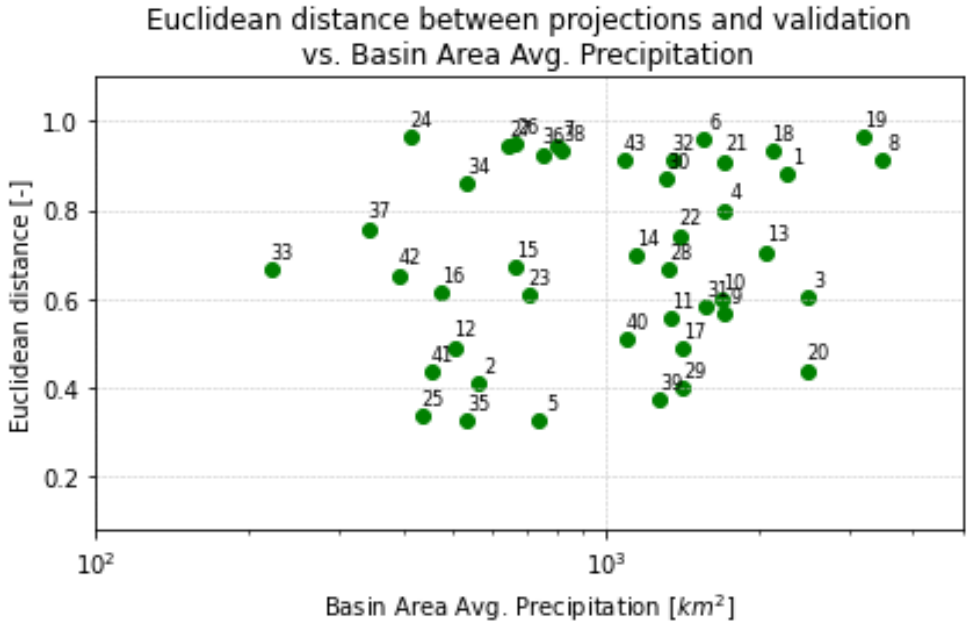

Figure B.4: Scaled Euclidean distance vs. Dunn's (2017) input variable 'Basin average precipitation [mm/a]'

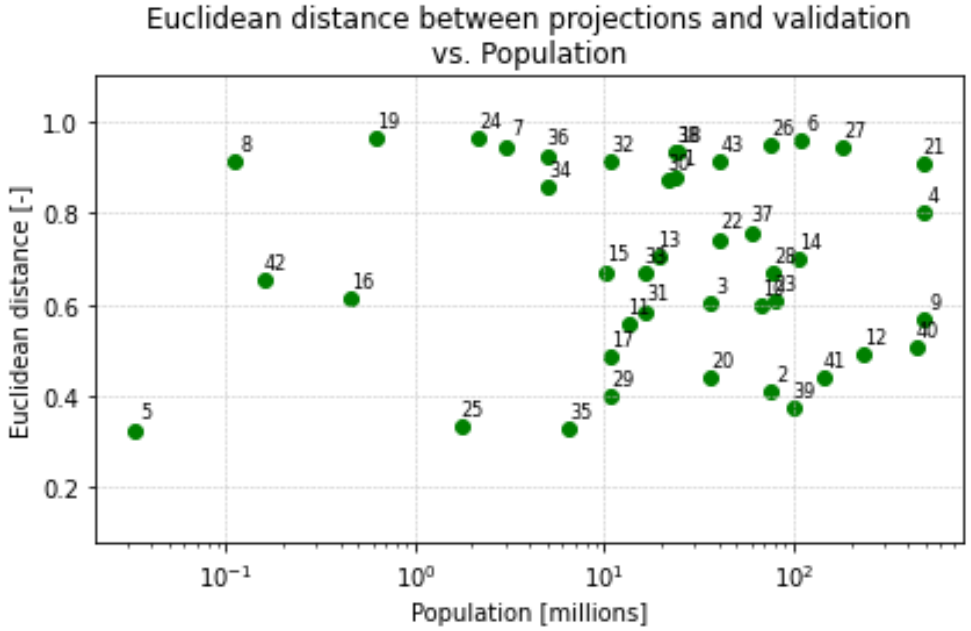

Figure B.5: Scaled Euclidean distance vs. Dunn's (2017) input variable 'Basin population [millions]'

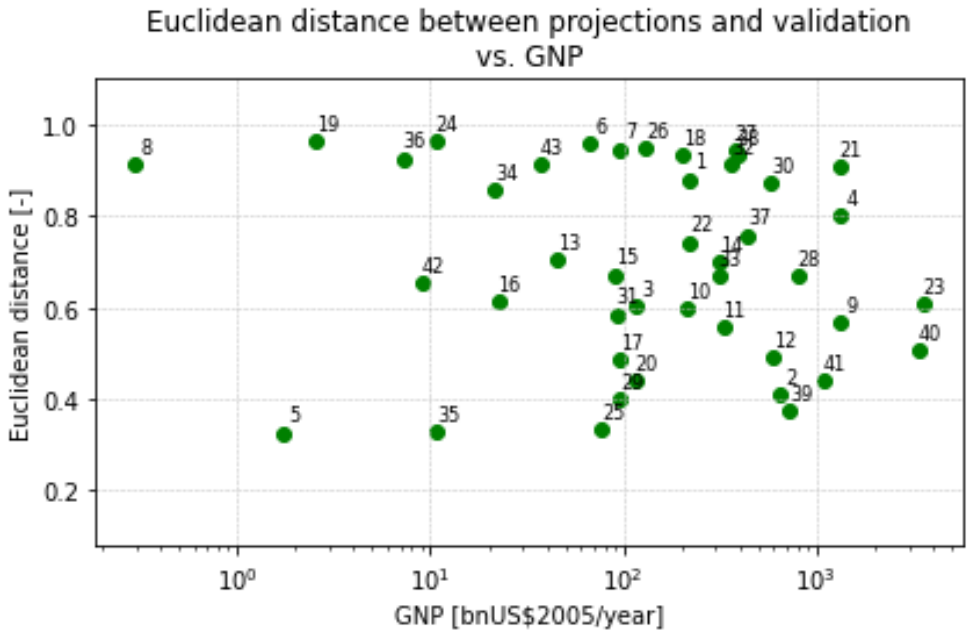

Figure B.6: Scaled Euclidean distance vs. Dunn's (2017) input variable 'Basin GNP [bnUS$2005/year]'

C. Significance test trendlines

Table C.1: T-test results significance testing trendline Dunn et al.(2019) 1984-2020

River	**T-value**	**P-value**	**Significant trendline (p-value<0.05)?**
Amazon	3.292685	0.002231	Yes
Amur	3.040471	0.004385	Yes
BrahmaniBaiterani	-3.33538	0.001985	Yes
Brahmaputra	4.699653	3.75E-05	Yes
Burdekin	-2.63517	0.012326	Yes
Congo	2.993102	0.004966	Yes
Ebro	-2.99792	0.004904	Yes
Fly	6.08023	5.43E-07	Yes
Ganges	-5.01444	1.44E-05	Yes
Godavari	-4.21787	0.000159	Yes
Han	-5.32731	5.51E-06	Yes
Indus	3.871043	0.000438	Yes
Irrawaddy	0.551158	0.58493	No
Krishna	-4.54835	5.92E-05	Yes
LimpopoChangane	-1.31197	0.197835	No
MacKenziePeel	0.472376	0.63951	No
MaeKlong	-1.44074	0.158299	No
MagdalenaBrazo	-1.34065	0.188434	No
Mahakam	6.064437	5.70E-07	Yes
Mahanadi	-1.15852	0.254279	No
Meghna	-3.91046	0.000391	Yes

Continued on next page

Table C.1: T-test results significance testing trendline Dunn et al.(2019) 1984-2020 (Continued)

Mekong	2.803062	0.008102	Yes
Mississippi	1.723821	0.093319	No
Moulouya	-2.0419	0.048541	Yes
Murray	-0.11186	0.911559	No
Niger	5.719292	1.65E-06	Yes
Nile	-5.5074	3.17E-06	Yes
Parana	-5.27046	6.56E-06	Yes
PasakMenam	-5.19715	8.21E-06	Yes
Po	6.05621	5.85E-07	Yes
Red	-4.7041	3.70E-05	Yes
Rhone	5.920246	8.88E-07	Yes
RioGrande	-5.4948	3.29E-06	Yes
Sebou	2.804704	0.008069	Yes
Senegal	-1.08327	0.285889	No
Tana	-2.36053	0.023785	Yes
TigrisEuphrates	-5.48521	3.39E-06	Yes
Vistula	2.715984	0.010088	Yes
Xijiang	-5.07796	1.18E-05	Yes
Yangtze	-5.58685	2.48E-06	Yes
Yellow	-1.9816	0.0552	No
Yukon	6.028595	6.36E-07	Yes
Zambezi	6.051238	5.94E-07	Yes

Table C.2: T-test results significance testing trendline Dethier et al. (2022) 1984-2020

River	**T-value**	**P-value**	**Significant trendline (p-value<0.05)?**
Amazon	4.004987	0.000297	Yes

Continued on next page

Table C.2: T-test results significance testing trendline Dethier et al. (2022) 1984-2020 (Continued)

Amur	4.11989	0.000212	Yes
BrahmaniBaiterani	-0.921	0.363181	No
Brahmaputra	-3.20391	2.84E-03	Yes
Burdekin	1.456183	0.154009	No
Congo	0.729254	0.470565	No
Ebro	-4.557	5.77E-05	Yes
Fly	1.670883	1.03E-01	No
Ganges	-2.90633	6.22E-03	Yes
Godavari	2.403709	0.021504	Yes
Han	-1.64709	1.08E-01	No
Indus	-4.66602	4.15E-05	Yes
Irrawaddy	-0.02994	0.976278	No
Krishna	0.470325	6.41E-01	No
LimpopoChangane	0.51247	0.611452	No
MacKenziePeel	2.108529	0.04201	Yes
MaeKlong	2.272481	0.029129	Yes
MagdalenaBrazo	4.723231	3.49E-05	Yes
Mahakam	4.909647	1.98E-05	Yes
Mahanadi	-0.98918	0.329178	No
Meghna	0.688077	0.495814	No
Mekong	-2.86512	0.006917	Yes
Mississippi	0.229842	0.819516	No
Moulouya	0.401274	0.690591	No
Murray	-2.43742	0.019862	Yes
Niger	5.221183	7.63E-06	Yes
Nile	-3.32874	2.02E-03	Yes

Continued on next page

Table C.2: T-test results significance testing trendline Dethier et al. (2022) 1984-2020 (Continued)

Parana	-2.92248	5.97E-03	Yes
PasakMenam	3.569279	1.04E-03	Yes
Po	1.187451	2.43E-01	No
Red	-5.25751	6.83E-06	Yes
Rhone	1.109383	2.75E-01	No
RioGrande	2.216089	3.31E-02	Yes
Sebou	-1.4789	0.147864	No
Senegal	4.195981	0.000169	Yes
Tana	4.494213	6.97E-05	Yes
TigrisEuphrates	2.022854	5.06E-02	No
Vistula	-0.11288	0.910749	No
Xijiang	-4.90564	2.00E-05	Yes
Yangtze	-5.21617	7.75E-06	Yes
Yellow	-4.24344	0.000147	Yes
Yukon	2.591051	1.37E-02	Yes
Zambezi	3.506084	1.24E-03	Yes

D. Projected vs. observed SSRI values

Table D.1: SSRI results of individual deltas for projections and observations

Delta(river)	**Projected SSRI**	**Observed SSRI**
Amazon	-0.00024	-0.0014
Amur	-0.00024	-0.0073
BrahmaniBaiterani	0.000108	0.000234
Brahmaputra	-1.65E-04	5.96E-05
Burdekin	0.00191	-0.00185
Congo	-0.00257	-0.00022
Ebro	1.49E-05	6.92E-05
Fly	-0.00061	-0.00044
Ganges	6.62E-04	8.95E-05
Godavari	0.006303	-0.00229
Han	5.06E-05	4.66E-06
Indus	-0.00162	0.002427
Irrawaddy	6.91E-07	-9.13E-05
Krishna	0.00104	-0.0004
LimpopoChangane	4.44E-05	-0.00028
MacKenziePeel	2.04E-05	-0.00039
MaeKlong	7.38E-06	-5.28E-06
MagdalenaBrazo	0.000871	-0.0035
Mahakam	-0.00018	-0.00026
Mahanadi	2.46E-04	-3.87E-05
Meghna	3.12E-04	-1.16E-07

Continued on next page

Table D.1: SSRI results of individual deltas for projections and observations (Continued)

Mekong	-5.12E-05	0.000333
Mississippi	-4.38E-06	1.36E-05
Moulouya	2.16E-05	-4.61E-06
Murray	1.33E-06	7.10E-05
Niger	-0.00038	-0.00068
Nile	2.73E-05	3.53E-06
Parana	0.001982	0.002275
PasakMenam	2.99E-05	-8.55E-05
Po	-0.00097	-0.0003
Red	0.002237	0.002887
Rhone	-0.00033	-0.00039
RioGrande	6.19E-06	-1.54E-06
Sebou	-0.00264	0.000191
Senegal	0.000381	-0.00085
Tana	0.000173	-0.00098
TigrisEuphrates	2.46E-03	-1.05E-05
Vistula	-4.68E-05	5.96E-06
Xijiang	4.84E-05	0.004831
Yangtze	0.003767	0.003745
Yellow	0.000371	0.004873
Yukon	-0.00012	-0.00216
Zambezi	-0.00012	-0.00022

Bibliography

Adger, W. N., Adams, H., Kay, S., Nicholls, R. J., Hutton, C. W., Hanson, S. E., Rahman, M. M., & Salehin, M. (2018). Ecosystem services, well-being and deltas: Current knowledge and understanding. *Ecosystem services for well-being in deltas: Integrated assessment for policy analysis*, 3–27.

Aguinis, H., Gottfredson, R. K., & Joo, H. (2013). Best-practice recommendations for defining, identifying, and handling outliers. *Organizational research methods*, *16*(2), 270–301.

Allen, M. P. (1997). The t test for the simple regression coefficient. *Understanding Regression Analysis*, 66–70.

Altman, D. G., & Bland, J. M. (2005). Standard deviations and standard errors. *Bmj*, *331*(7521), 903.

Barrett, P. (2005). Euclidean distance: Raw, normalised, and double-scaled coefficients. *The technical whitepaper series*, *6*, 1–26.

Besset, M., Anthony, E. J., & Bouchette, F. (2019). Multi-decadal variations in delta shorelines and their relationship to river sediment supply: An assessment and review. *Earth-science reviews*, *193*, 199–219.

Best, J., & Darby, S. E. (2020). The pace of human-induced change in large rivers: Stresses, resilience, and vulnerability to extreme events. *One Earth*, *2*(6), 510–514.

Birkmann, J., Cutter, S. L., Rothman, D. S., Welle, T., Garschagen, M., Van Ruijven, B., O'neill, B., Preston, B. L., Kienberger, S., Cardona, O. D., et al. (2015). Scenarios for vulnerability: Opportunities and constraints in the context of climate change and disaster risk. *Climatic Change*, *133*, 53–68.

Çakmak, S., Demir, T., Canpolat, E., & Aytaç, A. S. (2021). Evaluation of the effects of precipitation and flow characteristics on suspended sediment transport in mountain-type mediterranean climate; korkuteli stream sample, antalya, turkey. *Arabian Journal of Geosciences*, *14*(19), 2053.

Cohen, S., Kettner, A. J., & Syvitski, J. P. (2014). Global suspended sediment and water discharge dynamics between 1960 and 2010: Continental trends and intra-basin sensitivity. *global and planetary change*, *115*, 44–58.

Cohen, S., Kettner, A. J., Syvitski, J. P., & Fekete, B. M. (2013). Wbmsed, a distributed global-scale riverine sediment flux model: Model description and validation. *Computers & Geosciences*, *53*, 80–93.

Cohen, S., Syvitski, J., Ashley, T., Lammers, R., Fekete, B., & Li, H.-Y. (2022). Spatial trends and drivers of bedload and suspended sediment fluxes in global rivers. *Water Resources Research*, *58*(6), e2021WR031583.

Dahiru, T. (2008). P-value, a true test of statistical significance? a cautionary note. *Annals of Ibadan postgraduate medicine*, *6*(1), 21–26.

Day, J. W., Agboola, J., Chen, Z., D'Elia, C., Forbes, D. L., Giosan, L., Kemp, P., Kuenzer, C., Lane, R. R., Ramachandran, R., et al. (2016). Approaches to defining deltaic sustainability in the 21st century. *Estuarine, coastal and shelf science*, *183*, 275–291.

Deboulet, A., & Mansour, W. (2022). *Middle eastern cities in a time of climate crisis*. CEDEJ - Égypte/Soudan. https://books.openedition.org/cedej/8534

Dethier, E. N., Renshaw, C. E., & Magilligan, F. J. (2022). Rapid changes to global river suspended sediment flux by humans. *Science*, *376*(6600), 1447–1452.

Dethier, E. N., Silman, M., Leiva, J. D., Alqahtani, S., Fernandez, L. E., Pauca, P., Çamalan, S., Tomhave, P., Magilligan, F. J., Renshaw, C. E., et al. (2023). A global rise in alluvial mining increases sediment load in tropical rivers. *Nature*, *620*(7975), 787–793.

Ding, H., Trajcevski, G., Scheuermann, P., Wang, X., & Keogh, E. (2008). Querying and mining of time series data: Experimental comparison of representations and distance measures. *Proceedings of the VLDB Endowment*, *1*(2), 1542–1552.

Dunn, F. E., Darby, S. E., Nicholls, R. J., Cohen, S., Zarfl, C., & Fekete, B. M. (2019). Projections of declining fluvial sediment delivery to major deltas worldwide in response to climate change and anthropogenic stress. *Environmental Research Letters*, *14*(8), 084034.

Dunn, F. E., Nicholls, R. J., Darby, S. E., Cohen, S., Zarfl, C., & Fekete, B. M. (2018). Projections of historical and 21st century fluvial sediment delivery to the ganges-brahmaputra-meghna, mahanadi, and volta deltas. *Science of the total environment*, *642*, 105–116.

Dunn, F. E. (2017). *Multidecadal fluvial sediment fluxes to major deltas under environmental change scenarios: Projections and their implications* [Doctoral dissertation, University of Southampton].

Edmonds, D. A., Caldwell, R. L., Brondizio, E. S., & Siani, S. M. (2020). Coastal flooding will disproportionately impact people on river deltas. *Nature communications*, *11*(1), 4741.

Ericson, J. P., Vörösmarty, C. J., Dingman, S. L., Ward, L. G., & Meybeck, M. (2006). Effective sea-level rise and deltas: Causes of change and human dimension implications. *Global and Planetary Change*, *50*(1-2), 63–82.

Evans, G. (2012). Deltas: The fertile dustbins of the continents. *Proceedings of the Geologists' Association*, *123*(3), 397–418.

Fairbridge, R. W. (1961). Eustatic changes in sea level. *Physics and Chemistry of the Earth*, *4*, 99–185.

Faloutsos, C., Ranganathan, M., & Manolopoulos, Y. (1994). Fast subsequence matching in time-series databases. *ACM Sigmod Record*, *23*(2), 419–429.

Fekete, B. M., Pisacane, G., & Wisser, D. (2016). Crystal balls into the future: Are global circulation and water balance models ready? *Proceedings of the International Association of Hydrological Sciences*, *374*, 41–51.

Ford, C. (2015). Understanding QQ Plots | UVA Library — library.virginia.edu.

Fryirs, K. (2013). (dis) connectivity in catchment sediment cascades: A fresh look at the sediment delivery problem. *Earth Surface Processes and Landforms*, *38*(1), 30–46.

Ghasemi, A., & Zahediasl, S. (2012). Normality tests for statistical analysis: A guide for non-statisticians. *International journal of endocrinology and metabolism*, *10*(2), 486.

Giosan, L., Syvitski, J. P., Constantinescu, S., & Day, J. (2014). Climate change: Protect the world's deltas. *Nature*, *516*(7529), 31–33.

Grill, G., Lehner, B., Lumsdon, A. E., MacDonald, G. K., Zarfl, C., & Liermann, C. R. (2015). An index-based framework for assessing patterns and trends in river fragmentation and flow regulation by global dams at multiple scales. *Environmental Research Letters*, *10*(1), 015001.

Grinstead, C. M., & Snell, J. L. (2006). *Grinstead and snell's introduction to probability*. Chance Project.

Hancock, G. (2009). A catchment scale assessment of increased rainfall and storm intensity on erosion and sediment transport for northern australia. *Geoderma*, *152*(3-4), 350–360.

Hillman, J. R., Stephenson, F., Thrush, S. F., & Lundquist, C. J. (2020). Investigating changes in estuarine ecosystem functioning under future scenarios. *Ecol. Appl.*, *30*(4), e02090.

Hoitink, A. J., Nittrouer, J. A., Passalacqua, P., Shaw, J. B., Langendoen, E. J., Huismans, Y., & van Maren, D. S. (2020). Resilience of river deltas in the anthropocene. *Journal of Geophysical Research: Earth Surface*, *125*(3), e2019JF005201.

Ibáñez, C., Day, J. W., & Reyes, E. (2014). The response of deltas to sea-level rise: Natural mechanisms and management options to adapt to high-end scenarios [Sustainable Restoration]. *Ecological Engineering*, *65*, 122–130. https://doi.org/https://doi.org/10.1016/j.ecoleng.2013.08.002

Ioannidis, J. P. (2007). Limitations are not properly acknowledged in the scientific literature. *Journal of Clinical Epidemiology*, *60*(4), 324–329. https://doi.org/https://doi.org/10.1016/j.jclinepi.2006.09.011

IPCC. (2007). 6.4.1.2 Deltas - AR4 WGII Chapter 6: Coastal Systems and Low-Lying Areas — archive.ipcc.ch.

Jenkins-Smith, H., Ripberger, J., Copeland, G. W., Nowlin, M. C., Hughes, T., Fister, A. L., & Wehde, W. (2017). *Quantitative research methods for political science, public policy and public administration (with applications in r)*. University of Oklahoma Libraries.

Jiang, G., Wang, W., & Zhang, W. (2019). A novel distance measure for time series: Maximum shifting correlation distance. *Pattern Recognition Letters*, *117*, 58–65. https://doi.org/https://doi.org/10.1016/j.patrec.2018.11.013

Jones, C. D., Hughes, J. K., Bellouin, N., Hardiman, S. C., Jones, G. S., Knight, J., Liddicoat, S., O'Connor, F. M., Andres, R. J., Bell, C., Boo, K.-O., Bozzo, A., Butchart, N., Cadule, P., Corbin, K. D., Doutriaux-Boucher, M., Friedlingstein, P., Gornall, J., Gray, L., … Zerroukat, M. (2011). The hadgem2-es implementation of cmip5 centennial simulations. *Geoscientific Model Development*, *4*(3), 543–570. https://doi.org/10.5194/gmd-4-543-2011

Jordan, C., Tiede, J., Lojek, O., Visscher, J., Apel, H., Nguyen, H. Q., Quang, C. N. X., & Schlurmann, T. (2019). Sand mining in the mekong delta revisited - current scales of local sediment deficits. *Sci. Rep.*, *9*(1), 17823.

Juracek, K. E., & Fitzpatrick, F. A. (2022). Geomorphic responses of fluvial systems to climate change: A habitat perspective. *River Res. Appl.*, *38*(4), 757–775.

Kondolf, G. M., Schmitt, R. J. P., Carling, P. A., Goichot, M., Keskinen, M., Arias, M. E., Bizzi, S., Castelletti, A., Cochrane, T. A., Darby, S. E., Kummu, M., Minderhoud, P. S. J., Nguyen, D., Nguyen, H. T., Nguyen, N. T., Oeurng, C., Opperman, J., Rubin, Z., San, D. C., … Wild, T. (2022). Save the mekong delta from drowning. *Science*, *376*(6593), 583–585. https://doi.org/10.1126/science.abm5176

Kondolf, G. M. (1997). Profile: Hungry water: Effects of dams and gravel mining on river channels. *Environmental Management*, *21*(4), 533–551. https://doi.org/10.1007/s002679900048

Lai, X., Yin, D., Finlayson, B., Wei, T., Li, M., Yuan, W., Yang, S., Dai, Z., Gao, S., & Chen, Z. (2017). Will river erosion below the three gorges dam stop in the middle yangtze? *Journal of Hydrology*, *554*, 24–31. https://doi.org/https://doi.org/10.1016/j.jhydrol.2017.08.057

Lee, K. J., Wiest, M. M., & Carlin, J. B. (2014). Statistics for clinicians: An introduction to linear regression. *J. Paediatr. Child Health*, *50*(12), 940–943.

Li, Y., Zhao, J., Miao, R., Huang, Y., Fan, X., Liu, X., Wang, X., Wang, Y., & Shen, Y. (2022). Analysis of the temporal and spatial distribution of extreme climate indices in central china. *Sustainability*, *14*(4). https://doi.org/10.3390/su14042329

Liao, X., Xu, W., Zhang, J., Li, Y., & Tian, Y. (2019). Global exposure to rainstorms and the contribution rates of climate change and population change. *Science of The Total Environment*, *663*, 644–653. https://doi.org/https://doi.org/10.1016/j.scitotenv.2019.01.290

Maaß, A.-L., Schüttrumpf, H., & Lehmkuhl, F. (2021). Human impact on fluvial systems in europe with special regard to today's river restorations. *Environ. Sci. Eur.*, *33*(1).

MacKenzie, K., Singh, K., Binns, A., Whiteley, H., & Gharabaghi, B. (2022). Effects of urbanization on stream flow, sediment, and phosphorous regime. *Journal of Hydrology*, *612*, 128283. https://doi.org/https://doi.org/10.1016/j.jhydrol.2022.128283

Maselli, V., & Trincardi, F. (2013). Man made deltas. *Sci. Rep.*, *3*(1), 1926.

McManus, J. (2002). Deltaic responses to changes in river regimes [6th International Symposium on Model Estuaries]. *Marine Chemistry*, *79*(3), 155–170. https://doi.org/https://doi.org/10.1016/S0304-4203(02)00061-0

Meier, M. F., Dyurgerov, M. B., Rick, U. K., O'Neel, S., Pfeffer, W. T., Anderson, R. S., Anderson, S. P., & Glazovsky, A. F. (2007). Glaciers dominate eustatic sea-level rise in the 21st century. *Science*, *317*(5841), 1064–1067. https://doi.org/10.1126/science.1143906

Milliman, J. D., & Meade, R. H. (1983). World-wide delivery of river sediment to the oceans. *The Journal of Geology*, *91*(1), 1–21. https://doi.org/10.1086/628741

Milliman, J. D., & Syvitski, J. P. M. (1992). Geomorphic/tectonic control of sediment discharge to the ocean: The importance of small mountainous rivers. *The Journal of Geology*, *100*(5), 525–544. https://doi.org/10.1086/629606

Minderhoud, P. S. J., Middelkoop, H., Erkens, G., & Stouthamer, E. (2020). Groundwater extraction may drown mega-delta: Projections of extraction-induced subsidence and elevation of the mekong delta for the 21st century. *Environ. Res. Commun.*, *2*(1), 011005.

Mitrovica, J. X., Tamisiea, M. E., Davis, J. L., & Milne, G. A. (2001). Recent mass balance of polar ice sheets inferred from patterns of global sea-level change. *Nature*, *409*(6823), 1026–1029.

Moragoda, N., & Cohen, S. (2020). Climate-induced trends in global riverine water discharge and suspended sediment dynamics in the 21st century. *Global and Planetary Change*, *191*, 103199. https://doi.org/https://doi.org/10.1016/j.gloplacha.2020.103199

Moragoda, N., Cohen, S., Gardner, J., Muñoz, D., Narayanan, A., Moftakhari, H., & Pavelsky, T. M. (2023). Modeling and analysis of sediment trapping efficiency of large dams using remote sensing [e2022WR033296 2022WR033296]. *Water Resources Research*, *59*(6), e2022WR033296. https://doi.org/https://doi.org/10.1029/2022WR033296

Morehead, M. D., Syvitski, J. P., Hutton, E. W., & Peckham, S. D. (2003). Modeling the temporal variability in the flux of sediment from ungauged river basins [The supply of flux of sediment along hydrological pathways: Anthropogenic influences at the global scale]. *Global and Planetary Change*, *39*(1), 95–110. https://doi.org/https://doi.org/10.1016/S0921-8181(03)00019-5

Murakami, D., & Yamagata, Y. (2017). Estimation of gridded population and gdp scenarios with spatially explicit statistical downscaling.

Nguyen, T. C., Schwarzer, K., & Ricklefs, K. (2023). Water-level changes and subsidence rates along the saigon-dong nai river estuary and the east sea coastline of the mekong delta. *Estuarine, Coastal and Shelf Science*, *283*, 108259. https://doi.org/https://doi.org/10.1016/j.ecss.2023.108259

Nicholls, R., Hutton, C., Lázár, A., Allan, A., Adger, W., Adams, H., Wolf, J., Rahman, M., & Salehin, M. (2016). Integrated assessment of social and environmental sustainability dynamics in the ganges-brahmaputra-meghna delta, bangladesh. *Estuarine, Coastal and Shelf Science*, *183*, 370–381.

Nicholls, R., Wong, P. P., Burkett, V., Codignotto, J., Hay, J., Mclean, R., Ragoonaden, S., Woodroffe, C., Abuodha, P., Arblaster, J., Brown, B., Forbes, D., Hall, J., Kovats, S., Lowe, J., Mcinnes, K., Moser, S., Armstrong, S., & Saito, Y. (2007). Coastal systems and low-lying areas. *Faculty of Science - Papers*.

Nicholls, R. J. (2004). Coastal flooding and wetland loss in the 21st century: Changes under the sres climate and socio-economic scenarios [Climate Change]. *Global Environmental Change*, *14*(1), 69–86. https://doi.org/https://doi.org/10.1016/j.gloenvcha.2003.10.007

Nicholls, R. J., & Cazenave, A. (2010). Sea-level rise and its impact on coastal zones. *Science*, *328*(5985), 1517–1520. https://doi.org/10.1126/science.1185782

Nienhuis, J. H., Kim, W., Milne, G. A., Quock, M., Slangen, A. B., & Tornqvist, T. E. (2023). River deltas and sea-level rise. *Annual Review of Earth and Planetary Sciences*, *51*(1), 79–104. https://doi.org/10.1146/annurev-earth-031621-093732

Nienhuis, J. H., & van de Wal, R. S. W. (2021). Projections of global delta land loss from sea-level rise in the 21st century [e2021GL093368 2021GL093368]. *Geophysical Research Letters*, *48*(14), e2021GL093368. https://doi.org/https://doi.org/10.1029/2021GL093368

Nugus, S. (2009). *Financial planning using excel: Forecasting, planning and budgeting techniques*. Elsevier Science. https://books.google.nl/books?id=7u6r3_BzJ0oC

O'Neill, B. C., Kriegler, E., Riahi, K., Ebi, K. L., Hallegatte, S., Carter, T. R., Mathur, R., & van Vuuren, D. P. (2014). A new scenario framework for climate change research: The concept of shared socioeconomic pathways. *Clim. Change*, *122*(3), 387–400.

Parker, A. (2020). Anthropogenic drivers of relative sea-level rise in the mekong delta – a review. *Quaest. Geogr.*, *39*(1), 109–124.

Parsons, T., Wu, P.-C., (Matt) Wei, M., & D'Hondt, S. (2023). The weight of new york city: Possible contributions to subsidence from anthropogenic sources [e2022EF003465 2022EF003465]. *Earth's Future*, *11*(5), e2022EF003465. https://doi.org/https://doi.org/10.1029/2022EF003465

Preciso, E., Salemi, E., & Billi, P. (2012). Land use changes, torrent control works and sediment mining: Effects on channel morphology and sediment flux, case study of the reno river (northern italy). *26*(8), 1134–1148.

Puri, C., Kooijman, G., Vanrumste, B., & Luca, S. (2022). Forecasting time series in healthcare with gaussian processes and dynamic time warping based subset selection. *IEEE Journal of Biomedical and Health Informatics*, *26*(12), 6126–6137. https://doi.org/10.1109/JBHI.2022.3214343

Rascher, E., Rindler, R., Habersack, H., & Sass, O. (2018). Impacts of gravel mining and renaturation measures on the sediment flux and budget in an alpine catchment (johnsbach valley, austria). *Geomorphology*, *318*, 404–420. https://doi.org/https://doi.org/10.1016/j.geomorph.2018.07.009

Refsgaard, J. C., Arnbjerg-Nielsen, K., Drews, M., Halsnæs, K., Jeppesen, E., Madsen, H., Markandya, A., Olesen, J. E., Porter, J. R., & Christensen, J. H. (2013). The role of

uncertainty in climate change adaptation strategies—a danish water management example. *Mitig. Adapt. Strateg. Glob. Chang.*, *18*(3), 337–359.

Reid, S. C., Lane, S. N., Berney, J. M., & Holden, J. (2007). The timing and magnitude of coarse sediment transport events within an upland, temperate gravel-bed river. *Geomorphology*, *83*(1), 152–182. https://doi.org/https://doi.org/10.1016/j.geomorph.2006.06.030

Riahi, K., Grübler, A., & Nakicenovic, N. (2007). Scenarios of long-term socio-economic and environmental development under climate stabilization [Greenhouse Gases - Integrated Assessment]. *Technological Forecasting and Social Change*, *74*(7), 887–935. https://doi.org/https://doi.org/10.1016/j.techfore.2006.05.026

Rignot, E., & Thomas, R. H. (2002). Mass balance of polar ice sheets. *Science*, *297*(5586), 1502–1506. https://doi.org/10.1126/science.1073888

Rovere, A., Stocchi, P., & Vacchi, M. (2016). Eustatic and relative sea level changes. *Curr. Clim. Change Rep.*, *2*(4), 221–231.

Saito, Y., Chaimanee, N., Thanawat, J., & Syvitski, J. (2007). Shrinking megadeltas in asia: Sea-level rise and sediment reduction impacts from case study of the chao phraya delta. *LOICZ Inprint*, *2007*, 3–9.

Sames, B., Wagreich, M., Conrad, C. P., & Iqbal, S. (2020). Aquifer-eustasy as the main driver of short-term sea-level fluctuations during cretaceous hothouse climate phases. *Geological Society, London, Special Publications*, *498*(1), 9–38. https://doi.org/10.1144/SP498-2019-105

Sanchez-Arcilla, A., Jiménez, J., & Valdemoro, H. (1998). The ebro delta: Morphodynamics and vulnerability. *Journal of Coastal Research*, *14*, 754–772.

Sargent, R. G. (2010). Verification and validation of simulation models. *Proceedings of the 2010 Winter Simulation Conference*, 166–183. https://doi.org/10.1109/WSC.2010.5679166

Scott, D. W. (2015). Probability density estimation. In *International encyclopedia of the social & behavioral sciences* (pp. 29–32). Elsevier.

Stoddard, A. M. (1979). Standardization of measures prior to cluster analysis. *Biometrics*, *35*(4), 765–773. Retrieved January 14, 2024, from http://www.jstor.org/stable/2530108

Streiner, D. L. (1996). Maintaining standards: Differences between the standard deviation and standard error, and when to use each [PMID: 8899234]. *The Canadian Journal of Psychiatry*, *41*(8), 498–502. https://doi.org/10.1177/070674379604100805

Syvitski, J., Harvey, N., Wolanski, E., Burnett, W. C., Perillo, G. M. E., & Gornitz, V. (2005). Dynamics of the coastal zone. In C. J. Crossland, H. H. Kremer, H. J. Lindeboom, J. I. M. Crossland, & M. D. A. Le Tissier (Eds.), *Coastal change and the anthropocene: The land-ocean interactions in the coastal zone project of the international geosphere-biosphere programme* (pp. 39–94). Springer.

Syvitski, J. (2008). Deltas at risk. *Sustainability Science*, *3*, 23–32. https://doi.org/10.1007/s11625-008-0043-3

Syvitski, J., Ángel, J. R., Saito, Y., Overeem, I., Vörösmarty, C. J., Wang, H., & Olago, D. (2022). Earth's sediment cycle during the anthropocene. *Nat. Rev. Earth Environ.*, *3*(3), 179–196.

Syvitski, J., & Kettner, A. (2011). Sediment flux and the anthropocene. *Philosophical transactions. Series A, Mathematical, physical, and engineering sciences*, *369*, 957–75. https://doi.org/10.1098/rsta.2010.0329

Syvitski, J. P. M., & Kettner, A. (2011). Sediment flux and the anthropocene. *Philosophical Transactions of the Royal Society A: Mathematical, Physical and Engineering Sciences*, *369*(1938), 957–975. https://doi.org/10.1098/rsta.2010.0329

Syvitski, J. P. (2003). Supply and flux of sediment along hydrological pathways: Research for the 21st century [The supply of flux of sediment along hydrological pathways: Anthropogenic influences at the global scale]. *Global and Planetary Change*, *39*(1), 1–11. https://doi.org/https://doi.org/10.1016/S0921-8181(03)00008-0

Syvitski, J. P., Kettner, A. J., Overeem, I., Hutton, E. W., Hannon, M. T., Brakenridge, G. R., Day, J., Vörösmarty, C., Saito, Y., Giosan, L., et al. (2009). Sinking deltas due to human activities. *Nature Geoscience*, *2*(10), 681–686.

Syvitski, J. P., & Saito, Y. (2007). Morphodynamics of deltas under the influence of humans. *Global and Planetary Change*, *57*(3-4), 261–282.

Thacker, B. H., Doebling, S. W., Hemez, F. M., Anderson, M. C., Pepin, J. E., & Rodriguez, E. A. (2004). Concepts of model verification and validation. https://doi.org/10.2172/835920

Truong, M. H., & Nguyen, D. T. (2020). Characteristics of consolidation settlements and sedimentary environments of the late Pleistocene–Holocene deposits in the mekong delta and ho chi minh city, vietnam. *Proc. Int. Assoc. Hydrol. Sci.*, *382*, 367–374.

Valle, D., Staudhammer, C. L., Cropper Jr., W. P., & Gardingen, P. R. (2009). The importance of multimodel projections to assess uncertainty in projections from simulation models. *Ecological Applications*, *19*(7), 1680–1692. https://doi.org/https://doi.org/10.1890/08-1579.1

van Oorschot, M., Kleinhans, M., Buijse, T., Geerling, G., & Middelkoop, H. (2018). Combined effects of climate change and dam construction on riverine ecosystems. *Ecological Engineering*, *120*, 329–344. https://doi.org/https://doi.org/10.1016/j.ecoleng.2018.05.037

van Vuuren, D. P., Edmonds, J., Kainuma, M., Riahi, K., Thomson, A., Hibbard, K., Hurtt, G. C., Kram, T., Krey, V., Lamarque, J.-F., Masui, T., Meinshausen, M., Nakicenovic, N., Smith, S. J., & Rose, S. K. (2011). The representative concentration pathways: An overview. *Clim. Change*, *109*(1-2), 5–31.

van Vuuren, D. P., Kriegler, E., O'Neill, B. C., Ebi, K. L., Riahi, K., Carter, T. R., Edmonds, J., Hallegatte, S., Kram, T., Mathur, R., & Winkler, H. (2014). A new scenario framework for climate change research: Scenario matrix architecture. *Clim. Change*, *122*(3), 373–386.

Vörösmarty, C. J., Meybeck, M., Fekete, B., Sharma, K., Green, P., & Syvitski, J. P. (2003). Anthropogenic sediment retention: Major global impact from registered river impoundments [The supply of flux of sediment along hydrological pathways: Anthropogenic influences at the global scale]. *Global and Planetary Change*, *39*(1), 169–190. https://doi.org/https://doi.org/10.1016/S0921-8181(03)00023-7

Vörösmarty, C. J., Moore III, B., Grace, A. L., Gildea, M. P., Melillo, J. M., Peterson, B. J., Rastetter, E. B., & Steudler, P. A. (1989). Continental scale models of water balance and fluvial transport: An application to south america. *Global Biogeochemical Cycles*, *3*(3), 241–265. https://doi.org/https://doi.org/10.1029/GB003i003p00241

Wagner, D., W.and Lague, Mohrig, D., Passalacqua, P., & Shaw, K., J.and Moffett. (2017). *Elevation change and stability on a prograding delta.* (Vol. 44). Wiley.

Waltham, T. (2002). Sinking cities. *Geology Today*, *18*(3), 95–100. https://doi.org/https://doi.org/10.1046/j.1365-2451.2002.00341.x

Wan, X., Wang, W., Liu, J., & Tong, T. (2014). Estimating the sample mean and standard deviation from the sample size, median, range and/or interquartile range. *BMC Med. Res. Methodol.*, *14*(1), 135.

Wisser, D., Fekete, B. M., Vörösmarty, C. J., & Schumann, A. H. (2010). Reconstructing 20th century global hydrography: A contribution to the global terrestrial network-hydrology (gtn-h). *Hydrology and Earth System Sciences*, *14*(1), 1–24. https://doi.org/10.5194/hess-14-1-2010

Wisser, D., Frolking, S., Douglas, E. M., Fekete, B. M., Vörösmarty, C. J., & Schumann, A. H. (2008). Global irrigation water demand: Variability and uncertainties arising from agricultural and climate data sets. *Geophysical Research Letters*, *35*(24). https://doi.org/https://doi.org/10.1029/2008GL035296

Wong, P. P., Losada, I., Gattuso, J.-P., Hinkel, J., Khattabi, A., Mcinnes, K., Saito, Y., & Sallenger, A. (2014, January). Coastal systems and low-lying areas. https://doi.org/10.1017/CBO9781107415379.010

Yin, J., Griffies, S. M., & Stouffer, R. J. (2010). Spatial variability of sea level rise in twenty-first century projections. *Journal of Climate*, *23*(17), 4585–4607. https://doi.org/https://doi.org/10.1175/2010JCLI3533.1

Zarfl, C., Lumsdon, A. E., Berlekamp, J., Tydecks, L., & Tockner, K. (2015). A global boom in hydropower dam construction. *Aquat. Sci.*, *77*(1), 161–170.

Zhang, T., Li, D., East, A. E., Walling, D. E., Lane, S., Overeem, I., Beylich, A. A., Koppes, M., & Lu, X. (2022). Warming-driven erosion and sediment transport in cold regions. *Nat. Rev. Earth Environ.*, *3*(12), 832–851.

Zhang, Y., Tian, P., Yang, L., Zhao, G., Mu, X., Wang, B., Du, P., Gao, P., & Sun, W. (2023). Relationship between sediment load and climate extremes in the major chinese rivers. *Journal of Hydrology*, *617*, 128962. https://doi.org/https://doi.org/10.1016/j.jhydrol.2022.128962

Zoccarato, C., Minderhoud, P. S. J., & Teatini, P. (2018). The role of sedimentation and natural compaction in a prograding delta: Insights from the mega mekong delta, vietnam. *Sci. Rep.*, *8*(1).

Zonneveld, W., & Nadin, V. (2020, December). *The randstad: A polycentric metropolis* (W. Zonneveld & V. Nadin, Eds.). Routledge. https://doi.org/10.4324/9780203383346